Rev7 is a novel regulator of chemotherapeutic response in drug-resistant lung cancer

By: Faye-Marie Vassel

B.S. Biochemistry
SUNY Stony Brook University, 2011

Submitted to the Department of Biology on July 27th, 2018 in partial fulfillment of the requirements for the degree of:
Doctorate of Philosophy in Biology at the Massachusetts Institute of Technology

~~July 2018~~ [September 2018]

Signature of Author: Signature redacted
Department of Biology
July 27, 2018

Certified by: Signature redacted
Graham C. Walker
Professor of Biology
Thesis Supervisor

Certified by: Signature redacted
Michael T. Hemann
Associate Professor of Biology
Thesis Supervisor

Accepted by: Signature redacted
Amy Keating
Professor of Biology
Co-chair, Biology Graduate Committee

Rev7 is a novel regulator of chemotherapeutic response in drug-resistant lung cancer

By: Faye-Marie Vassel

Submitted to the Department of Biology on July 27th, 2018 in partial fulfillment of the requirements for the degree of Doctorate of Philosophy in Biology at the Massachusetts Institute of Technology

Abstract

Most malignant cancers are treated with chemotherapeutic agents that target and damage cellular DNA. While genotoxic chemotherapies have proven to be highly effective agents for cancer therapy, it is well known that intrinsic and acquired cancer drug resistance is a problem that severely limits the successful elimination of a wide range of malignancies. This point is particularly important in the context of genotoxic chemotherapies, because the DNA damaging agents used in cancer treatment induce a diverse spectrum of toxic lesions that are recognized by a variety of DNA damage response (DDR) mechanisms.

In this thesis I used CRISPR-Cas9 gene-editing and other molecular biology and biochemical techniques to examine the functional relevance of that Rev7, a multi-functional translesion synthesis (TLS) DNA damage tolerance protein in drug-resistant cancers. In particular, I employed CRISPR-Cas9 gene-editing technologies to generate Rev7 knockout (KO) drug-resistant lung cancers cell to use as a tool to investigate the impact that Rev7 loss may have on chemotherapeutic efficacy. Excitingly, this work reveals that Rev7 loss sensitizes intrinsically drug-resistant lung tumors to cisplatin and drastically enhances the overall survival of syngeneic mice transplanted with drug-resistant lung tumors. Additionally, in this thesis I conducted immunoprecipitation and mass spectrometry to better elucidate the Rev7's functional relevance. Mass spectrometry findings in this thesis reveal that when Rev7 is immunoprecipitated under different cellular conditions (i.e. G2/M arrested or DNA damaged cells), Rev7 interacts with novel and diverse Rev7 protein interactors. Intriguingly, my mass spectrometry findings also reveal that Rev7 forms protein-protein interactions with many proteins that play a role in regulating double-strand break (DSB) repair. Given these findings we conducted DSB repair

studies investigating if Rev7 plays a role regulating DSB repair in drug-resistant lung cancer. Notably, these studies suggest that Rev7 loss results in a decrease in DSB repair capacity and increases in DSBs in drug-resistant lung cancer cells.

Altogether, this thesis demonstrates that Rev7 has functional relevance in modulating chemotherapeutic response in drug-resistant lung cancer. Further, this thesis presents findings that strongly argue that the development of small molecule inhibitors targeting Rev7 may provide a new way to enhance chemotherapeutic efficacy in drug-resistant tumors in the clinic.

Thesis Supervisor: Graham C. Walker
Title: Professor of Biology

Thesis Supervisor: Michael T. Hemann
Title: Associate Professor of Biology

Acknowledgments

There are many people who have contributed to helping me along on my journey here at MIT. I feel fortunate to have had such a wonderful support team and owe these individuals many thanks. I'd like to thank my advisors Graham Walker and Michael Hemann for allowing me to work on a project that was somewhat out of the main focus of both labs. By doing so, during my years here I was able to gain valuable skills that have helped me to become an independent researcher. To this point, being co-advised by both Graham and Mike permitted me the freedom to try and learn a variety of techniques that span many areas, from use of functional genetics techniques to understand how a protein's function may impact cancer treatment approaches, to molecular biology and biochemical assays that have allowed me to probe some basic biology questions. Most importantly, Mike and Graham's distinct work styles have given me deep insights into the value of applying diverse perspectives to problem solving. I believe the latter has been most valuable and I will take these insights with me to my next professional endeavors. I also would like to thank my thesis committee members, Jacqueline Lees and Bevin Engelward for taking the time to listen and provide thoughtful suggestions about my project. Their contributions have been incredibly useful and have helped me make great strides over the years with my project.

Additionally, I'd like to thank the many people who I have worked with in the Walker and Hemann labs- I've had a number of memorable times with you all, from Friday night hangs in the nook, to the annual lobster party at Rockport. In particular, I'd like to thank former Walker lab post-docs Kinrin Yamanaka, Sanjay D'Souza, and Asha Jacobs, for all their help, confidence in my abilities, and unwavering support during the early years of my PhD. I'd also like to thank former Hemann lab graduate students Peter Bruno, Boyang Zhao, Silvia Fenoglio, and Yadira Soto-Feliciano, for encouraging me to ask the right questions, being sounding boards for experiments, and providing me a space in lab where I could be myself. These individuals knowingly and perhaps unknowingly were incredible mentors to me and I thank them immensely for their time and patience because in many ways they have helped me become the scientist I am today.

While grad school is an illuminating experience, it is no secret that the journey can also be a trying one, so I'd also like to thank my friends, new and old for their emotional support. My time here has opened my eyes to a lot of social progress that still needs to be met in the realm of the sciences and society at large. Were it not for the support of some wonderful individuals I met during my years at MIT (Tracy, Antonn, Chris); my classmates: Dave, David, Audra, and Xinchen; minority student associations on campus, like BGSA and ACME, and the wonderful friends and support systems I made there (Jasmine, Tsehai, and Mareena, just to name a few), my time at MIT would have been incredibly challenging. To my best friends: Anita, Polina, and Reginald, your support during my time at MIT means the world to me. Your visits to Boston, late night phone calls, and the belief that I could do this helped keep me going each step of the way. Lastly, I'd like to thank my parents, Lee and Svetlana Vassel. My parents have been incredible sources of strength, encouragement, beacons of patience, and undoubtedly my biggest champions. I thank them so much for their unconditional love and raising me to become the compassionate, curious, independent-thinker that I am today.

Table of Contents

Chapter 1

Introduction

The regulation of DDR mechanisms is a critical determinant of chemotherapeutic outcome in many malignancies. Consequently, the key components of many DDR pathways have been exploited therapeutically to aid in the efficacy of cancer treatment. This is particularly important in the context of this thesis because much of this work has been centered on better elucidating how perturbing key components of the translesion synthesis (TLS) DNA damage tolerance pathway may impact chemotherapeutic efficacy. In particular, this thesis focuses on applying gene editing technologies, such as CRISPR-Cas9, and other molecular biology and biochemical techniques to allow us to uncover the role that Rev7, a multi-functional TLS DNA damage tolerance protein, plays in modulating chemotherapeutic efficacy in drug-resistant cancers. My hope is that by further characterizing the biological relevance of Rev7, my work will ultimately contribute to the development of adjuvant therapies that can aid in the efficacy of chemotherapy for cancer treatment in clinic.

I. The DNA damage response

Summary of the DNA damage response

Cells are constantly bombarded with damage from endogenous agents, such as reactive oxygen species (ROS) that can generate DNA breaks, and exogenous agents, such as ultraviolet (UV) light from sunlight that can generate thymine-thymine adducts, which can have potentially

devastating effects on genomic integrity and ultimately lead to genomic instability (Harper and Elledge, 2007). To counteract DNA damage, cells have evolved highly intricate and efficient DNA damage response mechanisms for many types of DNA damage (Harper and Elledge, 2007). These mechanisms sense the presence of DNA damage and induce signaling pathways that lead to DNA damage checkpoints cell cycle arrest and DNA repair (Harper and Elledge, 2007). In turn, if these DNA damage response processes are not executed correctly, normal cells are triggered to undergo cell death to ensure that the damage sustained is not propagated in subsequent rounds of replication. In the following section, I will provide an overview of the key components of the DNA damage response (DDR) mechanisms most relevant to Rev7's ability to regulate DNA damage induced by genotoxic agents, such as cisplatin. Specifically, this section will include a summary of relevant: (1) DNA damage repair processes, (2) DNA damage tolerance processes, (3) DNA damage signaling and checkpoint arrest (4) and finally the processes that can trigger senescence and cell death.

Mechanism of action for the DNA damaging agent Cisplatin:

To begin my examination of the DNA damage response mechanisms particularly relevant in the context of the platinum-based DNA damaging agent cisplatin, I will first provide an overview of the mechanism of action for this drug. Cisplatin was discovered by Rosenberg and colleagues at Michigan State University in 1965 where, while conducting experiments on bacteria, they observed that when bacteria were exposed to an electrical field, that was generated by platinum electrodes, long filamentous strands were formed (Rosenberg, Van Camp, Grimley, & Thompson, 1967). This observation prompted Rosenberg to search for mediators of this effect, which ended with the identification of cisplatin and demonstration of its potential as an antitumor agent. It is widely used in the clinic to treat a host of malignancies, such as: ovarian cancer, lung

cancer, and testicular cancer (where it is curative) and as such has been studied extensively(Chang, 2011; Litchfield, Levy, Huddart, Shipley, & Turnbull, 2016; Matulonis et al., 2016; Shaloam Dasari and Paul Bernard Tchounwou, 2015). Platinum-based agents like cisplatin exert their cytotoxic effects via covalently modifying the DNA (Alcindor & Beauger, 2011; Kelland, 2007).

These covalent modifications occur after the compounds are activated by the replacement of the three platinum agents' respective leaving groups via aquation. The modified compounds are then able to attack the DNA at the N7 position of purine residues, generating 1,2 and 1,3-intrastrand crosslinks, as well as interstrand crosslinks (ICL), although ICLs occur at a much lower frequency (October, Zamble, & Lippard, 1995; D. Wang & Lippard, 2005). Platinum-based agents like cisplatin generate covalent modified DNA lesions by attacking the N7 atoms of purine bases (October et al., 1995; D. Wang & Lippard, 2005).The first reactive event that takes place is the production of mono-functional DNA adducts, which after subsequent reactions, can result in a variety of DNA lesions, including: (1) DNA monoadducts, (2) intrastrand crosslinks, and (3) ICLs (October et al., 1995; D. Wang & Lippard, 2005).

I. DNA damage response mechanisms

(1) DNA damage repair processes

1.1 Single Strand DNA repair mechanisms

NER:

The nucleotide excision repair (NER) pathway (Fig.1a) is typically employed for bulkier DNA lesions and, as such, is one of the key repair mechanisms for cisplatin-induced DNA damage. The critical steps in the NER pathway are the recognition of the site of damaged DNA, followed by the binding of the NER pathway protein XPC/hHR23B to helix-distorting DNA lesions (Marteijn, Lans, Vermeulen, & Hoeijmakers, 2014). Once the XPC/hHR23B heterodimer successfully binds to the DNA lesion, another NER pathway enzyme, TFIIH, is recruited to the site of damage and can proceed in the excise and repair the damaged DNA (Marteijn et al., 2014). In the context of cisplatin-induced DNA lesions, studies have shown that two NER pathway components, excision repair cross-complementation group 1 (ERCC1) and XPF, are particularly important in the repair of these lesions (Marteijn et al., 2014). ERCC1 carries out its function by dimerizing with XPF, which is required for the excision of cisplatin-induced DNA lesions (Marteijn et al., 2014). In turn, several in vitro studies have revealed that loss of ERCC1 results in increased sensitization to cisplatin in intrinsically resistant ovarian cancer cells and a host of cisplatin resistant cancer cell lines (Martin, Hamilton, & Schilder, 2008; Matulonis et al., 2016).

1.2 DSB repair pathways

Double strand break (DSB) repair pathways have also been shown to play key roles in repairing of cisplatin-induced DNA damage. Specifically, cisplatin has been shown to induce stalled replication forks that collapse and are converted into DSB (Sears & Turchi, 2012). DSB repair is carried out in cells by two DSB repair key pathways, the homologous recombination (HR) and non-homologous end-joining (NHEJ). While these two pathways play key roles in the repair of DSBs, they differ greatly in their fidelity of the damaged DNA (Ceccaldi, Rondinelli, & D'Andrea, 2016; Chapman, Taylor, & Boulton, 2012). Given that these two pathways diverge at the early step of end resection and have different outcomes, it has been shown that end resection and other downstream factors play important roles in deciding which DSB pathway choice will be employed (Ceccaldi et al., 2016; Chapman et al., 2012). For example, it is known that the cell cycle phase and the activity of various cyclin-dependent kinases (CDKs), largely through their phosphorylation of multiple substrates, plays crucial roles in the DSB pathway choice decision (Ceccaldi et al., 2016; Chapman et al., 2012).

HR DSB Repair Pathway:

HR carries out DSB repair in an "error-free" manner (Fig.1b), using homologous copies of DNA present on sister chromatids as a template to replace the damaged that was lost due to damage (Ceccaldi et al., 2016; Chapman et al., 2012). As such, HR only occurs as a DSB repair mechanism in S and G2 phases of the cell cycle (Ceccaldi et al., 2016; Chapman et al., 2012). The critical components for DSB repair by the HR pathway are BRCA1 and BRCA2 and nucleases that carryout 5' end resection, such as endonuclease CTIP and endo/exonuclease MRE11(Ceccaldi et al., 2016; Chapman et al., 2012). In the case of cisplatin-induced damage, the HR pathway fills in the DNA gaps that are generated by the NER step of the ICL pathway.

Interestingly, HR-deficient cancers, such as those bearing loss-of-function mutations in the genes encoding BRCA1 or BRAC2 are generally more susceptible to cisplatin-induced DNA damage than HR-proficient cancers of the same type (Helleday, 2010). As such, the appearance of mutations that restore BRCA1 or BRCA2 dependent functions of HR have been shown to result in cisplatin.

NHEJ DSB Repair Pathway:

In contrast to HR, NHEJ does not use the genetic information in homologous DNA strands to repair DSB, rendering DSB repair by NHEJ being very error-prone. NHEJ carries out DSB repair (Fig.1c) throughout the cell cycle by inhibiting resection of DSB and directly ligating broken DNA ends. This form of "error-prone" DSB repair is largely accomplished by the end-binding of key NHEJ pathway components, KU70/80 heterodimer complex and DNA-dependent protein kinase catalytic subunits (DNA-PKCs) (Ceccaldi et al., 2016; Chapman et al., 2012). Specifically, it has been shown that the KU70/80 heterodimer complex binds to the DNA ends and activates DNA-PKCs subunits, which results in the recruitment of protein factors essential for carrying out NHEJ DSB repair. These factors include: the exonuclease Artemis, which is responsible for 5'->3' exonuclease activity around the DSB, DNA ligases such as DNA ligase IV, and the recruitment of DNA polymerases such as Pol mu and Pol lambda, which depending on the nature of the DSB are recruited if a lesion needs to be removed and gap filling is necessary (Ceccaldi et al., 2016; Chapman et al., 2012). Given that these are error-prone processes, the sequence damaged at the site of a DSB is altered as a result NHEJ. Interestingly, there are few studies that directly implicate the protein factors important for NHEJ in the repair of cisplatin-induced DNA lesions or cisplatin resistance (Sears & Turchi, 2012).

1.3 ICL Repair pathway

Unlike intrastrand crosslinks, which are the predominant form of DNA crosslinks introduced by platinum-based agents like cisplatin, ICLs cannot be resolved solely by repair pathways like the NER because ICLs introduce lesions that span both strands of DNA (Deans & West, 2011; Huang & Li, 2013; Muniandy, Liu, Majumdar, Liu, & Seidman, 2010). As such, while cisplatin-induced DNA damage rarely results in the generation of ICL, these lesions are incredibly toxic because ICL result in an absolute block to DNA strand separation (Deans & West, 2011; Huang & Li, 2013; Muniandy et al., 2010). Consequently, these lesions can interrupt essential DNA processes such as replication and transcription. This, in turn, means if left unrepaired, ICLs can be extremely detrimental to dividing cells and can ultimately lead to cell death (Deans & West, 2011; Huang & Li, 2013; Muniandy et al., 2010).

The key steps of the ICL repair pathway (Fig.1d) are detection of a stalled of the replication fork, removal of the lesion introduced by the crosslinking agent, translesion synthesis carried out by core components of the translesion synthesis (TLS) DNA damage tolerance pathway, gap filling carried out by NER proteins, and homologous recombination (Deans & West, 2011; Huang & Li, 2013; Muniandy et al., 2010). The initial steps of the ICL repair pathway are largely carried out by key components of the Fanconi anemia (FA) pathway (Lopez-Martinez, Liang, & Cohn, 2016; L. Wang & Gautier, 2011). In particular, the FA pathway component FANCM is recruited first to the site of the ICL, which results in the initiation step of the ICL repair pathway (Lopez-Martinez et al., 2016; L. Wang & Gautier, 2011). The initial activity of FA pathway proteins like FANCM helps to recruit and activate the rest of the FA) repair complex . When assembled into the core complex, key components of the FA pathway, i.e.

FANCD2 and FANCI, are monoubiquinated (Lopez-Martinez et al., 2016; L. Wang & Gautier, 2011). This monoubiquination step signals for phosphorylation by DNA damage signaling kinases ATM and ATR, which results in full activation of the FA core complex (Lopez-Martinez et al., 2016; L. Wang & Gautier, 2011). Once the FA core complex is fully activated, nucleases, polymerases and other repair proteins are recruited to the site of ICL and proper ICL repair can occur (Lopez-Martinez et al., 2016; L. Wang & Gautier, 2011)

(2) DNA damage tolerance processes

2.1 TLS DNA damage tolerance pathway

In contrast to the DNA damage response mechanisms highlighted so far, the translesion synthesis (TLS) pathway responds to DNA damage induced by platinum-based agents like cisplatin to promote DNA damage tolerance rather than DNA damage repair. TLS DNA damage tolerance pathway (Fig.2) is activated when replication fork stalling, caused by the induction of DNA lesions by genotoxic agents like cisplatin, results in the mono-ubiquitination of PCNA that, in turn signals, for the recruitment of specialized DNA polymerases, called TLS DNA polymerases, to the site of damage (Goodman & Woodgate, 2013; Lehmann et al., 2007; Waters et al., 2009). These TLS polymerases are uniquely poised to bypass and leave intact sites of DNA damage, for they lack exonuclease activity and have large, accommodating active sites that readily allow them to bypass a variety of bulky DNA lesions (Goodman & Woodgate, 2013; Lehmann et al., 2007; Waters et al., 2009). The specialized polymerases that make up TLS DNA polymerases primarily belong to the Y-family of DNA polymerases, which include key TLS polymerases like Rev1 (Hoege et al., 2002; Kannouche et al., 2004; Terai et al., 2010). One exception to this is the key TLS polymerase, Pol ζ, which belongs to the B-family of DNA polymerases (Hoege et al., 2002; Kannouche et al., 2004; Terai et al., 2010). When TLS

polymerases are recruited to the site of DNA damage they can replace highly processive, error-free replicative polymerases and carry out DNA synthesis in an error-free or error-prone manner (Goodman & Woodgate, 2013; Lehmann et al., 2007; Waters et al., 2009). Once this happens, DNA damage bypass is typically thought to occur in a two-step manner. Specifically, it is thought that once the DNA lesion is detected one TLS DNA polymerase inserts a nucleotide across from the DNA lesion and a separate TLS DNA polymerase, typically Pol ζ, help extends the distorted primer-end (Goodman & Woodgate, 2013; Lehmann et al., 2007; Waters et al., 2009).

As mentioned, the TLS DNA damage tolerance bypass of DNA lesions can occur in an error-free manner, in which TLS DNA polymerases like polymerase η can correctly insert nucleotides across from the encountered DNA lesion (Goodman & Woodgate, 2013; Lehmann et al., 2007; Waters et al., 2009). On the other hand, the TLS DNA damage tolerance bypass of DNA lesions can also carry out DNA lesion bypass in an error-prone manner in which TLS DNA polymerases incorrectly insert a nucleotide across from the encountered DNA lesion (Goodman & Woodgate, 2013; Lehmann et al., 2007; Waters et al., 2009). If the incorrect nucleotides that are inserted during error-prone TLS are not corrected before the next round of DNA replication, the resulting base-pair mutation is made permanent (Goodman & Woodgate, 2013; Lehmann et al., 2007; Waters et al., 2009). Consequently, the TLS DNA tolerance pathway is responsible for much of the mutagenesis occurring in eukaryotes (Goodman & Woodgate, 2013; Lehmann et al., 2007; Waters et al., 2009).

The error-prone arm of the TLS pathway potentially poses a challenge to treatment response when tumor cells are treated with genotoxic agents like cisplatin. The three translesion polymerases most relevant to platinum agent treatment are Rev1, polymerase ζ (composed of the

catalytic subunit Rev3 and non-catalytic subunits: which include, Rev7/Mad2l2, and two components of polymerase delta) and polymerase η (Goodman & Woodgate, 2013; Lee, Gregory, & Yang, 2014; Lehmann et al., 2007; Waters et al., 2009). While Rev1 is capable of carrying out TLS by lesions via its unique dCMP transferase enzymatic function that allows it to exclusively insert cytosine across from DNA lesions and abasic sites, Rev1's non-catalytic function is particularly important in the TLS pathway (Lehmann et al., 2007). The latter function has been revealed in large part by experiments carried out in a $Rev1^{-/-}$ background, that show that TLS activity is rescued by a catalytically dead Rev1 (Ross, Simpson, & Sale, 2005). Thus, Rev1's crucial TLS role lies in its ability to promote TLS activity by recruiting and scaffolding other TLS polymerases at the site of damage(Kikuchi, Hara, Shimizu, Sato, & Hashimoto, 2012). Rev1 is able to carry out this crucial role via its association with the mono-ubiquitination site of PCNA and its interaction (via the C-terminal domain of Rev1) with other TLS polymerases (Ohashi et al., 2004). The importance of Rev1-mediated regulation of the TLS pathway has also been shown in studies where Rev1 knockdown leads to sensitization to the genotoxic agents like cisplatin and cyclophosphamide (Xie, Doles, Hemann, & Walker, 2010).

Numerous studies have revealed that Rev3, the catalytic subunit of Pol ζ, and Pol eta, play important roles in bypassing cisplatin induced DNA GG adducts (Albertella, Green, Lehmann, & O'Connor, 2005; Hicks et al., 2010; Lee et al., 2014). Additionally, both polymerases are mutagenic in their bypass of cisplatin adducts (Bassett et al., 2004; Doles et al., 2010). Consequently, loss of either protein is likely to result in enhanced sensitivity to cisplatin, as well as reduction in the mutagenic capability of genotoxic agents like cisplatin. These data have led to TLS polymerases being pursued as possible adjuvant treatments with cisplatin in the clinic (Lange, Takata, & Wood, 2011; Sail et al., 2017; M.K. Zafar et al., 2018; Maroof K. Zafar &

Eoff, 2017).

Interestingly, in recent year studies have revealed that Rev7/Mad2l2, a non-catalytic subunit of Pol ζ, also appears to play an important role in helping cells deal with DNA damage induced by genotoxic agents like cisplatin. In particular, structure-function studies have revealed that Rev3-mediated TLS DNA damage tolerance of cisplatin-induced lesions is not possible without Rev3 interacting with Rev7 (Tomida et al., 2015). Other studies also suggest that Rev7 may help cells deal with DNA lesions, such as those caused by cisplatin, in a TLS-independent manner . Targeting these Rev7 functions may prove as promising ways to improve existing genotoxic chemotherapy regimens. Subsequently, many DNA damage groups have also turned their attention to trying to better understand Rev7's non-TLS functions, for targeting these Rev7 functions may prove to be a promising way to improve existing genotoxic chemotherapy regimens.

(3) DNA damage signaling and checkpoint arrest

3.1 DNA damage signaling

While the processes of DNA damage tolerance and ultimately DNA damage repair are possible outcomes when cells sustain DNA damage, they are only one facet of DNA damage response (Ciccia & Elledge, 2010; Harper & Elledge, 2007). Namely, for processes like DNA repair to occur, the cell must halt DNA replication and all others cellular processes that may enhance existing damage (Ciccia & Elledge, 2010; Harper & Elledge, 2007). For this to happen, the appropriate DNA damage signaling machinery must be activated. DNA damage-signaling pathways involve two distinct kinase signaling cascades, the ATM-CHK2 and the ATR-CHK1

pathways (Blackford & Jackson, 2017; Ciccia & Elledge, 2010; Harper & Elledge, 2007) . The ATM-CHK2 pathway is typically thought to be activated by DNA double-strand breaks and the ATR-CHK1 pathway is typically activated following the detection of single-stranded DNA and replication fork stalling (Blackford & Jackson, 2017; Ciccia & Elledge, 2010; Harper & Elledge, 2007).

ATM's kinase signaling activity (Fig.3a) is activated once the DNA damage response protein MRN detects DSB (Blackford & Jackson, 2017). Following this, ATM serves as a major DNA damage signaling protein by recruiting and phosphorylating key DNA damage response proteins like H2AX and BRCA1 (Blackford & Jackson, 2017). In contrast, for ATR- signaling pathways (Fig.3b) to be activated, two key events must happen (Blackford & Jackson, 2017). Namely, single-stranded DNA (ssDNA) breaks must form and then the protein RPA, which has a high affinity for binding ssDNA, must coat ssDNA (Blackford & Jackson, 2017). Following this, ATR is able to detect RPA-coated ssDNA and then the ATRIP (ATR- interacting protein) can be recruited to RPA-ssDNA (Blackford & Jackson, 2017). Finally, ATR signaling occurs once the ATR-ATRIP complex co-localizes with the Rad9-Rad1-Hus1 (9-1-1) complex (Blackford & Jackson, 2017). Similar to ATM, once ATR is activated, it is able to phosphorylate a host of downstream DNA damage signaling effector proteins like BRCA1.

3.2 DNA damage checkpoints

In addition to playing crucial roles in activating DNA damage response proteins, the ATM and ATR DNA signaling pathways also help facilitate DNA damage checkpoint activation (Abraham, 2001; Zhou & Elledge, 2000). Specifically, once DNA damage is sensed, the ATM and ATR signaling pathways can phosphorylate downstream effector proteins that induce cell

cycle delays (Abraham, 2001; Zhou & Elledge, 2000). These cell cycle arrest checkpoints typically occur at the G1/S, S, and G2/M transitions. Halting the cell cycle at these checkpoints helps to further ensure that damaged DNA is not carried over into subsequent stages in the cell cycle.

In the case of G1 arrest via the ATM-signaling pathway, ATM helps to activate DNA damage checkpoint arrest by phosphorylating the checkpoint kinase Chk2 and the transcription factor p53 (Abraham, 2001; Zhou & Elledge, 2000). Specifically, following ATM phosphorylation, Chk2 phosphorylates of Cdc25A and p53 (Abraham, 2001; Zhou & Elledge, 2000). The latter can lead to the upregulation of CDK inhibitor p21 and degradation of Cdc25A, ultimately causing G1 arrest (Abraham, 2001; Zhou & Elledge, 2000). There is also evidence that ATR phosphorylation of the checkpoint kinase CHK1 can also lead to G1 arrest via phosphorylation of p53 (Abraham, 2001; Zhou & Elledge, 2000).

S phase arrest occurs via an ATM-dependent pathway when a DSB break is detected in S-phase (Abraham, 2001; Zhou & Elledge, 2000). Specifically, the S-phase checkpoint occurs when ATM phosphorylation of CHK2 helps to signal for proteosome-mediated degradation of Cdc25A, and, in turn, inhibition of DNA synthesis (Abraham, 2001; Zhou & Elledge, 2000). In contrast, G2/M arrest can be activated via ATM or ATR dependent DNA damage signaling (Abraham, 2001; Zhou & Elledge, 2000). G2/M arrest occurs via an ATM-dependent manner when DNA damage is detected G2 (Abraham, 2001; Zhou & Elledge, 2000). In this case, ATM activates Chk2, which ultimately leads to phosphorylation and inhibition of the Cdk1-activating Cdc25C phosphatase. In contrast, G2/M arrest typically occurs via an ATR-dependent manner when cells incur DNA damage while going through S phase (Abraham, 2001; Zhou & Elledge, 2000).Once damage is detected, ATR-dependent G2/M arrest takes place when ATR activates

Chk1, which results in the phosphorylation of CDC25C and the subsequent inactivation of the mitotic cyclin B·cdc2 complex (Abraham, 2001; Zhou & Elledge, 2000). Thus, for the DNA damage response to occur most effectively, it is crucial that protein factors that regulate the DNA damage checkpoint activation are functioning correctly at the time that damage occurs.

(4) DNA damage induced apoptosis and senescence:

While the typical outcome of DNA damage response is the repair of DNA lesions, if cells sustain too much damage or the damage is irreparable cells undergo apoptosis (programmed cell death) or senescence (permanent cell arrest) (Elmore, 2007). The following section will provide a brief overview of DNA damage induced apoptosis and senescence.

4.1 Apoptosis

For DNA damage induced apoptosis (Fig. 4a) to occur, p53 and its negative regulatory protein MDM2 must be phosphorylated by key components of the DNA damage response (DDR) pathway (i.e. ATM, ATR, and CHK2) to inhibit p53's interaction with MDM2 (Elmore, 2007). Once p53 is stabilized and activated, it is able to transcriptionally activate numerous pro-apoptotic target genes of the mitochondrial cell death pathway such as BAX, PUMA, and NOXA (Elmore, 2007). It has also been shown that p53 plays a crucial role in signaling for DNA damage induced apoptosis by represses the expression of anti-apoptotic proteins like BCL-2 (Elmore, 2007). In addition to its transcription regulatory roles, p53 can modulate death via transcription-independent mechanisms (Elmore, 2007). For example, it has been shown that p53 can promote apoptosis in a transcription-independent manner by functioning similarly to a BH3-only pro-apoptotic proteins (Elmore, 2007). It has also been shown that, when in the cytosol or in

the mitochondria, p53 can promote apoptosis by directly activating and inducing oligomerization of the pro-apoptotic protein BAX (Elmore, 2007). Thus, correct p53 activity is crucial in regulating in how cells respond to genotoxic therapies, and aberrant p53 function can lead to the dysregulation of DNA damage induced apoptosis and promote tumorigenesis (Ciccia & Elledge, 2010; Harper & Elledge, 2007; Ouyang et al., 2012; Wong, 2011).

4.2 Senescence

Senescence (Fig.4b) is an irreversible cell-cycle arrest induced by DDR signaling and classically involves the activation of p53 dependent pathways (D'Adda Di Fagagna, 2008). While cellular senescence was originally believed to be caused solely by telomere shortening, numerous studies have revealed that there are a number of inducers of senescence, which include the activation of DNA damage response pathways by genotoxic agents (D'Adda Di Fagagna, 2008). Indeed, the senescence phenotype induced by genotoxic agents may prove to be a desired treatment outcome in certain cancers due to its resulting anti-proliferative effects (Acosta & Gil, 2012; Collado, Blasco, & Serrano, 2007; D'Adda Di Fagagna, 2008). However, senescence can also promote tumorigenesis in a non-cell autonomous fashion due to the senescence associated secretory phenotype (SASP) (Acosta & Gil, 2012; Collado et al., 2007; D'Adda Di Fagagna, 2008). Specifically, via SASP, senescence can promote tumor growth due the secretion of various cytokines and chemokines by senescent cells, which can induce dedifferentiation and consequently increased cell division and even metastasis in neighboring cells (Acosta & Gil, 2012; Collado et al., 2007; D'Adda Di Fagagna, 2008). In turn, the induction of senescence is a double-edged sword in the context of cancer treatment and tumor development (Acosta & Gil, 2012; Collado et al., 2007; D'Adda Di Fagagna, 2008).

II. Genomic Instability and Cancer

Genomic instability is a major driving force of tumorigenesis (Abbas, Keaton, & Dutta, 2013; Negrini, Gorgoulis, & Halazonetis, 2010). This occurs because failure to correctly duplicate the genome can result in an abnormally high-frequency of secondary chromosome segregation errors that induce genome alterations in the daughter cells (Abbas et al., 2013; Negrini et al., 2010). In particular, these detrimental genomic alterations include amplifications, deletions and rearrangements of chromosome segments and gains or losses of entire chromosomes. Consequently, genetic instability may promote tumorigenic properties in cells via the overexpression or mutation of genes that promote cell growth or survival (Abbas et al., 2013; Negrini et al., 2010).

Genomic instability can occur due to the loss of DNA repair genes, which can also result in oncogenic cellular transformation (Abbas et al., 2013; Negrini et al., 2010; Tubbs & Nussenzweig, 2017). An elevated mutation load has been shown to be associated with defective DNA repair and other DNA damage response proteins (Abbas et al., 2013; Negrini et al., 2010; Tubbs & Nussenzweig, 2017). Furthermore, genomic instability that promotes the acquisition of genetic alterations in DNA damage repair or DNA damage response genes may result chemotherapy resistance in a host of cancers (Abbas et al., 2013; Negrini et al., 2010; Tubbs & Nussenzweig, 2017).

III. Cancer treatment: Modes of chemotherapeutic action and resistance

DNA-damaging agents have a long history of use in cancer chemotherapy. The following section will provide an overview of the modes of action and chemoresistance for commonly used genotoxic chemotherapies. Additionally, due to the crucial role that cisplatin treatment plays in cancer treatment in clinic and in work examined in this thesis, this section will also briefly focus on common modes cisplatin resistance.

Chemoresistance can broadly be classified into two groups, intrinsic resistance and acquired resistance. Specifically, some cancers exhibit an innate resistance and fail to respond to initial treatment (Zheng, 2017). In contrast, acquired resistance is thought to arise from a combination of selection of pre-existing genetic alterations within the tumor cell population and/or from the acquisition of new alterations under the selective pressure imposed by chemotherapy (Zheng, 2017).

Genotoxic Agents:

Historically, cancer treatment regimens have relied on the use of chemotherapeutic agents that target highly proliferative cancer cells via inducing DNA damage. In turn, these DNA damaging chemotherapies initiate DNA damage cell cycle checkpoints that can lead to cell cycle arrest and/or cell death . DNA damaging chemotherapies are typically characterized based on the type of DNA damage induced and their mechanism of action. The four main groups of DNA damaging chemotherapies that will be discussed in this section are: (1) alkylating agents, (2) anti-metabolites, (3) topoisomerase poisons, and (4) platinum agents.

1. Alkylating agents mechanism of action

DNA-damaging alkylating agents are chemotherapeutics that covalently transfer alkyl-groups onto the DNA bases and consist of several chemical groups, which include nitrogen mustards (i.e. cyclophosphamide) and imidazotetrazines (i.e. temozolomide). The mechanism of action for alkylating agents can vary depending on their functional group (Fig.5a,b). For example, nitrogen mustards are bifunctional alkylating agents that typically damage DNA by forming guanine-guanine and guanine-adenine intrastrand or interstrand crosslinks (Fu, Calvo, & Samson, 2012). Thus, the damage often introduced by nitrogen mustards is typically repaired by the NER pathway (Fu et al., 2012). In contrast, imidazotetrazines are monofunctional alkylating agents that typically methylate DNA at the N7 or O6 positions of guanine residues and in turn introduce mono-functional groups to DNA, which often results in attempted repair by the MMR pathway (Fu et al., 2012). Further, the DNA lesions induced by alkylating agents typically result in a block of the replication machinery, which if not repaired can ultimately lead to DNA strand breaks (Fu et al., 2012).

2. Anti-metabolites mechanism of action

Antimetabolites used in chemotherapy regimens typically mimic the chemical structure of nucleotide metabolites. Introduction of these agents often results in a block of nucleotide metabolism or the incorporation of these nucleotide mimics into nucleic acids such as DNA and RNA (Longley et al., 2003). Consequently, cells treated with anti-metabolites are often depleted of their deoxynucleotide triphosphates (dNTPs) pools. This is the case with cells treated with the chemotherapeutic agent 5-fluorouracil (5-FU) (Fig.6), which is an anti-metabolite that can replace uracil or thymidine (Longley et al., 2003). Additionally, the incorporation of anti-metabolites, such as 5-FU, into DNA or RNA during the S phase of the cell cycle prevents

correct base pairing, which often results in replication fork stalling and strand breaks (Longley et al., 2003). In turn, the resulting stalled/collapsed replication forks often result in DSBs that are repaired by the HR pathway (Longley et al., 2003).

3. Topoisomerase poisons mechanism of action

Topoisomerase poisons are a unique class of genotoxic agents that function by targeting and trapping the DNA- topoisomerase enzyme intermediate as a complex (Pommier, 2013). Topoisomerases consist of two classes of enzymes, topoisomerase I and II, which are responsible for releasing the torsional strain of the DNA double helix. Topoisomerase I (Topo I) functions by creating a transient break in the complementary DNA strand, which allows for the passage of a single strand of DNA through the enzyme to unwind supercoiled DNA. In contrast, topoisomerase II (Topo II) functions by making a cut in both strands of DNA to allow the passage of an intact helix to unwind supercoiled DNA (Pommier, 2013). Topo I poisons, including agents like campthothecin, function by binding the DNA-topoisomerase complex to inhibit strand re-ligation (Pommier, 2013). In contrast, Topo II poisons, which include anthracylines like doxorubicin, carry out their function by directly binding and intercalating into DNA, which in turn interferes with Topo II activity and can ultimately induce apoptosis (Pommier, 2013). Subsequently, due to their respective mechanism of action topoisomerase poisons ultimately inhibit replication fork progression, which if not resolved can lead to toxic DSBs (Pommier, 2013). Repair of the stalled/collapsed replication forks and resulting DSBs often require repair by the HR pathway (Pommier, 2013).

4. Cisplatin modes of resistance

Cisplatin is a platinum-based genotoxic agent that forms covalent bonds between the N7

position of the purine bases and functions similar to many alkylating agents making either mono-functional adducts or intra and interstrand and DNA-protein crosslinks (October et al., 1995; D. Wang & Lippard, 2005). If not accurately repaired, the various DNA lesions induced by cisplatin can block the replication machinery that can collapse and result in lethal DSB.

While cisplatin is frequently used with success as a front-line chemotherapy to treat a variety of disseminated malignancies, the emergence of cisplatin resistance is major limitation to its long-term success in the clinic (Martin et al., 2008; Shaloam Dasari and Paul Bernard Tchounwou, 2015; Siddik, 2003). The issue of cisplatin resistance is particularly challenging because cisplatin resistance is often multifactorial. As such, to establish a better understanding of when cisplatin treatment might be optimal, it is important to understand the different mechanisms that can lead to resistance to cisplatin treatment.

When exploring mechanisms by which cancer cells escape the genotoxic activity of platinum DNA-damaging agents like, cisplatin, it is helpful to think about the modes of resistance in three broad categories, which include: (1) changes in intracellular accumulation or export of cisplatin, (2) alterations in apoptotic response to cisplatin; (3) aberrant DNA damage repair pathway and/ or DNA damage tolerance pathway activity to cisplatin.

4.1 Changes in export or intracellular accumulation of cisplatin

Studies investigating common mechanisms of chemotherapeutic resistance reveal that many cancers treated with genotoxic agents acquire multidrug resistance (MDR). MDR is a phenomenon where cancer drugs undergo increased efflux via relatively nonselective members of the ATP- binding cassette (ABC) family of ATPases like the P-glycoprotein (Luqmani, 2008). For example, MDR has been observed in some cisplatin-resistant cell lines, such as in drug-

resistant ovarian cancer cells, which display high expression of ABC drug transporters and increased efflux of cisplatin (Luqmani, 2008). Interestingly, cisplatin resistance has also been observed when nucleophilic species, such as glutathione (GSH) and other cysteine-rich proteins, act as cytoplasmic scavengers and bind to cisplatin (Luqmani, 2008). For example, several studies have revealed that cancer cells that exhibit elevated levels of GSH display cisplatin resistance due to increased GSH-cisplatin conjugation, which helps to facilitate cisplatin extrusion (Luqmani, 2008).

Alterations in cisplatin uptake have also been shown to play a role in the emergence of cisplatin resistance in drug resistant cancer cell lines. For example, copper transporters have been shown to play a role in the emergence of cisplatin resistance. In particular, the latter has been observed in drug-resistant cancers that down-regulate the expression of copper transporters such as copper transporter 1 (Ctr1) (Luqmani, 2008).

4.2 Alterations in apoptotic response to cisplatin

While data from various studies indicate the changes in cisplatin uptake and export can play a role in the emergence of cisplatin resistance, a more commonly observed cause for cisplatin resistance is cellular alterations in the apoptotic response. Indeed, considerable research focused on better understanding how changes the latter can lead to cisplatin resistance. Cisplatin treatment results in the introduction of a variety of DNA-adducts that can trigger DNA damage signaling response pathways, such as the apoptotic response, to help cells cope with the damage sustained. Cisplatin-induced apoptosis can occur in a number of ways, such as through the extrinsic death receptor pathway or through pro-apoptotic signaling pathways like the JNK signaling cascade (Martin et al., 2008; Shaloam Dasari and Paul Bernard Tchounwou, 2015;

Siddik, 2003). In turn, cisplatin-resistance can emerge due to decreased expression/ loss of pro-apoptotic factors or increased expression of anti-apoptotic proteins, like BCL-2 (Martin et al., 2008; Shaloam Dasari and Paul Bernard Tchounwou, 2015; Siddik, 2003). One common way that deregulation of apoptotic signaling can result in cisplatin resistance is via inactivation of p53 function or complete loss of p53 (Martin et al., 2008; Shaloam Dasari and Paul Bernard Tchounwou, 2015; Siddik, 2003). Cisplatin resistance has observed in a variety of tumor types, such as in ovarian and colorectal cancers, which lack functional p53 (Martin et al., 2008; Shaloam Dasari and Paul Bernard Tchounwou, 2015; Siddik, 2003).

4.3 Aberrant DNA damage repair pathway and/ or DNA damage tolerance pathway activity to cisplatin

In addition to triggering an apoptotic response, cisplatin treatment introduces DNA adducts that can also activate a variety of DNA damage repair and/ or DNA damage tolerance mechanisms that help cells manage cisplatin-induced DNA damage (Chen et al., 2016; Hicks et al., 2010; Martin et al., 2008; Shaloam Dasari and Paul Bernard Tchounwou, 2015; S. Sharma, Shah, Joiner, Roberts, & Canman, 2012). Thus, regulation of these repair and tolerance pathways can play an important role in the emergence of cisplatin-resistance (Chen et al., 2016; Hicks et al., 2010; Martin et al., 2008; Shaloam Dasari and Paul Bernard Tchounwou, 2015; S. Sharma et al., 2012). For example, upregulation of DNA damage repair components or increased DNA damage repair pathway activity has been associated with cisplatin resistance (Martin et al., 2008; Shaloam Dasari and Paul Bernard Tchounwou, 2015; Siddik, 2003). Indeed, cisplatin resistance has been observed in a variety of tumor types, such as non-small cell lung cancer (NSCLC), that have aberrant NER pathway function (Martin et al., 2008; Rosell et al., 2003; Shaloam Dasari and Paul Bernard Tchounwou, 2015; Siddik, 2003). Key NER pathway components, like

ERCC1, have emerged as potential biomarkers for cisplatin resistance, because tumors that lack NER components like ERCC1 appear to respond better to cisplatin treatment (Martin et al., 2008; Shaloam Dasari and Paul Bernard Tchounwou, 2015; Siddik, 2003).

Given that cisplatin treatment can also induce DNA-adducts that may generate DSB, dysregulation of DSB repair can also contribute to cisplatin resistance (Martin et al., 2008; Sears & Turchi, 2012). Moreover, tumors that have inactivated or sustained a loss-of-function in key DSB repair components, like BRCA1 or BRCA2, are typically more sensitized to cisplatin than HR-proficient tumors (Martin et al., 2008; Sears & Turchi, 2012) and cisplatin resistance is often observed in tumors that have sustained compensatory mutations in HR proteins, like BRCA1 and BRCA2, that restore the functionality of DSB repair (Martin et al., 2008; Sears & Turchi, 2012). The TLS DNA damage tolerance pathway also plays an important role in modulating cisplatin response and in turn cisplatin resistance. To this point, a number of studies reveal that tumors with functional defects in key TLS DNA damage tolerance components, like TLS polymerases Pol eta, Rev1, or Pol ζ, display increased sensitivity to cisplatin (Chen et al., 2016; Hicks et al., 2010; Martin et al., 2008; Shaloam Dasari and Paul Bernard Tchounwou, 2015; S. Sharma et al., 2012)

IV. NSCLC and Chemotherapeutic resistance

Given that a key focus of my thesis is the role that Rev7 plays in modulating chemotherapeutic efficacy in drug-resistant lung cancer, this section will provide an overview of lung cancer that is seen frequently the clinic, as well as discuss some key mechanisms of resistance for commonly used chemotherapeutic agents in lung cancer.

As the most commonly diagnosed cancer and the primary cause of cancer-related deaths among adults, lung cancer is a major health concern worldwide (Herbst, Morgensztern, & Boshoff, 2018; Molina, Yang, Cassivi, Schild, & Adjei, 2008). There are two main subtypes of lung cancer: small cell lung carcinoma (SCLC) and non-small-cell lung carcinoma (NSCLC) (Herbst et al., 2018). NSCLC represents ~90% of the lung cancer and can be further classified into three types: squamous-cell carcinoma, large-cell carcinoma, and adenocarcinoma (Herbst et al., 2018; Molina et al., 2008) As such, studying chemotherapeutic response in NSCLC is of great importance largely because the majority of lung cancer patients treated in the clinic will have some form of this disease.

Additionally, studying chemotherapeutic response in an epithelial cancer like NSCLC is of great value, for epithelial cancers not only represent the majority of human malignancies; studies also suggest these tumors are typically less response to chemotherapeutic intervention than hematopoietic malignancies (Herbst et al., 2018; Molina et al., 2008). Subsequently, better elucidation of NSCLC disease progression and its mechanisms of chemotherapeutic response may provide great insight into resistance mechanisms uniquely employed by NSCLC and other commonly occurring epithelial cancers.

Due to the genetic makeup of the disease there are a number of treatment options for patients who have NSCLC (Ahsan, 2016; Herbst et al., 2018; Molina et al., 2008). Namely, since approximately two-thirds of patients with NSCLC have an oncogenic driver mutation, such as in oncogenes like EFGR, BRAF, and KRAS, patients with NSCLC often have therapeutically targetable lesions, which expands the potential for treatment options beyond the realm of non-specific genotoxic chemotherapies to targeted chemotherapy options (Ahsan, 2016; Herbst et al., 2018; Molina et al., 2008). To this point, activating genetic mutations or fusions in genes such

as EGFR or BRAF are now targets for kinase-inhibitor therapy in NSCLC and have led to the use of tyrosine kinase inhibitors (TKI), like afatinib (EGFR specific) and dabrafenib (BRAF specific) in the clinic in the treatment of NSCLC (Ahsan, 2016; Herbst et al., 2018; Molina et al., 2008). Additionally, in the last five years personalized therapies that target the immune response to treat NSCLC have emerged in the clinic (Ahsan, 2016; Herbst et al., 2018; Molina et al., 2008). Namely, immunotherapies, such as the anti-PD1 antibody nivolumab, have been used in the clinic as a single agent or in conjunction with genotoxic chemotherapies to treat advanced or metastatic NSCLC (Ahsan, 2016; Herbst et al., 2018; Molina et al., 2008).

Nevertheless, while treatment with personalized therapies often improves the outcome in patients with NSCLC, responses to these agents are generally temporary due to the emergence of resistance to these therapies, such as in the development of secondary inactivating mutations in genes that are targeted by TKIs (Ahsan, 2016; Herbst et al., 2018; Molina et al., 2008). The latter is further confounded by the fact that 70% of patients with NSCLC present with locally advanced or metastatic disease at the time of diagnosis (Ahsan, 2016; Herbst et al., 2018; Molina et al., 2008). Such tumors are often intrinsically non-responsive to or will acquire resistance to personalized treatment (Ahsan, 2016; Herbst et al., 2018; Molina et al., 2008). These factors underscore the importance of better understanding the nature of chemotherapeutic response, particularly because genotoxic chemotherapy is remains the standard of care in the clinic for patients with metastatic or stage IV NSCLC (Ahsan, 2016; Herbst et al., 2018; Molina et al., 2008).

Currently, Platinum-based agents like cisplatin, are still the mainstay of genotoxic chemotherapy for NSCLC with no detectable genetic alterations or stage IV NSCLC/ metastatic NSCLC (Chang, 2011; Herbst et al., 2018; Molina et al., 2008). In such cases the treatment of

NSCLC, cisplatin is often used as a combination therapy with other genotoxic chemotherapies, like campthothecin or gemcitabine as frontline therapies, as well as adjuvant therapies following surgery or radiotherapy (Chang, 2011; Herbst et al., 2018; Molina et al., 2008). In Further, a better understanding the mechanisms involved in chemotherapeutic response in NSCLC is important, for treatment of NSCLC with genotoxic agents like cisplatin have been shown to consistently increase survival rates among NSCLC patients, regardless of stage of disease (Chang, 2011; Herbst et al., 2018; Molina et al., 2008). However, as in seen in the case with a host of other solid malignancies NSCLC patients often develop resistance to cisplatin.

The emergence of chemoresistance in NSCLC to genotoxic agents like cisplatin is thought to be driven by many of the cisplatin resistance mechanisms I have explored earlier in this chapter. For example, reduced uptake of cisplatin has been demonstrated in cisplatin-resistant NSCLC cells and studies have shown that there is correlation between intratumoral tissue platinum concentrations and tumor response in NSCLC (Chang, 2011; d'Amato et al., 2007; Herbst et al., 2018; Molina et al., 2008). Additionally, there is a growing body of evidence indicates that dysregulation of DNA damage repair capacity is a major factor in conferring cisplatin resistance (O'Connor, 2015). As such, in recent years, targeting of DNA repair pathways in NSCLC has emerged as a strategy for overcoming cisplatin resistance because studies have shown that key components of DNA damage repair pathways, such as NER pathway protein ERCC1, are often overexpressed in cisplatin-resistant NSCLC (Martin et al., 2008; Rosell et al., 2003). DNA damage tolerance mechanisms have also been shown to play an important role in cisplatin resistance observed in NSCLC. In particular, several studies have revealed that key components of the TLS DNA damage tolerance pathway, like Rev3, play a key

role in promoting intrinsic and acquired cisplatin resistance in NSCLC tumors (Doles et al., 2010).

Nevertheless, while the reality of drug resistance to personalized and systemic chemotherapies makes the treatment of NSCLC seem daunting, a multitude of strategies ranging from the development of more potent and selective TKIs, to the discovery of novel biomarkers may better inform what NSCLC tumors are particularly sensitive to treatment by genotoxic agents like cisplatin, provide hope for improvement of NSCLC treatment. Additionally, the continued study of NSCLC tumor evolution may also aid in the development of novel therapeutics for improved NSCLC treatment. Most importantly, since genotoxic agents like cisplatin remain the mainstay of treatment for many patients with NSCLC, there is much value in better elucidation of the cellular mechanisms that control how NSCLC responds to cisplatin, for the latter may lead to the development of adjuvant therapies that can enhance cisplatin efficacy in NSCLC tumors and other relevant solid tumor malignancies.

PART V - Introduction to Rev7

Due to the focus of this thesis, in this section I will provide a brief introduction of Rev7 biology. In particular, I will describe advances in understanding Rev7's functions, from: (1) Rev7's discovery, to (2) Rev7's gene and protein expression, to (3) more recent studies describing some of Rev7's diverse cellular functions and (4) also highlight studies that examine Rev7's role in cancer.

(1) Discovery of Rev7

Rev7 is a multi-functional TLS DNA damage tolerance protein whose existence was

unknown until 1985, when it was discovered in yeast S. cervisiae in a screen for mutants conferring a "reversionless" phenotype (Lawrence, Das, & Christensen, 1985; Torpey, Gibbs, Nelson, & Lawrence, 1994). This work was spurred by work done a decade earlier that resulted in the identification of genes associated with UV-induced mutagenesis (Lemontt et al., 1971). In the original screen for mutants conferring a "reversionless" phenotype, a set of genes, which included the TLS DNA damage tolerance proteins Rev1 and Rev3, were identified in cells with reduced UV radiation-induced mutagenesis. In turn, the identification of novel "reversionless" genes led to an intensive investigation by Lawrence's group for additional genes that may be a crucial role in this pathway, which ultimately led to the discovery of Rev7 (Lawrence et al., 1985; Torpey et al., 1994).

Rev7's discovery was further advanced years later by protein interaction studies, first conducted in in S. cerevisiae, that revealed that Rev7 interacts with Rev3 and as such is a key component of the TLS polymerase pol ζ (Gan, Wittschieben, Wittschieben, & Wood, 2008; Torpey et al., 1994; Zhu & Zhang, 2003). This study was crucial for advancing the field of Rev7 biology, for it also discovered that Rev7 interaction with Pol ζ's catalytic with Rev3 is crucial, because Rev7's interactions with Rev3 enhances the catalytic activity of polymerase ζ (Gan et al., 2008; Torpey et al., 1994; Zhu & Zhang, 2003).

(2) Rev7 gene and protein expression

Mammalian REV7 is a HORMA (Hop1,Rev7,Mad2) domain containing protein, of 211 amino acids and it has 23% sequence identity and 53% similarity to S. cerevisiae Rev7. The HORMA domain is a unique multifunctional protein–protein interaction domain found in only a handful of proteins other than Rev7, such as the meiotic protein Hop1 and the mitotic regulatory protein Mad2 (Aravind & Koonin, 1998; Muniyappa, Kshirsagar, & Ghodke, 2014). HORMA

domain containing proteins, like Rev7, regulate a diverse set of signaling pathways such as the TLS DNA damage tolerance pathway and the spindle activity checkpoint (Aravind & Koonin, 1998; Muniyappa et al., 2014). Rev7's sequence is conserved across higher eukaryotes and the gene maps to chromosome 1p36 in humans, which is a region that has been shown to be deleted in a variety of cancers (Aravind & Koonin, 1998; Muniyappa et al., 2014). Rev7 protein expression is observed across tissue types in mammalian cells and expression studies carried out in 293T cells have recently shown that Rev7 is expressed at about 5.7×10^5 molecules per cell, which other studies reveal is 4000 more than Rev3 expression (Tomida et al., 2015).

Rev7's abundant expression has been linked to Rev7's ability to interact with proteins beyond the TLS pathway, this point will be explored later in this section. Much is still to be uncovered about regulation of Rev7 expression but a few studies have emerged suggesting regulation of Rev7 expression may be complex, for it has been shown that in some contexts Rev7 expression displays cyclical behavior dependent on the cell cycle and it has also been observed that Rev7 expression may in part be regulated by Rev3 (Listovsky & Sale, 2013). Interestingly, in contrast to studies that have revealed that loss of Rev3, the catalytic subunit of Pol ζ, is embryonic lethal in mice, studies reveal that even though there is a decrease in the expected number of mice, some $Rev7^{-/-}$ mice are viable (Watanabe et al., 2013). Additionally, of the surviving mice it has been observed that loss of Rev7 expression, among other things, yields defects in cell cycle regulation and DNA damage response (Watanabe et al., 2013).

(3) Rev7 cellular functions

Historically, due to Rev7s discovery in the yeast reversion-less screen and subsequent studies, Rev7's biological relevance has largely been confined to the TLS DNA damage tolerance pathway. However, in the last decade a number of studies have emerged that reveal that Rev7 is

actually a multi-functional TLS protein. Namely, Rev7 has been shown to play regulatory roles pathways beyond the TLS DNA damage tolerance pathway, which include diverse functions like: epigenetic reprogramming, gene regulation, cell cycle regulation, and DSB break repair. In this section I will focus on Rev7's most well characterized non-TLS DNA damage tolerance roles, which are Rev7's role in the cell cycle regulation and DSB repair pathway choice regulation.

Rev7 and the cell cycle

While Rev7's is typically referred to in the literature as a TLS DNA damage tolerance protein, about two decades ago, due to its striking sequence and structural similarity to the spindle activity checkpoint (SAC) protein MAD2 (human REV7 has a 23% sequence identity and 54% structural to Mad2), Rev7 was rediscovered as a cell cycle regulator and thus is also known as Mad2l2 (Aravind & Koonin, 1998; Muniyappa et al., 2014). Importantly, due to these similarities is have led to work that has revealed that similar to Mad2, Rev7 also plays a role regulating spindle activity checkpoint functions (Bhat, Wu, Maher, McCormick, & Xiao, 2015; Listovsky & Sale, 2013).

Several cell cycle studies have revealed that cells also employ Rev7 to further ensure that the switch from activation of the anaphase-promoting complex/cyclosome (APC/C) by interacting proteins CDC20 to CDH1 during anaphase is crucial for accurate, which aids in proper mitosis (Bhat et al., 2015; Listovsky & Sale, 2013). In particular, work done in mammalian cells has revealed that Rev7 also functions as an APC/C inhibitor via interactions that Rev7 makes with the APC/C co-activator CDH1, (Bhat et al., 2015; Listovsky & Sale, 2013). These studies have uncovered that Rev7 does this by sequestering CDH1 away from the APC/C during prometaphase, which in turn aids in preventing CDH1 from from binding and prematurely

activating the APC/C (Bhat et al., 2015; Listovsky & Sale, 2013). There are also studies that suggest Rev7 may control APC/C function via interactions it makes with another APC/C co-activator CDC20 (Bhat et al., 2015; Listovsky & Sale, 2013).

In addition to being characterized as an APC/C inhibitor, Rev7 is thought to play a role in mitotic spindle organization and faithful chromosome segregation via interactions it makes with the cell cycle related proteins, like RAN and the chromosome alignment-maintaining phosphoprotein (ZNF828/CAMP) (Hara et al., 2017). Interestingly, yeast-two hybrid interaction studies also suggest that Rev7 may be tied to the cell cycle via interactions it can make with the SAC protein Mad2, which suggest that Rev7 may also function as an DNA damage signaling adapter protein linking the TLS DNA damage tolerance pathway and the SAC activity (Cahill et al., 1999).

Rev7 and DSB repair

Intriguingly, in addition to playing a key role in regulating TLS DNA damage bypass and cell cycle progression, Rev7 has also emerged as a key regulatory protein in DSB repair pathway choice. As explored earlier, DNA DSBs are highly toxic DNA lesions that, if not repaired, can lead to genomic instability and cell death. Cells employ highly efficient DSB repair mechanisms, which if dysregulated can result in a host of human disorders like cancer (Harper & Elledge, 2007; Jeggo, Pearl, & Carr, 2016; Negrini et al., 2010). The fact that unrepaired DSBs can promote tumorigenesis has resulted in a growing interest in better elucidating the mechanisms that regulate DSB repair. As mentioned in previous sections, studies characterizing repair mechanisms employed following the induction of DSB have revealed that cells employ two main DSB repair pathways: NHEJ DSB repair pathway and the HR DSB repair pathway. Both DSB

repair pathways are highly regulated and have a host of regulatory proteins that promote each pathway's respective function. In particular, one key way that cells regulate the type of DSB repair that occurs at a given time is by regulating the expression of NHEJ and HR promoting proteins in a cell cycle dependent manner (Ceccaldi et al., 2016; Chapman et al., 2012). This is to say, even though NHEJ can occur throughout the cell cycle since its function is typically promoted in the G1 phase of the cell cycle, many of the key NHEJ protein factors, such as 53BP1, are expressed at high levels in G1 (Ceccaldi et al., 2016; Chapman et al., 2012). In contrast, due to its dependence on an intact sister chromatid, HR is restricted to S/G2 and many of its key protein factors, like BRCA1, are expressed at high levels in S/G2 (Ceccaldi et al., 2016; Chapman et al., 2012). While many of the components crucial for sensing DSBs and signaling for NHEJ or HR have been identified, yet there is still much to be known about how some of the downstream processes in DSB repair, like resection DNA end protection, are regulated.

Interestingly, in recent years Rev7 has emerged an important regulator of DSB repair pathway choice due its ability to modulate DSB repair pathway choice by acting as an inhibitor of CTIP-dependent 5' end resection (Boersma et al., 2015; Xu et al., 2015). Rev7's DSB repair regulatory role was initially discovered in two genetic screens carried out in mammalian cells that revealed Rev7 deficient cells display a decrease in NHEJ DSB repair activity, immunoglobulin class-switch recombination (CSR), and an increase in 5'end resection (Boersma et al., 2015; Xu et al., 2015). Importantly, these studies have revealed that Rev7 is recruited to DSBs in an ATM-dependent manner and acts downstream of the NHEJ promoting factors 53BP1 and RIF1, yet much of how Rev7-dependent NHEJ activity occurs remains unknown (Boersma et al., 2015; Xu et al., 2015).

However, this year, two separate studies have emerged that have shed more light on some new functional interactions that play a key role in how Rev7 regulates DSB repair pathway choice (Gupta et al., 2018; Tomida et al., 2018). Namely, via quantitative mass spectrometry experiments these studies have uncovered a novel Rev7 mediated protein complex called the "shieldin" complex (Gupta et al., 2018). This complex is comprised of Rev7 and three previously uncharacterized proteins called RINN1-3 (Gupta et al., 2018). These studies discovered that the recruitment of shieldin to DSBs occurs in an ATM-dependent manner and promotes NHEJ-dependent repair, immunoglobulin CSR, and fusion of unprotected telomeres (Gupta et al., 2018). Further, this work shows that via interactions Rev7 makes with RINN1-3 it is able to act as a downstream effector of 53BP1-RIF1, which ultimately promotes the inhibition of 5' end resection (Gupta et al., 2018). Additionally, this work revealed that the expression of the shieldin complex may be an important biomarker for PARP inhibitor (PARPi) resistant cancers, for, via Rev7-dependent interactions the shieldin complex is able to sensitize BRCA1-deficient cells to PARPi (Gupta et al., 2018).

While the majority of this section has focused on the key role Rev7 plays in promoting NHEJ, there is evidence that Rev7 may actually play dual roles in DSB repair pathway choice, i.e. as seen work that suggest that Rev7 deficient HeLa cells have decrease HR DSB repair activity (Shilpy Sharma et al., 2012). Furthermore, it is clear that Rev7s role in DSB repair regulation may be complex, which highlights the fact that there is still much to be learned about the cellular processes Rev7 helps to regulate.

(4) Rev7 roles in cancer

Earlier in this thesis I explored the role that dysregulation of DNA damage response pathways and DNA damage cell cycle regulation can play in oncogenesis and modulating how

cells respond to DNA-damaging anticancer therapy. In turn, it is no surprise that a multifunctional TLS protein like Rev7 may play a role in modulating chemotherapeutic efficacy. However, to date, only a handful of studies have investigated Rev7s potential in regulating how cells respond to chemotherapy and the studies that have examined this role have focused on Rev7s role in promoting mutagenic TLS. As such, many of these studies have been carried in cancers cells that are intrinsically resistant to, or acquire resistance to, genotoxic agents like cisplatin. These studies have revealed that Rev7 loss can sensitize a variety of tumors, including ovarian cancer, nasopharyngeal, and colorectal cancer to genotoxic therapies (Cheung et al., 2006; Niimi et al., 2014). Interestingly, a couple of these studies have even revealed that Rev7 expression levels may correlate with disease progression and chemotherapeutic response, as seen in the case of radio-resistant glioma, where Rev7 mRNA was overexpressed in more aggressive glioma tumors that respond poorly to radiotherapy (Zhao J et al., 2011).

With the emergence of Rev7s new found role in DSB repair pathway choice researchers have also started to investigate how Rev7s role beyond the TLS DNA damage tolerance pathway may alter chemotherapeutic efficacy. Such studies have revealed that via its DSB break repair roles, Rev7 interacts in a synthetic viable manner in HR-deficient tumors. To date, similar to NHEJ proteins like 53BP1, Rev7s loss has been shown to result in PARPi resistance in BRCA1/2 deficient breast cancers; as well as in HR-deficient prostate tumors (Kurfurstova et al., 2016; Xu et al., 2015). This work has resulted in sequencing analysis that have uncovered that in certain tumors contexts there is aberrant loss of Rev7, which may be used as a biomarker to assess how tumors may respond to treatment with PARPi (Xu et al., 2015).

Figures

Fig.1a: Schematic of the Nucleotide excision repair (NER) pathway

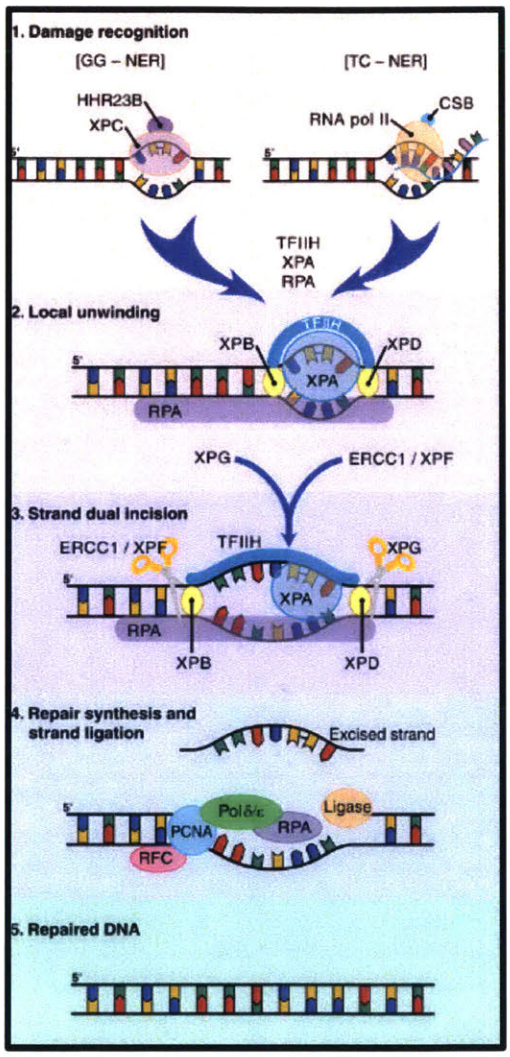

Fig. 1b: Schematic of homoglous recombination (HR) double strand break repair

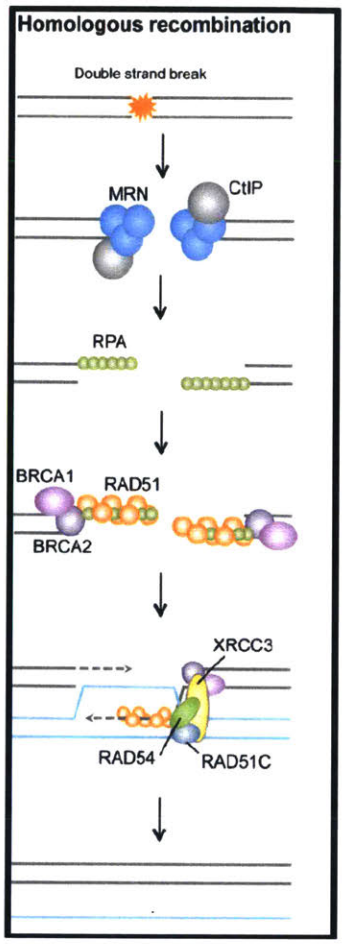

Fig 1d: Schematic of non-homologous end joining (NHEJ) double strand break repair

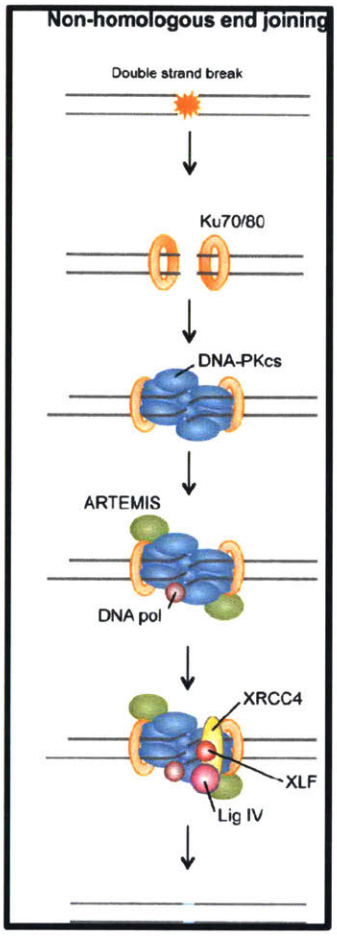

Fig 1d: Schematic of Interstrand crosslink (ICL) repair. ICL is mediated by coordinated action of Fanconi anemia (FA), translesion synthesis (TLS), and homologous recombination (HR) processes.

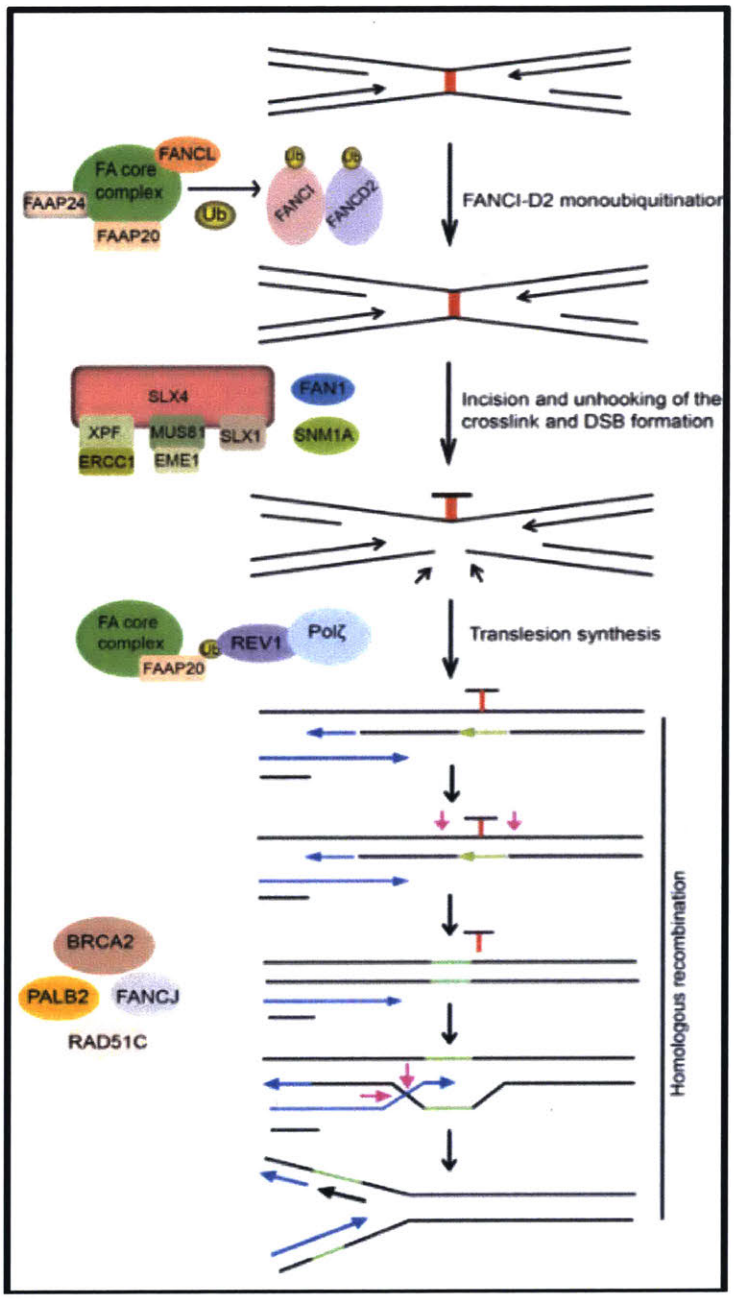

Fig 2: Schematic of the translesion synthesis (TLS) DNA damage tolerance pathway

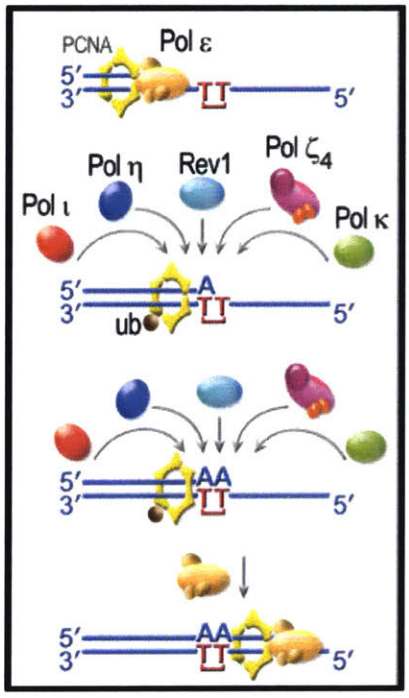

Fig 3a: Schematic of ATM-dependent DNA damage signaling response

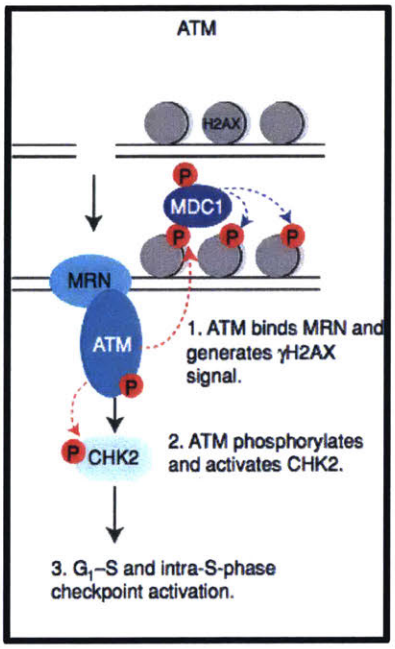

Fig 3b: Schematic of ATR-dependent DNA damage signaling response

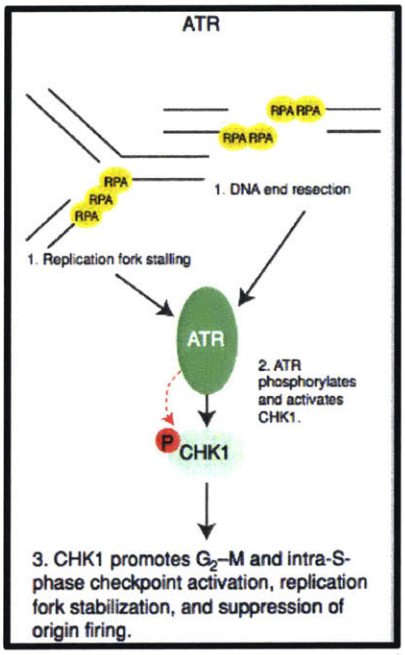

Fig 4a: Schematic of DNA damage-induced apoptotic signaling. The recruitment of ATM, ATR or DNA-PK to the site of DNA damage is a central event during DDR signaling. ATM and ATR transduce the DDR signal by phosphorylation of the checkpoint kinases CHK1/CHK2, which results in cell cycle arrest and either DNA repair or DNA damage-induced apoptotic signaling

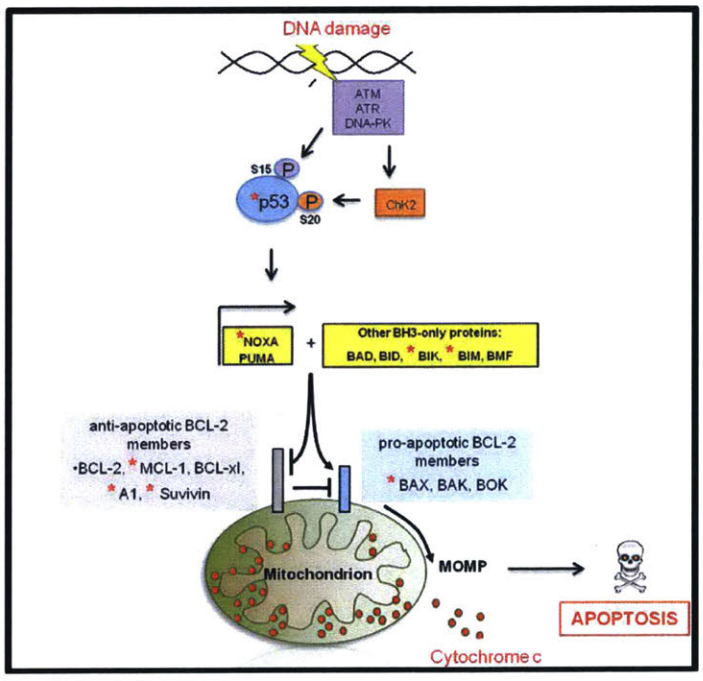

Fig 4b: Schematic of senescence stimuli, such as DNA damage, strong mitogenic signals, overexpression of oncogenes, epigenomic disruption, telomere dysfunction, and ROS engage in cell signaling cascades that cause activation of 1 or both of the pathways that regulate cell senescence

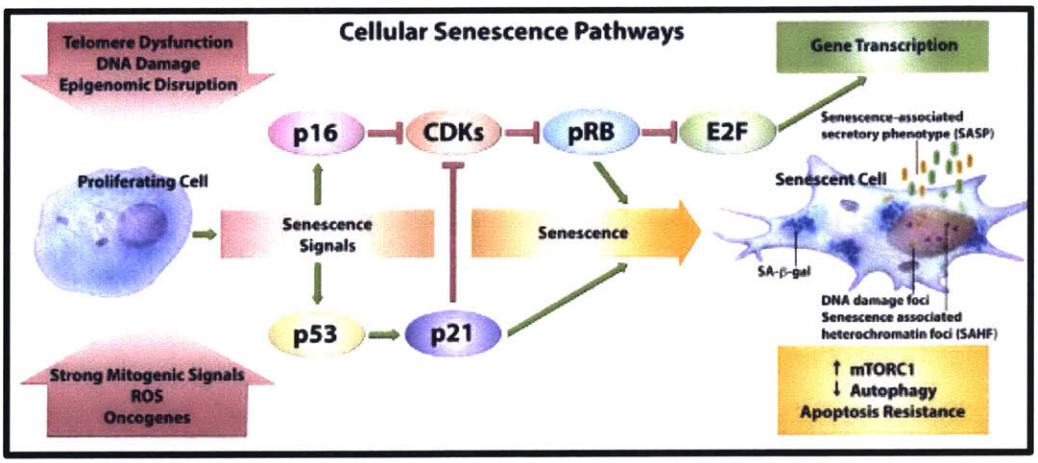

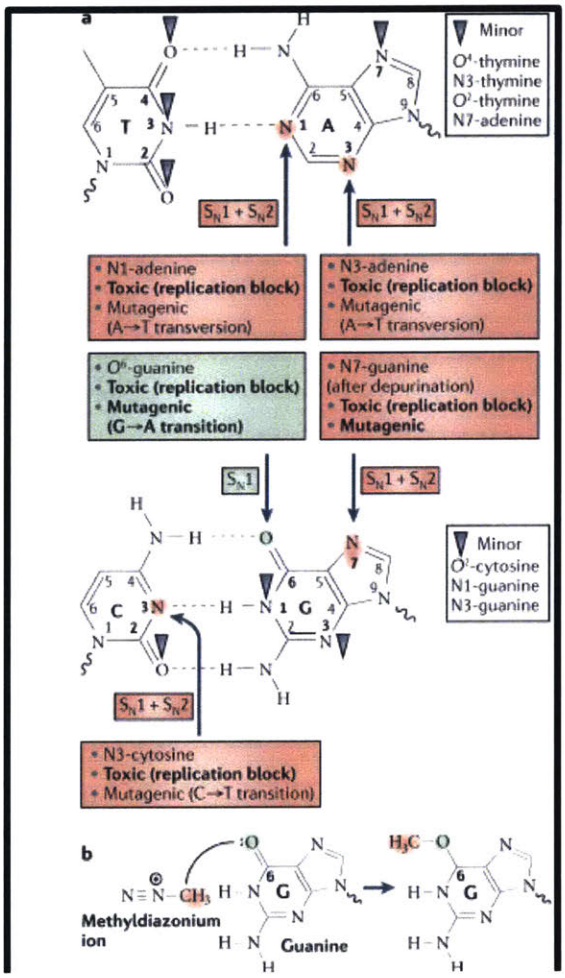

Fig 5: Sites of alkylation on DNA bases.
(5a) Alkylating agents react with the nitrogen and oxygen cancer atoms of DNA bases to form covalent alkyl lesions. The major sites of alkylation on the DNA bases and biological effects of alkylation are shown in red and green, with minor lesions denoted by grey arrow heads. (5b) An example of a DNA alkylation reaction between the methyldiazonium ion of the chemotherapeutic alkylating agent temozolomide with the O6 -position of guanine to form the O6 -methylguanine DNA lesion.

Fig 6: Schematic depicting the activation of 5-Fluorouracil. 5- Fluorouracil (5-FU) can activate p53 by more than one mechanism: incorporation of fluorouridine triphosphate (FUTP) into RNA, incorporation of fluorodeoxyuridine triphosphate (FdUTP) into DNA and inhibition of thymidylate synthase (TS) by fluorodeoxyuridine monophosphate (FdUMP) with resultant DNA damage. TS-directed cytotoxicity is abrogated by increased TS expression, whereas RNAdirected cytoxicity can be abrogated by increasing the intracellular levels of uridine

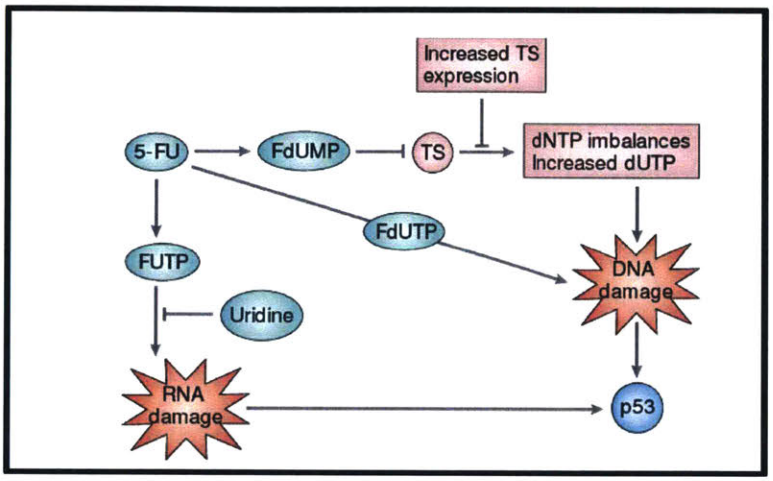

Chapter 2

Rev7 loss sensitizes drug-resistant lung tumors to chemotherapy

Faye-Marie Vassel[1], Graham C. Walker[2] and Michael T. Hemann[1,2],

[1] Department of Biology, Massachusetts Institute of Technology, Cambridge, MA 02139, USA

[2] The David H. Koch Institute for Integrative Cancer Research, Massachusetts Institute of Technology, Cambridge, MA 02139, USA

Contributions F.M.V., G.C.W., and M.T.H. conceived the idea for the research, designed experiments and interpreted data. F.M.V., G.C.W., and M.T.H. wrote the paper.

Abstract

Platinum-based chemotherapeutics, such as cisplatin, are the mainstay of treatment for non-small cell cancer (NSCLC) in the clinic. While treatment of NSCLC tumors with platinum agents can be efficacious, relapse is not uncommon. One major impediment to cisplatin efficacy in NSCLC is intrinsic drug resistance. Recent studies suggest that loss of Rev7, a multi-functional translesion synthesis (TLS) protein, can enhance cisplatin sensitivity in human cell lines such as HEK293T and multiple ovarian cancer cell lines (Lee et al., 2014; Niimi et al., 2014). However, the relevance of Rev7 role in modulating cisplatin efficacy in chemoresistant tumors remains unclear.

Here, I used a pre-clinical model of NSCLC to examine the effect of Rev7 activity on cisplatin response in this aggressive late stage lung cancer model. Using this model, I have discovered that when Rev7 is deleted, chemoresistant NSCLC lung tumors display a striking enhancement in sensitivity to cisplatin, which leads to a significant extension in overall survival of treated recipient mice. Intriguingly, my work also revealed that cisplatin-treated Rev7KO cells display an increase in DNA damage accumulation. Furthermore, my data illustrate that Rev7 inhibition may be a promising approach for enhancing cisplatin efficacy in other chemoresistant tumor models. This work provides a rationale for Rev7 inhibition as an adjuvant therapy for the treatment of chemoresistant NSCLC cancer in the clinic.

Introduction

Lung cancer is the most commonly diagnosed malignancy worldwide and is the primary cause

of cancer-related deaths among adults (Herbst et al., 2018; Molina et al., 2008). While cancer detection methods and treatment regimens have dramatically improved in the last two decades, the high incidence of lung cancer worldwide indicates that a better understanding of the mechanisms of disease progression and chemotherapeutic response is desperately needed to more effectively treat lung cancer patients. Among the two main subtypes of lung cancer, small cell lung carcinoma (SCLC) and non-small-cell lung carcinoma (NSCLC), NSCLC represents ~90% of lung cancer cases and can be further classified into three types: squamous-cell carcinoma, large-cell carcinoma, and adenocarcinoma, with adenocarcinoma being the most commonly occurring type of NSCLC (Herbst et al., 2018; Molina et al., 2008). Owing to its prevalence in the clinic, much of the work investigating chemotherapeutic efficacy in lung cancer has been carried out in NSCLC tumor models.

Due to the diverse set of driver mutations in lung cancer there are a number of treatment options for patients who have NSCLC. One such treatment option that generated great excitement when it was first introduced were tyrosine kinase inhibitors (TKI) that target a tumor's oncogenic driver mutations (Ahsan, 2016; Baudino, 2015; Herbst et al., 2018; Molina et al., 2008). One major impediment to treating NSCLC using these targeted therapies is that 70% of patients with NSCLC present with locally advanced or metastatic disease at the time of diagnosis (Ahsan, 2016; Baudino, 2015; Herbst et al., 2018; Molina et al., 2008). These advanced lung tumors are often intrinsically non-responsive to chemotherapy and frequently acquire resistance to targeted therapies (Ahsan, 2016; Baudino, 2015; Herbst et al., 2018; Molina et al., 2008). Thus, most front-line treatment regimens for lung cancer still consist of surgery, for tumors that can still be resected, and then radiotherapy and/or treatment with cytotoxic chemotherapeutic agents like cisplatin (d'Amato et al., 2007; Li et al., 2016; Molina et al., 2008).

Nevertheless, while conventional chemotherapies like cisplatin are the mainstay of genotoxic chemotherapy for NSCLC with no detectable genetic alterations and stage IV NSCLC/ metastatic NSCLC, the five-year survival rate of NSCLC is less than 15% (Chang, 2011; Herbst et al., 2018; Molina et al., 2008).

Considering the dismal survival rate of advanced stage NSCLC patients treated with frontline chemotherapies like cisplatin, there is dire need for a greater understanding of the mechanisms of cisplatin resistance in NSCLC. Importantly, the molecular mechanism(s) underlying cisplatin resistance are likely complex and as such are still largely undefined. A better understanding of cisplatin resistance mechanisms may reveal aberrations that can be targeted to improve the efficacy of cisplatin treatment in advanced NSCLC and drug-resistant lung cancer at large. Additionally, the identification of novel mechanisms of cisplatin resistance in lung cancer may aid in the development of biomarker profiles that will inform which patients may benefit from cisplatin therapy.

Like most cytotoxic agents, cisplatin functions by introducing DNA adducts, which trigger the DNA damage response (DDR) and in turn can ultimately lead to apoptosis (Basu & Krishnamurthy, 2010; October et al., 1995; Siddik, 2003). When cisplatin covalently binds to DNA, it can form intrastrand and interstrand DNA adducts between the N7 position of two purine bases (Basu & Krishnamurthy, 2010; October et al., 1995; Siddik, 2003). In particular, the predominant form of cisplatin-induced DNA damage is intrastrand 1,2 (GpG) crosslinks, which account for about 65% of the cisplatin adducts formed (Basu & Krishnamurthy, 2010; October et al., 1995; Siddik, 2003). In contrast, cisplatin interstrand adducts, though the most toxic to cells, account for less than 3% of cisplatin adducts formed (Basu & Krishnamurthy, 2010; October et al., 1995; Siddik, 2003).

Following cisplatin treatment, the DDR is activated, which induces repair mechanisms which depend on the DNA lesion. The key DNA repair mechanisms responsible for repairing cisplatin-induced DNA damage are the nucleotide excision repair (NER) and interstrand crosslink (ICL) repair pathways. Additionally, cells also employ DNA damage tolerance mechanisms, such the translesion synthesis (TLS) DNA damage tolerance pathway, to help protect cells from genomic instability and/or cell death. Therefore, to better understand the factors that regulate cisplatin response in cancer cells, it is critical to further dissect the DNA repair pathway-related and DNA damage tolerance proteins responsible for modulating a tumor cell's response to cisplatin.

The TLS DNA damage tolerance pathway in particular has been shown to play an important role in resistance to cisplatin (Doles et al., 2010; Jiang et al., 2017; Lin, 2006). However, there is still much to be known about how exactly the TLS DNA damage tolerance pathway impacts cisplatin efficacy in different tumors (Combs-cantrell et al., 2009). The TLS DNA damage tolerance pathway is a DNA damage bypass mechanism, which helps cells tolerate DNA damage until DNA lesions can be repaired. TLS DNA damage tolerance is carried out by a group of specialized DNA polymerases that have large accommodating active sites and lack proof-reading activity which allows them to synthesize DNA through DNA adducts which halt regular polymerases (Fattah et al., 2014; Goodman & Woodgate, 2013; Lehmann et al., 2007; Shcherbakova, P. V., 2006; Taggart, Fredrickson, Gadkari, & Suo, 2014; Waters et al., 2009; Maroof K. Zafar & Eoff, 2017). These specialized DNA polymerases can carry out TLS DNA damage tolerance mechanisms in an error-free manner, such as via the TLS DNA polymerase η's bypass activity over UV-induced thymine-thymine cyclobutane dimers (Yoon, Prakash, & Prakash, 2009). In contrast, specialized DNA polymerases can employ TLS DNA damage

tolerance mechanisms in an error-prone manner, such as via the TLS DNA polymerase ι's bypass activity over UV-induced thymine-thymine dimers, where incorrect nucleotide base-pairing occurs upon bypass and can result in the introduction of base-pair mutations (Tissier, McDonald, Frank, & Woodgate, 2000). The Rev1/3/7-dependent branch of the TLS DNA damage tolerance pathway can be mutagenic and so a better understanding of its mechanisms may shed light on modulators of chemoresistance in cancer cells.

Mutagenic TLS bypass is largely carried out by the activity of TLS DNA polymerases Rev1 and the multi-subunit TLS DNA polymerase Pol ζ, which is comprised of two main subunits: its catalytic subunit, Rev3, and it's structural subunit, Rev7. Studies investigating the role of TLS DNA damage tolerance in chemotherapeutic response have revealed that the core components of the mutagenic TLS pathway, Rev1 and Rev3, play a critical role in regulating cisplatin efficacy in cells due to their ability to promote mutagenic TLS activity over intrastrand DNA adducts, as well as participate in the repair of both cisplatin-induced interstrand crosslinks (Hicks et al., 2010). In particular, several studies have revealed that Rev1 or Rev3 activity can prevent cisplatin cytotoxicity and promote cisplatin resistance in various human cancer cells, such ovarian and lung cancer cells, *in vitro* (Doles et al., 2010; Jiang et al., 2017; Lin, 2006). Intriguingly, seminal studies have revealed that depleting Rev3 or Rev1, either individually or together using siRNAs drastically sensitizes tumor cells from multiple cancer types (X. et al., 2013).

In particular, one crucial study using a mouse model of NSCLC lung adenocarinoma demonstrated that Rev3 loss drastically sensitizes intrinsically drug-resistant lung tumors to cisplatin (Doles et al., 2010). This work strongly suggests that targeting Rev1 or Rev3 function may aid in the development of targeted inhibitor that can help overcome cisplatin resistance in

the clinic.

While these studies have significantly furthered our understanding of how the TLS DNA damage tolerance pathway can impact cisplatin efficacy there is still much that remains unknown. For example, the majority of these studies have investigated the importance of Rev1 and Rev3 in promoting chemoresistance. In contrast, little is known about Rev7's relevance in this context because very few studies have investigated the role that Rev7 may play in modulating cisplatin efficacy in tumor cells. However, there is some evidence that Rev7 may play an important role in this process. Work investigating Rev7's impact on chemotherapeutic response has shown that depletion of REV7 by RNAi enhances sensitivity to DNA-damaging agents in a handful of tumor cell lines, such as ovarian and nasopharyngeal cancer cells (Cheung et al., 2006; Niimi et al., 2014).

Additionally, it has recently been discovered that BRCA1-mutant cancer cells, which are defective in homologous recombination, become resistant to PARP inhibitors following inactivation of Rev7 (Barazas et al., 2018; Gupta et al., 2018; Xu et al., 2015). In turn, it is clear that a deeper dissection of Rev7s role in modulating chemotherapeutic response is needed for it is possible that depending on the tumor type or mutational background, Rev7 may regulate chemotherapeutic response in varied ways. Furthermore, because Rev7 has been shown to play a crucial role in regulating Pol ζ's TLS DNA damage tolerance activity, its ability to regulate other DDR pathways that have also been shown to modulate chemotherapeutic response in cancer cells, such as the DSB repair pathway, strongly suggests that abrogating Rev7's functions may reveal novel ways to enhance the efficacy of chemotherapeutic agents like cisplatin in drug-resistant cancer models.

Notably, Rev7 has been shown to play regulatory roles in pathways beyond the TLS DNA damage tolerance pathway, including regulating diverse functions such as: epigenetic reprogramming, gene regulation, cell cycle regulation, and DSB break repair pathway choice (Bhat et al., 2015; Leland, Chen, Zhao, Wharton, & Megan, 2018; Pirouz, Pilarski, & Kessel, 2013; Rahjouei, Pirouz, Di Virgilio, Kamin, & Kessel, 2017; Sale, 2015; Tomida et al., 2018; Xu et al., 2015).

Results:

I. Development of a Rev7-knockout (Rev7 KO) cell line

Given the diverse roles that Rev7 plays in mediating interactions that are critical for both the assembly of the Polζ-Rev1 TLS complex and in the regulation of cellular processes beyond the mutagenic TLS pathway, I became interested better elucidating the role Rev7 plays in modulating the chemotherapeutic response in drug-resistant cancers. For this study I chose to use intrinsically drug-resistant lung adenocarcinoma cells derived from a previously described KrasG12D; $p53^{-/-}$ mouse model (abbreviated KP), as tumors from this model have been shown to recapitulate the phenotype of human NSCLC (Oliver et al., 2010).

To study the effect of Rev7 loss on lung adenocarcinoma chemotherapeutic response, I employed CRISPR/Cas9 mutagenesis knockout Rev7 in a KP-derived cell line. I designed five different guide RNAs (sg1, sg2, … sg5: Fig.1a) targeting the coding sequence of mouse Rev7 and cloned these guide RNAs into the CAS9, GFP expression plasmid PX459 (Ran et al., 2013). Following cloning, KP cells were transfected with guide RNAs and twenty hours after transfection cells were single cell sorted into 96-well plates. Clones derived from all five guides were screened via immunoblotting and qPCR to identify Rev7 knockout cells. Immunoblotting

analysis of Rev7 protein levels revealed that two clones from sg2 showed a complete loss of Rev7 protein (Fig.1b). This was further confirmed by qPCR data showing that both clones also have significantly reduced transcriptional levels of Rev7 (Fig.1c). The mutation introduced by sg2 that resulted in Rev7 loss was later found to be an insertion that resulted in a frame-shift and a subsequent premature stop-codon (Fig.S1).

II. Rev7KO sensitizes $Kras^{G12D}$; $p53^{-/-}$ Lung Adenocarcinoma cells to cisplatin *in vitro*

Because Rev7 plays an important role regulating numerous processes beyond the TLS DNA damage tolerance pathway, such as the cell cycle, I sought to determine if, in the absence of DNA damage, Rev7 knockout has any deleterious effects on cell growth and cell-cycle progression. Colony formation assays did not reveal any significant differences in cell growth and cell cycle analysis did not reveal any notable cell cycle defects. These results suggested that Rev7 loss was not grossly affecting normal KP cell growth, as seen in colony formation ability (Fig. 2a-c).

Having established that there are not any major aberrations in cell growth in unstressed Rev7 KO KP cells, I sought to elucidate whether Rev7 regulates chemotherapeutic response. To investigate if Rev7 plays a role in regulating chemotherapeutic efficacy, I began by examining the effect of Rev7 knockout on drug response in KP cells *in vitro*. I performed Cell Titer-Glo (CTG) survival assays and discovered that Rev7KO cells, are drastically sensitized to cisplatin cells relative to WT cells (Fig.2d).

I also sought to investigate the impact that Rev7 loss may have on cells treated with a high-dose of cisplatin by evaluating long-term survival. These data revealed that following a high-dose of cisplatin, Rev7KO severely inhibits cell recovery, as seen in the drastic reduction of colony formation ability of Rev7KO KP cells compared to KPWT cells (Fig.2e)

To verify that the enhanced sensitivity to cisplatin observed in the Rev7 KO KP cells was due to the loss of Rev7, I generated Rev7 KO KP cells that re-expressed wild-type Rev7 (Fig.S2). I assayed these cells for cisplatin sensitivity. These data reveal that rescuing Rev7 KO KP cells with wild-type Rev7 does indeed complement the cisplatin sensitivity phenotype (Fig.2f)

III. Rev7 loss promotes cisplatin-induced DNA damage response and causes accumulation of DNA double-strand breaks after cisplatin treatment in KP cells

Having observed that Rev7 loss enhances cisplatin sensitivity, I examined the effect of Rev7 loss on DNA damage response signaling in KP cells. To do this, I examined DNA damage accumulation by assessing the phosphorylation status of ATM (pATM, Ser1981). Protein expression data reveal that loss of Rev7 results in a cisplatin-induced DNA damage response in KP cells, as seen by an increase in pATM (Fig. 3a).

Intriguingly, since recent work has also shown that loss of Rev7 is associated with alterations in double-strand break repair pathway choice and chromosomal instability, I investigated the impact the Rev7KO may have on DSB repair following cisplatin treatment. I used immunofluorescence assays to assess DSB induction by staining for γH2AX levels. These immunofluorescence assays revealed that Rev7 KO KP cells exhibit greater γH2AX staining in comparison to control cells after cisplatin treatment (Fig. 3b). Thus, these findings indicate that Rev7 loss also results in an accumulation of double-strand breaks in response to cisplatin treatment.

IV. Loss of Rev7 suppresses caspase-3 and PARP-mediated apoptosis / senescence

To investigate whether the effect of reduced cell viability in Rev7 KO KP cells was due to

apoptosis, I assessed the levels of cleaved caspase-3 and PARP proteins in the cells following cisplatin treatment. Interestingly, after cisplatin treatment, I observed suppression of cleaved caspase 3 and cleaved PARP levels in Rev7 KO KP cells (Fig. 4a,b). These data suggest that the loss of cell viability observed in Rev7 KO KP cells may be due to mechanisms besides an increase in apoptosis.

Another process that might limit cell viability following cisplatin treatment is senescence. To see if Rev7 KO KP cells had reduced viability due to an increase in senescence, I performed β-galactosidase activity staining following cisplatin treatment *in vitro*. These data indeed revealed that Rev7KO cells exhibit characteristics of DNA-damage induced senescence, including the appearance of a flattened, vacuolized cell morphology and the induction of senescence-associated β-galactosidase activity (Fig. 4c). Thus, Rev7 loss impairs the repair of cisplatin-induced DNA damage leading to DNA-damage induced senescence.

V. Rev7KO sensitizes lung adenocarcinoma transplants to cisplatin *in vivo*

Motivated by the impressive cisplatin sensitivity phenotype I observed in Rev7 deficient cells *in vitro*, I decided to further evaluate the potential of Rev7 inhibition as novel adjuvant therapy to enhance response to cisplatin by assessing the impact of Rev7KO *in vivo*. To investigate this question, I transplanted Rev7KO or KPWT into syngeneic recipient mice and used an *in vivo* imaging-based Micro CT platform to assess tumor presence 3–4 weeks after transplantation. Tumor bearing mice were then treated with 10mg/kg cisplatin. Mice were sacrificed 2 days after cisplatin treatment and cisplatin-treated tumors were examined using immunohistochemistry (IHC) to analyzed the effects of cisplatin response in *vivo*. These IHC analyses of tumors reveal that Rev7 loss suppressed tumor-cell proliferation as well as apoptosis in KP tumors, as seen by decreases in KI-67 and decreases in caspase 3 levels, respectively (Fig.

5a,b). These results recapitulate the phenotype of Rev7 loss in vitro. I also conducted IHC analyses to investigate the impact that Rev7 loss may have lead to an increase in DNA accumulation in KP tumors (not shown).

To further elucidate the impact that Rev7 loss has on cisplatin response in lung adenocarcinoma tumors, I used a microCT imaging platform to study lung tumor dynamics over the course of cisplatin therapy. Using data from these microCT imaging experiments, I constructed 2D axial and 3D isosurface images from Rev7 WT and KO tumors imaged before and 14 days following the initiation of cisplatin treatment (10 mg/kg cisplatin on day 0). In these experiments, Rev7KO tumors exhibited a strikingly enhanced response to cisplatin relative to controls. This response was apparent at the level of individual tumors (Fig. 6a,b) and the entire lung (Fig.6c). Additionally, Kaplan-Meier analysis of overall survival showed that mice harboring Rev7KO transplants survived at more than twice as long as that of the control cohort (Fig.6d). Taken together, these days suggest that Rev7 inhibition may be an effective mechanism to sensitize tumors to cisplatin and enhance its therapeutic efficacy.

Discussion:

This study provides the first evidence of the functional relevance of Rev7 in drug-resistant lung adenocarcinoma. Namely, here I have demonstrated that loss of Rev7, a key structural subunit of TLS Pol ζ, , can strikingly enhance the chemotherapeutic efficacy of cisplatin-based chemotherapy in a mouse model of NSCLC. Additionally, I have also discovered that Rev7 loss likely results in a reduction in DSB repair capacity, as seen in an increase in DNA damage accumulation. As a result, these findings strongly suggest that Rev7 is a promising adjuvant chemotherapeutic target for drug-resistant lung cancer.

The striking enhancement in cisplatin efficacy that I have shown in Rev7KO NSCLC tumors is particularly interesting because it is likely a result of Rev7's dual ability to both promote cisplatin resistance via the TLS DNA damage tolerance pathway and to regulate DSB repair pathway choice. The latter is potentially important because numerous studies have shown that both Rev1/Pol ζ-mediated TLS replicative bypass and DSB DNA damage repair are needed to help cells deal with the diverse DNA lesions that can result from cisplatin-induced DNA damage (Hicks et al., 2010; S. Sharma et al., 2012; Shilpy Sharma, Canman, & Arbor, 2017; Shilpy Sharma et al., 2012). This is particularly of value for there is precedence for inhibiting aspects of the DDR to improve the efficacy of chemotherapy, as seen in clinical successes observed in BRCA deficient tumors that were treated with PARP inhibitors (Barazas et al., 2018). Interestingly, a recent study has also revealed that Rev7 is highly expressed in NSCLC cancer and Rev7's overexpression may promote processes associated with metastasis in lung cancer (Zheng et al., 2017). These findings are particularly intriguing, for they suggest that in addition to reducing Rev7's TLS and DSB functions that may promote chemoresistance, Rev7 inhibition may prove to be beneficial because it may also help to prevent lung cancer metastasis (Zheng et al., 2017).

As seen in the development of small molecule inhibitors targeting other TLS proteins like polymerase η and Rev1 (Sail et al., 2017; M.K. Zafar et al., 2018) it is evident that there could be great value in the development of small molecule inhibitors that specifically target Rev7. Importantly, the development of small molecule inhibitors that specifically target Rev7-mediated interactions may provide a way to specifically target Rev7's TLS dependent functions, as well as its cellular functions beyond the TLS pathway, such as Rev7's DSB repair dependent capabilities, which may prove to be particularly valuable adjuvant therapeutic in different cancer

contexts.

Materials and Methods

Cell culture and chemicals:

Mouse $Kras^{G12D}$; $p53^{-/-}$ lung adenocarcinoma cells were cultured in standard DMEM/10% FBS media. Cisplatin was purchased from Calbiochem and used at the indicated concentrations (0–15 μM). For in vivo studies, cisplatin was dissolved in a 0.9% NaCl solution, protected from light, and immediately injected intraperitoneally into tumor-bearing mice. X-gal for senescent cell identification was purchased from Cell Signaling Technologies.

CRISPR/Cas9-Mediated Gene Editing:

We targeted Rev7 via SpCas9-mediated genome editing in mouse $Kras^{G12D}$; $p53^{-/-}$ lung adenocarcinoma cells. To do so, we designed an sgRNA-targeting coding sequence of the mouse Rev7 gene. The designed sgRNA strands were phosphorylated and cloned into the pSpCas9(BB)-2A-GFP plasmid (Addgene: PX458). After 24 h, GFP positive cells were placed into 96 well plates for a 3-week expansion by fluorescence assisted cell sorting (FACS). Cells were functionally assessed by qRT-PCR and Western blot for Rev7 gene and protein levels respectively. Rev7 knockout cell mutations were sequence validated by Sanger sequencing.

RT-qPCR, Immunohistochemistry, and Immunofluorescence:

RT-qPCR was performed using SYBR green on a BioRad thermal cycler. GAPDH and Rev7 primer sequences are available upon request.

For immunohistochemistry assays, mice were killed by CO2 asphyxiation and lungs were fixed overnight in 10% neutral-buffered formalin. Lung lobes were separated and embedded in

paraffin according to standard procedures. Lungs were sectioned at 4 μm and stained with H&E for tumor pathology. For detection of cleaved caspase 3 (1:500; Cell Signaling) and KI67 (1:200; Cell Signaling), tissue sections were subjected to antigen retrieval in citrate buffer, blocked in 3% H2O2 for 10 min, blocked for 1 h in 5% serum/PBS-T, and stained overnight at 4 °C. Secondary antibodies were used according to Vectastain ABC kits (Vector Laboratories).

Cells for immunofluorescence were grown and treated with cisplatin on poly-L-lysine coated coverslips, fixed with 100% methanol for 5 min at −20 °C, and stored for later use. Anti–γ-H2AX (1:1000; Cell Signaling Technologies) was used along with an Alexa secondary (568) antibody (Molecular Probes) to visualize γ-H2AX foci. Stained coverslips were imaged and analyzed using Applied Precision DeltaVision instruments and deconvolution software.

***In vitro* viability assays and FACS:**

For short-term viability assays, cells were seeded in triplicate (8×10^3 per well) in 96-well plates and treated as indicated with cisplatin. After 48-h treatment, cell viability was measured using Cell- Titer-Glo (Promega) on an Applied Biosystems microplate luminometer. Long-term viability assays were performed by initially treating 4×10^5 lung adenocarcinoma cells with 15 μM cisplatin for 24 h. Four days following treatment, cells were split 1:20 onto a fresh 10-cm plate and allowed to form colonies for ~10 d.

To visualize colonies in the colony formation assay, cells were fixed with formaldehyde for 10min, 0.5% crystal violet solution in 25% methanol for 10min. Images were processed and colonies counted using ImageJ software.

***In vivo* transplantation and MicroCT imaging:**

Lung adenocarcinoma cells (~5×10^4) were intravenously injected into the tail vein of

syngeneic C57BL6/Jx129-JAE female recipient mice and monitored weekly using a GE Healthcare microCT imaging device (45-μm resolution, 80 kV, with 450-μA current) beginning ~3 weeks following injection. Images were acquired and processed using GE eXplore software. The Massachusetts Institute of Technology Committee on Animal Care reviewed and approved all mouse experiments described in this study.

Figures

Fig. 1a: sgRNA sequences targeting mRev7 coding sequence for CRISPR-Cas9 gene editing

Guide #1	GTGCGCGAGGTCTACCCGGTGGG
Guide #2	CCTGATTCTCTATGTGCGCGAGG
Guide #3	GTTGAGGTCTTGGCGCGTGAGGG
Guide #4	CTATGTGCGCGAGGTCTACCCGG
Guide #5	GCGCAAGAAGTACAACGTGCCGG

Fig. 1b: Western blot analysis of Rev7 protein expression in Rev7KO KP cells

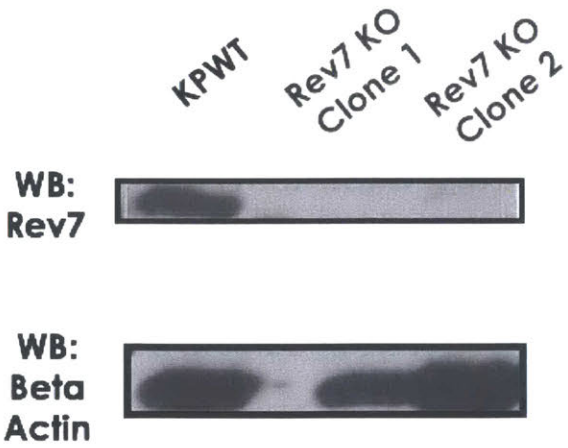

Fig. 1b: qPCR analysis of Rev7 mRNA transcript levels in Rev7KO KP cells

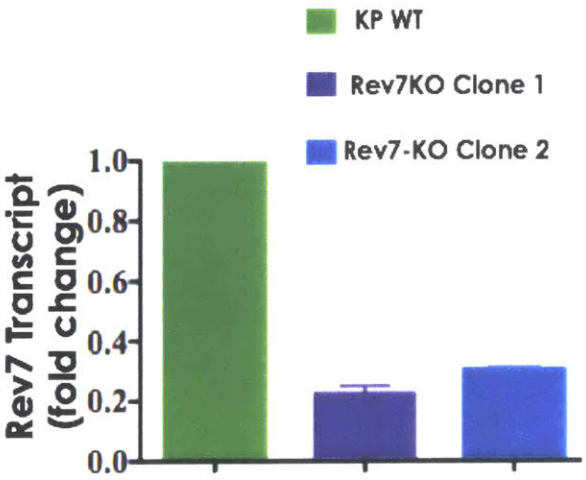

Fig. 2a: Colony formation analysis of untreated KPWT and Rev7 KO cells

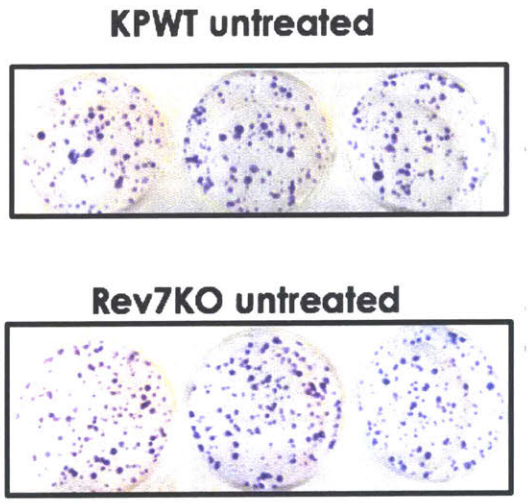

Fig. 2b: Quantification of colony forming ability of untreated KPWT and Rev7 KO cells

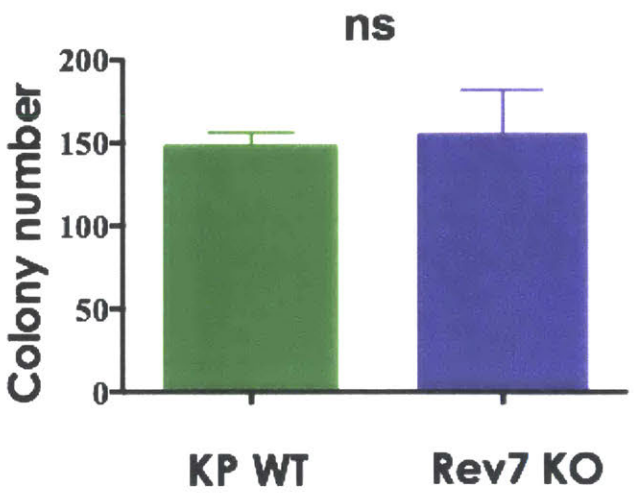

:

Fig. 2c: Cell cycle analysis of untreated KPWT and Rev7KO cells

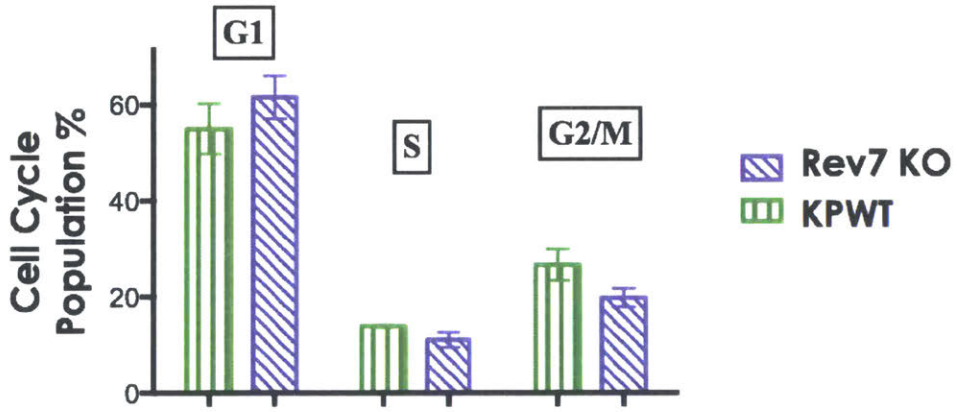

Fig. 2d: Cell viability analysis of cisplatin treated KPWT and Rev7KO cells, p-value <0.001

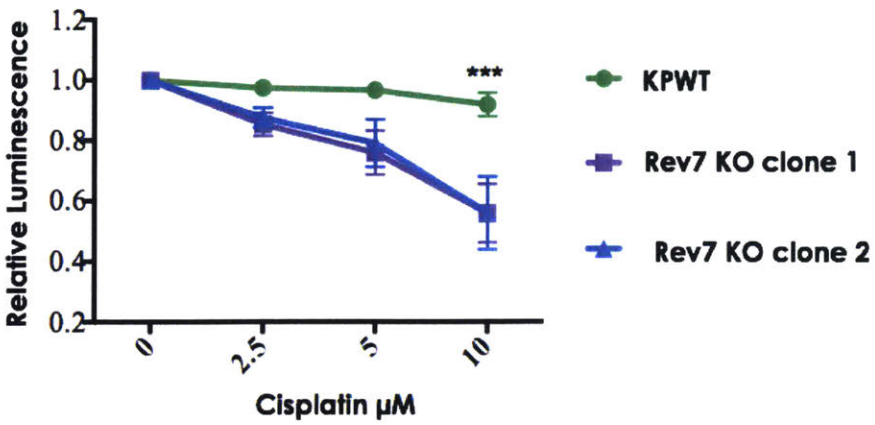

Fig. 2e: Colony formation analysis of cisplatin treated KPWT and Rev7KO cells

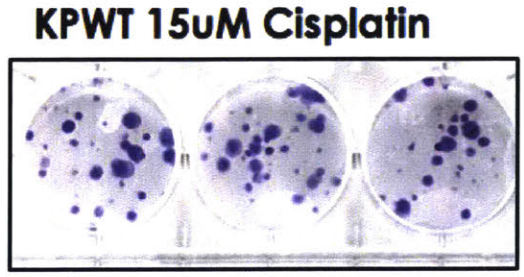

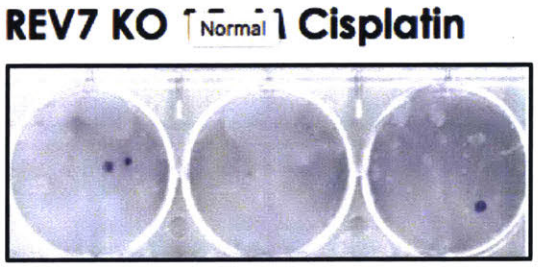

Fig. 2f: Quantification of colony formation ability of cisplatin treated KPWT and Rev7KO cells, p-value <0.001

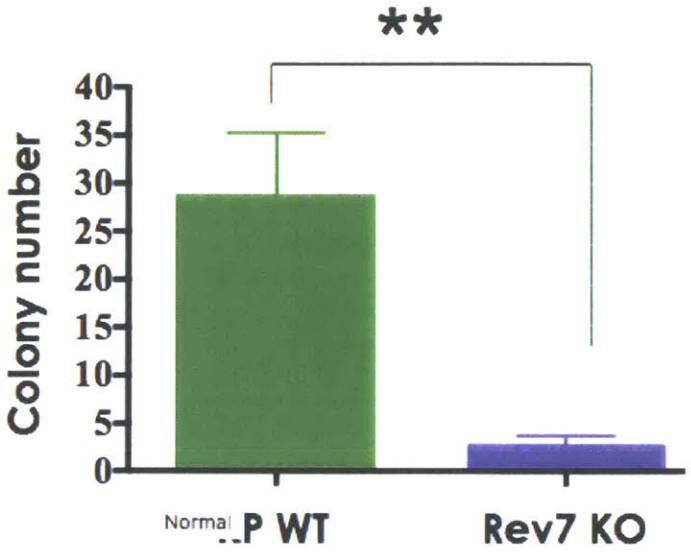

Fig. 2g: Cell titer glo cisplatin sensitivity analysis of cisplatin treated wild-type Rev7 rescue cells, p-value <0.001

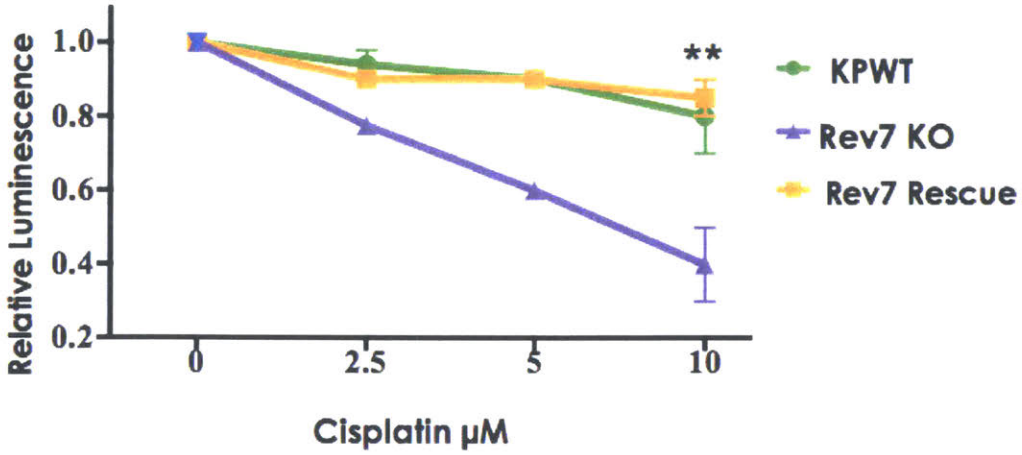

Fig. 3a: Western blot analysis of pATM induction in cisplatin treated KPWT and Rev7KO cells

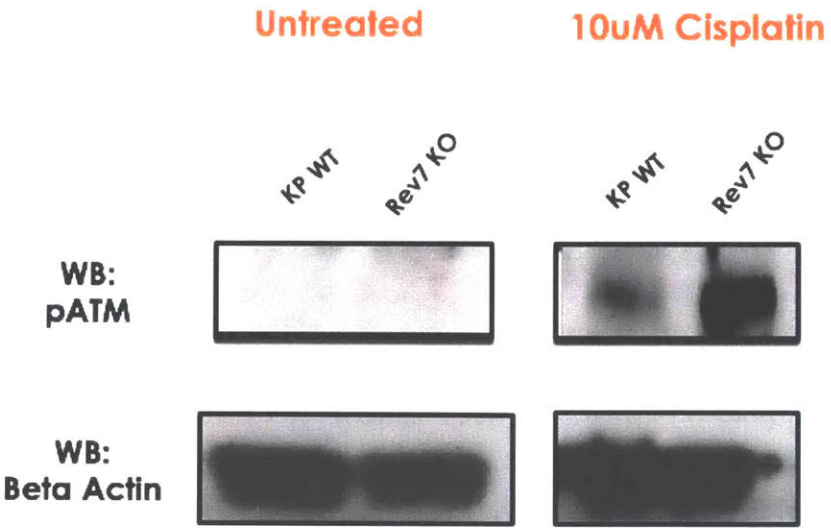

Fig. 3b: Immunofluorescence analysis of H2AX induction in cisplatin treated KPWT and Rev7KO cells

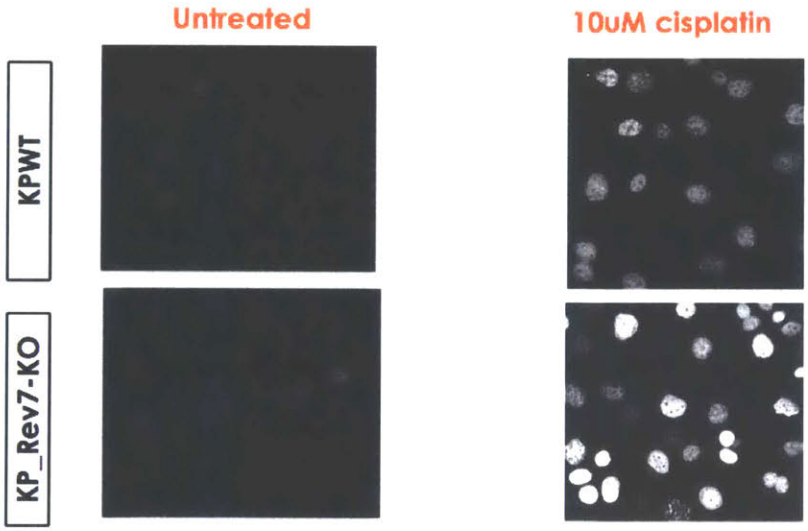

Fig. 3c: Quantification of immunofluorescence analysis of H2AX induction in cisplatin treated KPWT and Rev7KO cells, p-value <0.001

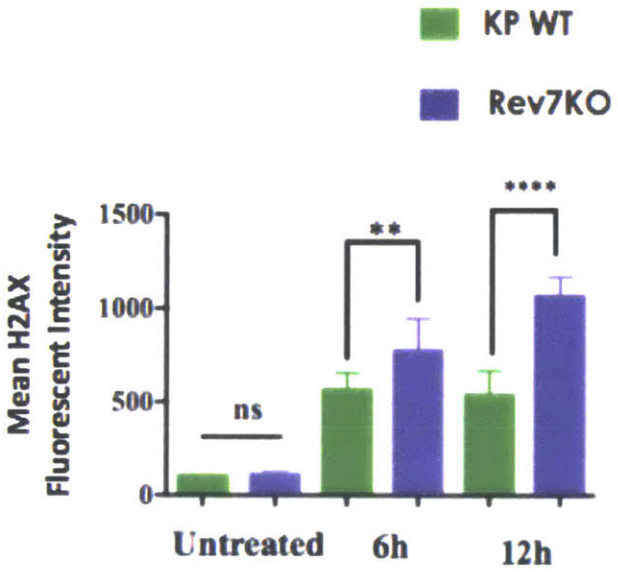

Fig. 4a: Western blot analysis of cleaved caspase 3 levels in cisplatin treated KPWT and Rev7KO cells

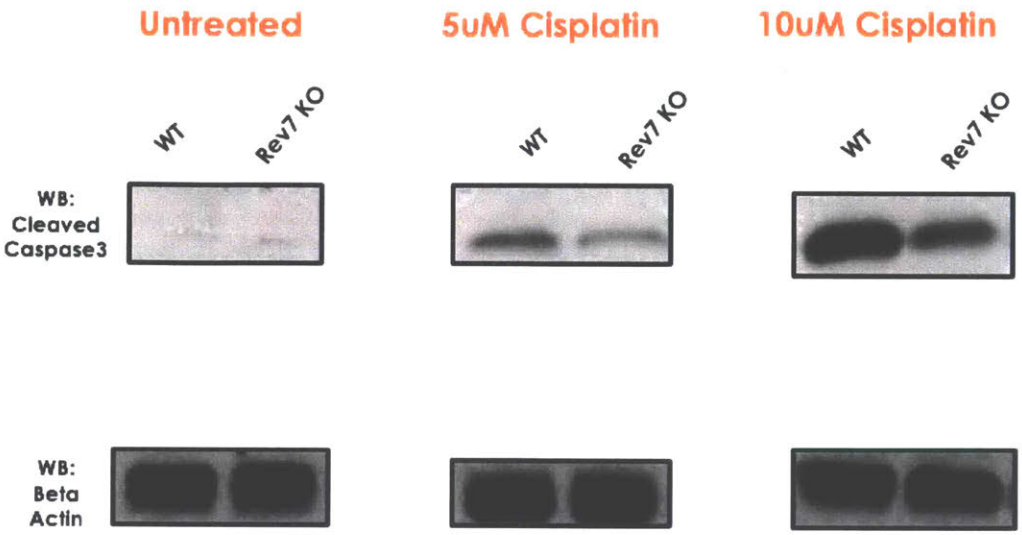

Fig. 4b: Western blot analysis of cleaved Parp levels in cisplatin treated KPWT and Rev7KO cells

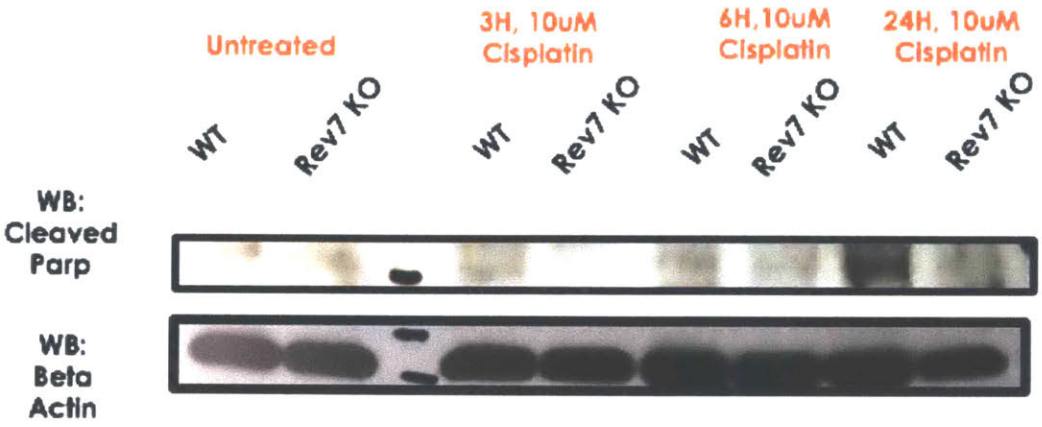

Fig. 4c: Beta-gal staining of cisplatin treated KPWT and Rev7KO cell lines

Cisplatin treated KP WT cells

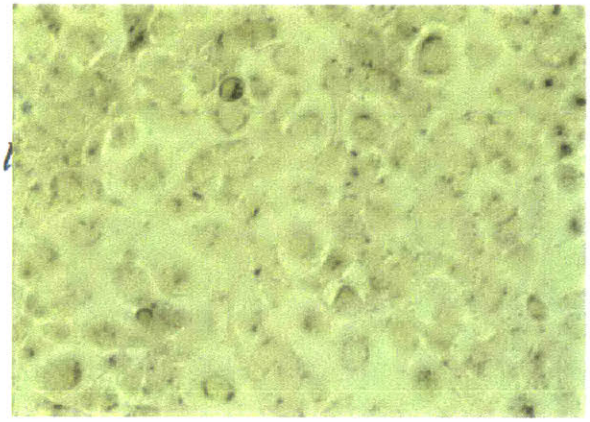

Cisplatin Treated Rev7KO cells

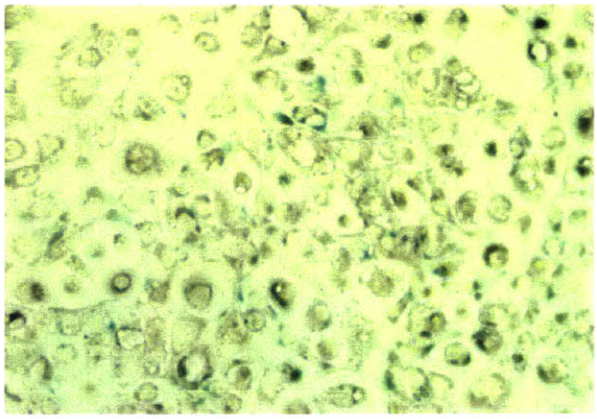

Fig. 5a: Immunohistochemistry analysis of KI-67 levels in cisplatin treated KP WT and Rev7KO tumors, 48 hours after 10mg/kg cisplatin treatment

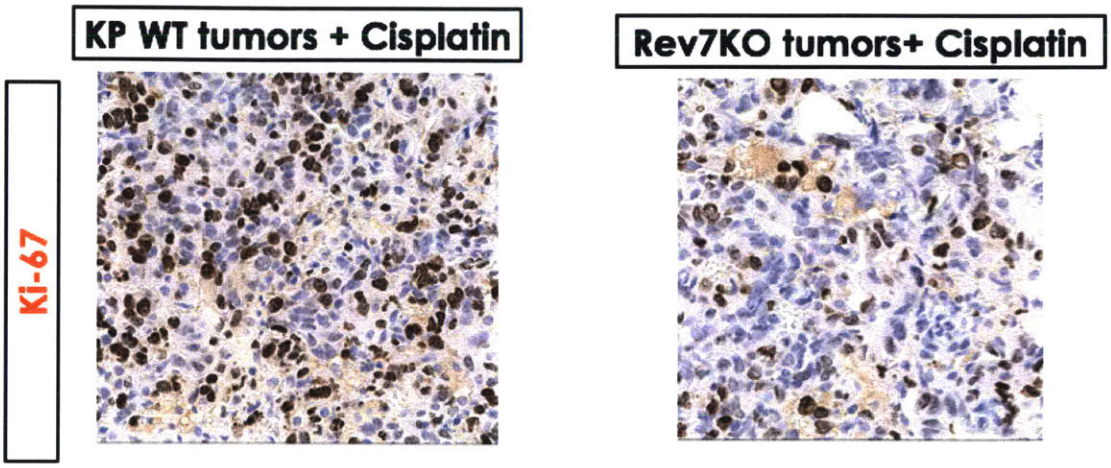

Fig. 5b: Immunohistochemistry analysis of cleaved caspase 3 levels in cisplatin treated KP WT and Rev7KO tumors, 48hours after 10mg/kg cisplatin treatment

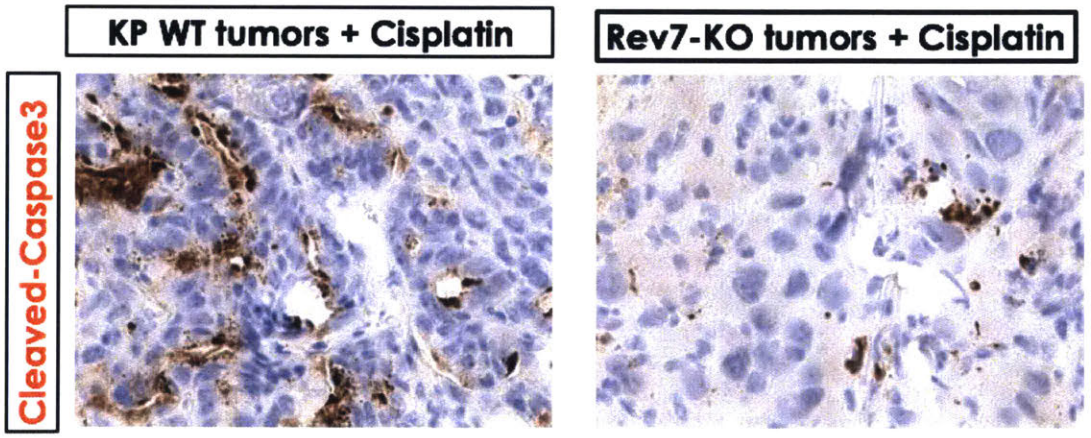

Fig. 6a: MicroCT axial images of mouse lungs transplanted with KPWT or Rev7KO cells before and 14 days after 10mg/kg cisplatin treatment

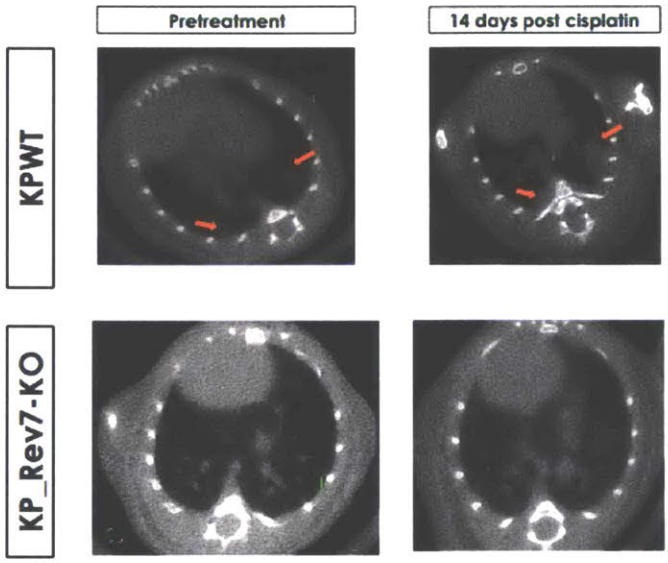

Fig. 6b: Individual tumor volume calculations for several KPWT and Rev7KO transplants before and 14 days after cisplatin treatment

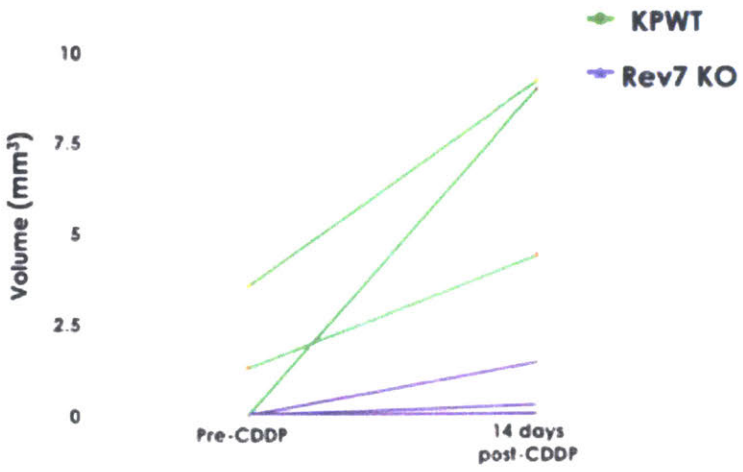

Fig. 6c: Inverse 3D isosurface projections of healthy lung volume in KPWT and Rev7KO transplanted mice before and 14 days after cisplatin treatment

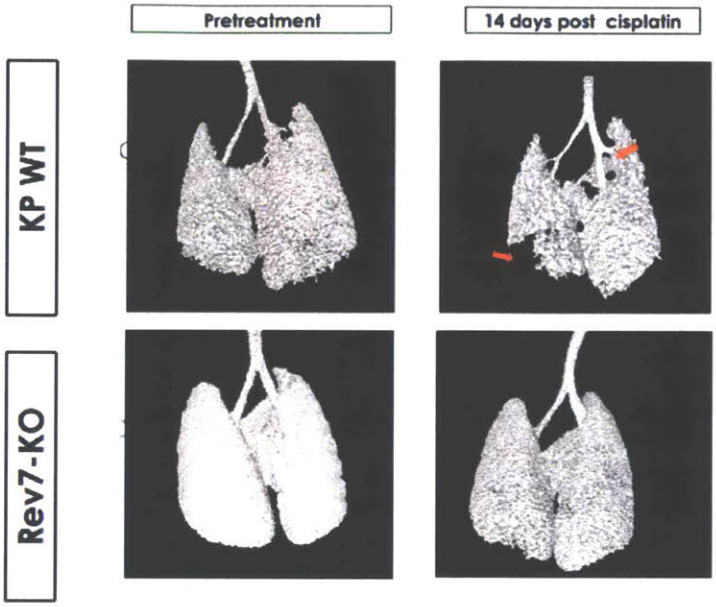

Fig. 6d: Kaplan-Meier curve comparing survival of mice bearing Rev7KO transplants versus mice bearing KPWT tumors following treatment with 10mg/kg cisplatin , p-value <0.001

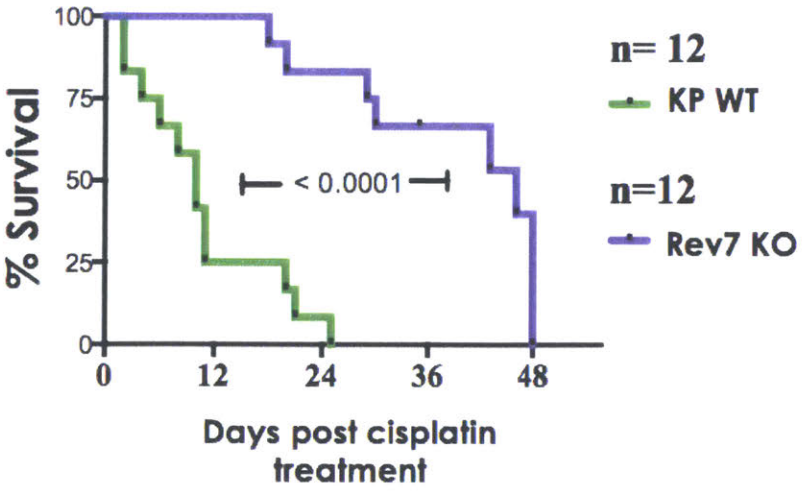

Supplemental Figures

Fig.S1: Western blot analysis of Rev7 protein expression is Rev7KO rescue cell lines

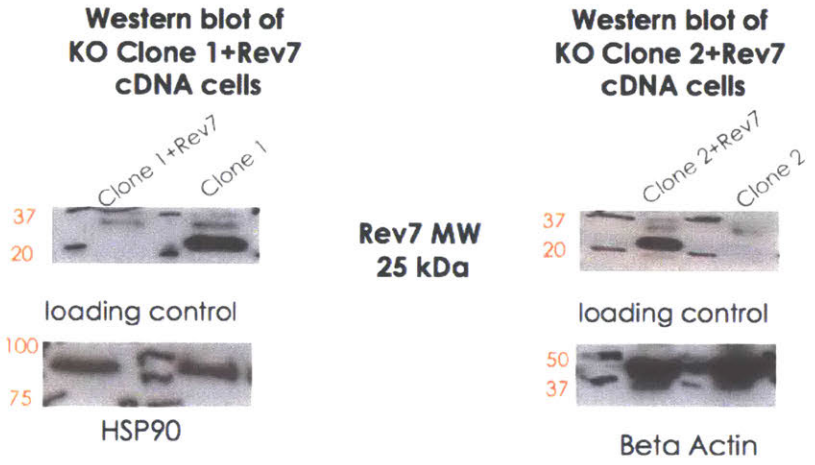

Fig.S2: qPCR analysis of p21 mRNA levels in untreated Rev7KO KP cells

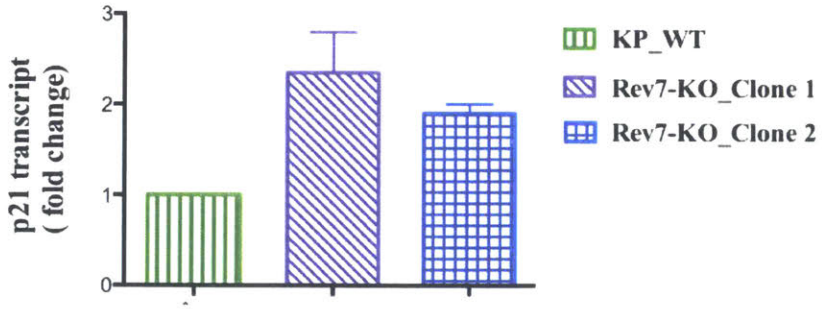

Fig.S3: Cell titer glo cisplatin sensitivity assay probing the impact co-depletion of Rev3 in Rev7KO KP cells has on cisplatin response in KP cells, p-value <0.001

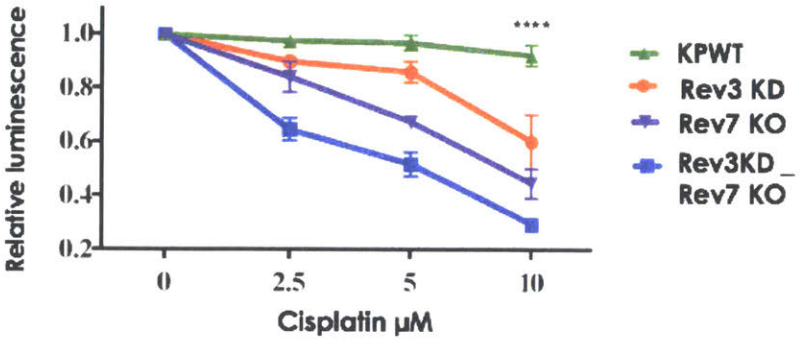

Fig.S4: Cell titer glo cisplatin sensitivity assay probing the impact mutating the Rev1 binding interface of Rev7 has on cisplatin response in KP cells

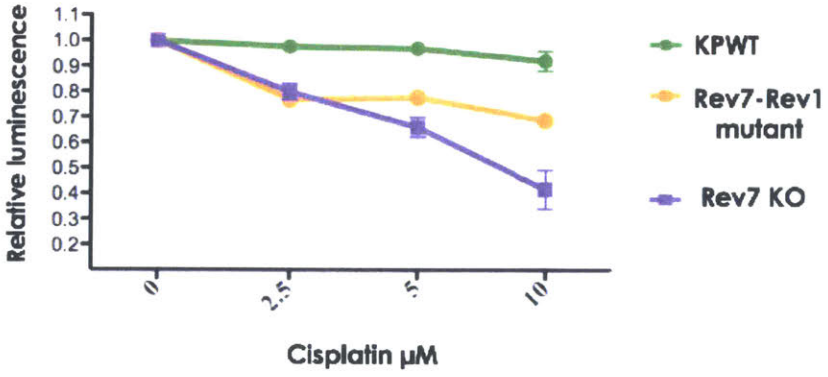

Fig.S5: Kaplan-Meier curve comparing survival of mice bearing Rev7KO transplants versus mice bearing KPWT tumors following treatment with saline vehicle

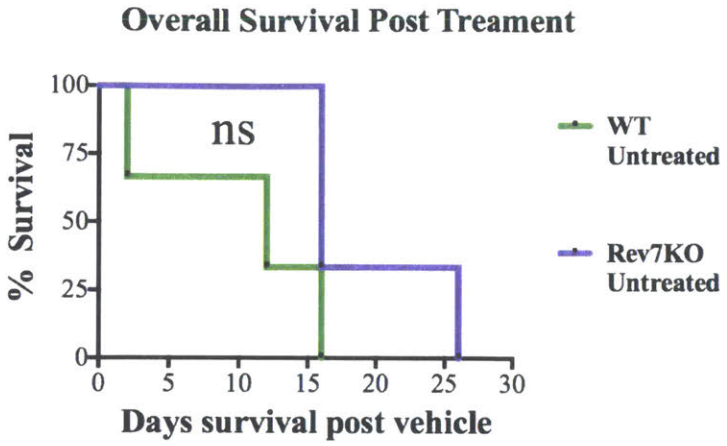

Chapter 3

Investigation of novel Rev7-mediated protein interactions using Localization Affinity Purification (LAP)-tagging and IP/Mass Spectrometry to explore Rev7's functional relevance beyond the TLS pathway

Faye-Marie Vassel[1], Iain Cheeseman[1,2], Alessandro A. Rizzo[3], Zachary Nagel[5],Dmitry M. Korzhnev[3], Michael T. Hemann[1,4], and Graham C. Walker[1]

[1]Department of Biology, Massachusetts Institute of Technology, Cambridge, MA 02139, USA

[2]Whitehead Institute for Biomedical Research Nine Cambridge Center, Suite 401 Cambridge, MA 02142, USA

[3]Department of Molecular Biology and Biophysics, University of Connecticut Health Center, Farmington, CT 06030, USA

[4]The David H. Koch Institute for Integrative Cancer Research, Massachusetts Institute of Technology, Cambridge, MA 02139, USA

[5]Department of Molecular Biology and Biophysics, University of Connecticut Health Center, Farmington, CT 06030, USA

[5]Department of Environmental Health, Harvard T.H Chan School of Public Health 220 Longwood Ave Goldenson 559C Boston, MA 02115, USA

Contributions: F.M.V., A.R., Z.N., I.C., G.C.W., and M.T.H. conceived the idea for the research, designed experiments and interpreted data. F.M.V., G.C.W., and M.T.H. wrote the paper.

Abstract

Given the critical role that Rev1 and Rev3 play in modulating therapeutic response in a variety of tumors, there has been a growing interest in better elucidation of the impact that the TLS protein Rev7 may also play in this context. To date, the studies examining Rev7's biological relevance have largely been focused on the role it plays as a structural DNA polymerase subunit in the TLS DNA damage tolerance pathway. However, in the last decade numerous studies have emerged indicating that Rev7 also regulates multiple cellular functions. In this study I sought to better elucidate Rev7's diverse cell regulatory roles by using a localization and Affinity Purification (LAP) Tagging system to identify Rev7 protein interactors via immunopreciptation and mass spectrometry analyses.

Findings from this work revealed that Rev7 has differential interactions with various protein partners, some previously unidentified, depending on the cellular conditions assayed. Additionally, from this work I have discovered that Rev7's regulatory roles beyond the TLS DNA damage tolerance pathway may aid in its ability to modulate chemotherapeutic efficacy in drug-resistant cancer cells. In particular, this work reveals that Rev7 loss results in a decrease in DSB repair following DSB induction in drug-resistant lung cells, in a manner that appears to be due to a reduction in HR DSB repair activity. Importantly, this work also demonstrates that identification of Rev7 protein interactors and better characterization of Rev7's non-TLS regulatory roles can reveal valuable insights into how Rev7 is able to promote such a diverse set of regulatory responses. This is particularly important, for a better understanding of Rev7's diverse cell regulatory roles may reveal how targeting Rev7 mediated functions can provide added insights for the development of Rev7 specific inhibitors that could potentially be used to

enhance chemotherapeutic efficacy in drug-resistant malignancies.

Introduction

Genomic instability is a crucial driver of tumorigenesis (Hanahan & Weinberg, 2011). Moreover, as the disease advances many malignancies have an extremely high propensity to accumulate DNA damage. In part, this is one key reason that chemotherapy is still a mainstay of treatment for many cancers. However, it is not uncommon for tumors to respond poorly to chemotherapy and/or acquire resistance to treatment over the course of chemotherapy (Zheng, 2017). Subsequently, innate and acquired chemoresistance poses a great challenge to chemotherapeutic efficacy. In recent years, to try and target this tumor vulnerability, there has been a drastic increase in the development of targeted therapies that inhibit the DNA damage response (DDR) in cancers.

One approach currently used in the clinic is to specifically target tumors bearing mutations in DNA damage repair pathways (Dietlein, Thelen, & Reinhardt, 2014; O'Connor, 2015). For example, the development of PARP inhibitors has made it possible to target the DNA repair defects in BRCA mutant tumors (Ashworth & Lord, 2018). While treatment of tumors with DNA damage repair inhibitors, such as olaparib, have yielded success in certain cancer populations, failure to respond and acquired resistance to these treatments still remains a major issue (Ashworth & Lord, 2018). Thus, there is an urgent need to develop novel therapies that target other therapeutically promising components of the DDR pathway.

In recent years there has been an increase in the number of studies suggesting that targeting crucial components of the translesion synthesis (TLS) DNA damage tolerance pathway may prove to be a promising way to overcome issues of chemoresistance in many different tumors.

Interest in the links between TLS and chemotherapeutic response has increased because a number of studies have revealed the error-prone TLS DNA damage pathway, which is largely carried out by TLS pol Rev1 and TLS pol ζ (Rev3, the catalytic subunit and Rev7, a structural subunit), can render cytotoxic anticancer drugs less effective by enabling direct bypass of the DNA lesions incurred following treatment (Murakumo et al., 2001). Notably, these studies have shown that, in addition to promoting chemoresistance by DNA damage bypass, key TLS proteins like Rev1 and Rev3 are involved in promoting mutagenesis following exposure to chemotherapeutic agents like cisplatin (Doles et al., 2010; Lin, 2006). These studies highlight that the development of DDR inhibitors that target proteins in the TLS DNA damage pathway is a promising anti-cancer strategy, as it may be able to both enhance the efficacy of chemotherapies in tumors, as well as reduce the emergence of chemotherapy induced mutagenesis in tumors. While elucidating Rev1's and Rev3's roles in chemotherapeutic response has proved to be very important, to truly understand how the error-prone TLS pathway modulates chemotherapeutic efficacy and can be targeted as a way to enhance chemotherapeutic response in tumors, it is also crucial to investigate the role that the TLS protein Rev7 may also play in this context.

In the last decade, numerous published Rev7 studies have revealed that Rev7 is actually a multi-functional TLS protein. Rev7's non-TLS regulatory roles affect such diverse functions as epigenetic reprogramming, cell cycle regulation, and DSB break repair (Bhat et al., 2015; Rahjouei et al., 2017; Xu et al., 2015). One leading thought is that Rev7 is able to regulate such a diverse set of cellular functions because of its special protein topology. Rev7's 211 amino acid structure is made up of the HORMA (Hop1, Rev7, Mad2) domain, which is a conserved, unique structural signaling motif. This motif allows Rev7 and other HORMA domain containing

proteins, such as the spindle activity checkpoint (SAC) protein Mad2, to form protein complexes with a diverse set of proteins through a characteristic "seat belt-like" interaction in which the C-terminus of the HORMA domain wraps entirely around a peptide segment of a binding partner (Aravind & Koonin, 1998; Muniyappa et al., 2014). It seems likely that interactions Rev7 makes via its HORMA domain with non-TLS protein partners may enable it to regulate cellular processes beyond the TLS pathway. To date, several studies have indicated that in addition to interacting with Rev1 and Rev3, Rev7 also interacts with non-TLS proteins linked to functions as diverse as spindle checkpoint regulation, (i.e. CDC20 and CDH1) and kinetochore regulation (i.e. ZNF828) (Hara et al., 2017; Listovsky & Sale, 2013). Moreover, recent structural work has also revealed that Rev7 forms a homodimer, which likely also helps to facilitate Rev7's ability to form interactions with many of its TLS and non-TLS binding partners (Rizzo, Vassel, et al 2018).

However, it still remains unclear exactly how Rev7-mediated protein interactions may control its ability to regulate such diverse cellular processes. An understanding of how Rev7 carries out its diverse functions would be extremely valuable, because identifying and targeting key Rev7 mediated protein interactions might potentially reveal if inhibiting key Rev7-mediated protein interactions could significantly enhance the efficacy of chemotherapy in tumors. This is a particularly intriguing point because several studies have revealed that Rev7 also plays a key role in regulating DDR cellular processes other than the error-prone TLS pathway, such as DSB repair pathway choice. Thus identifying targeting Rev7-mediated interactions, such as those that regulate DSB repair, in tumors may prove to be an important Achilles heel in cancer therapy because inhibiting Rev7 function may serve to sensitize cancer cells to chemotherapy by abrogating the activity of DDR mechanisms beyond the TLS DNA damage tolerance pathway.

Furthermore, uncovering when and how Rev7 interacts with its various protein partners will provide new insights into how Rev7-mediated dependencies on DNA damage tolerance, mutagenesis, and repair may contribute to its ability to modulating chemotherapeutic response.

In this study I used a localization and Affinity Purification (LAP) Tagging system to better elucidate Rev7's diverse regulatory functions. Using this system, I conducted immunoprecipitation and mass spectrometry analyses to that led to the identification of novel Rev7 protein interactors. Here I show that it is possible to immunopurify hRev7-LAP tagged complexes from asynchronous, G2/M arrested, and mitomycin C (MMC) treated cells. Mass spectrometry analysis of G2/M arrested cells revealed that Rev7 interacts with previously characterized partners such as transcription factor TFII-I. These analyses also revealed that in asynchronous, G2/M arrested, and MMC treated cells Rev7 interacts with several relatively uncharacterized protein partners - POGZ, ZNF828, and HP1-gamma – that are most likely in a complex.

Intriguingly, mass spectrometry analysis of MMC-treated cells revealed two novel Rev7 interactions partners: the AAA+ ATPase TRIP13 and the anti-apoptotic protein P75 (p75). The discovery of Rev7 mediated interactions with these two proteins was of particular interest because, like Rev7, both TRIP13 and P75 have been shown to play key roles in DSB pathway choice (Banerjee et al., 2014; Daugaard et al., 2012). Thus, I characterized the Rev7/TRIP13 and Rev7/ p75 interactions in an effort to further elucidate the role that Rev7 plays in modulating DNA damage response and present a more detailed picture of how Rev7's interaction with TRIP13 or P75 may also modulate chemotherapeutic efficacy.

Additionally, I also sought to further characterize Rev7's role beyond the TLS DNA damage tolerance pathway by examining the role that Rev7 plays in regulating DSB repair. Specifically, I

investigated the impact that Rev7 may have on DSB repair because much is still unknown about when and how Rev7 regulates DSB repair. To explore this question, I conducted DSB repair activity assays in drug-resistant lung cancers and assessed the impact that Rev7 loss has on DSB repair in these cells. These DSB repair analyses reveal that Rev7 loss increases the presence of DSBs in these lung cancers cells and in turn Rev7 loss also reduces DSB repair capacity in these cells. Interestingly, these DSB repair studies also suggest that Rev7 loss may specifically result in an increase in DSBs due to a decrease in HR DSB repair activity.

Results:

I. Identification of the Rev7-interacting proteins in HeLa cells via IP/Mass Spectrometry analysis

I believe that a better understanding of Rev7's diverse cell regulatory functions will be greatly aided by the identification of Rev7's protein partners. To investigate how Rev7-mediated protein interactions may impact Rev7's ability to regulate diverse cellular functions I used the Localization and Affinity Purification (LAP) Tagging and GFP immunoprecipitation system (Cheeseman & Desai, 2005). This system is attractive because it readily allows the identification of novel protein interactors via the use of immunoprecipation/mass spectrometry analyses. Thus, to use this system to further dissect Rev7's cellular functions, I created HeLa cell lines stably expressing human Rev7 (hRev7) fused at its C and N termini with a LAP tag, respectively. The N-terminal tagged hRev7-LAP cell line was used in all immunoprecipitation and mass spectrometry experiments conducted in this study.

Using our hRev7-LAP HeLa cell lines, I first investigated how different cellular conditions may modulate Rev7 protein-protein interactions. In particular, I immunopurified

hRev7-LAP tagged complexes from lysates of untreated asynchronous, nocodazole treated (~12 hours nocodazole treatment), or MMC-treated (24 hours MMC treatment) HeLa cells. I examined these particular cellular conditions because of the key roles that Rev7 plays crucial roles in regulating the cell cycle, the TLS DNA damage tolerance, and DNA damage repair. Encouragingly, my initial overall assessment of my mass spectrometry data (Fig. 1) detected the presence of previously characterized Rev7 protein interactors, such as the transcription factor TFII-I and the kinetochore protein ZNF828/CAMP (Fattah et al., 2014; Hara et al., 2017). This is important, for it strongly suggests that immunopurifying hRev7 protein complexes using the LAP system can reliably detect characterized Rev7 interactors and thus has the potential to detect novel Rev7-mediated protein-protein interactions.

II. Identification of uncharacterized Rev7 protein-protein interactions suggest Rev7 may interact in various uncharacterized protein complexes and may localize at sites of heterchromatin DNA

Encouraged by the ability to use hRev7-LAP tagged constructs to identify previously characterized Rev7 interactors, I carried out a more in-depth analysis of all three hRev7-LAP mass spectrometry data sets. This analysis revealed that in asynchronous, G2/M arrested, and MMC treated cells Rev7 may form interactions with several characterized and relatively uncharacterized protein partners (Fig. 2a,b), which include characterized Rev7 protein interactors: TFII-I, ZNF828/CAMP and uncharacterized putative Rev7 protein interactors: Mad2, HP1-beta, POGZ, and HP1-gamma. This was intriguing, for the identification of these proteins in all sample conditions suggests that Rev7 may interact in a complex with a set and/or all of these proteins. The detection of the SAC protein Mad2 in all hRev7-LAP samples was a particularly interesting finding, for one way Rev7 has been linked to controlling cell cycle

regulation is via interactions it makes with other SAC proteins such as CDH1, but there are no published IP/ mass spectrometry data suggesting that Rev7 interacts with Mad2.

Interestingly, an analysis of the literature revealed that several of the uncharacterized putative Rev7 protein interactors detected in these samples, specifically HP1-beta, POGZ, and HP1-gamma, have been previously shown to localize to heterochromatin DNA (Vermeulen et al., 2010). In particular, two of the uncharacterized Rev7 protein interactors identified, HP1-beta and HP1-gamma, are known heterochromatin proteins. Additionally, a previously published genome-wide mass spectrometry analysis has revealed that several of these relatively uncharacterized putative Rev7 protein interactors, namely: HP1 gamma, HP1-beta, and POGZ, all have been shown to interact in IP/mass spectrometry studies with each other and localize to the heterochromatin marker H3K9me3 (Vermeulen et al., 2010). Interestingly, this same genome-wide interaction study revealed that the previously characterized Rev7 interacting protein ZNF828 also interacts with two of the heterochromatin proteins detected in the hRev7-LAP mass spectrometry analyses, HP1-beta and HP1-gamma (Vermeulen et al., 2010). Taken together, the enrichment of heterochromatin proteins and proteins that interact with heterochromatin markers like H3K9me3 in the hRev7-LAP mass spectrometry data suggests that Rev7 likely localizes to sites of heterochromatin under certain cellular conditions.

III. Identification of novel Rev7 protein interactors suggest Rev7 may interact with HORMA domain remodeling proteins and DSB repair proteins

A major goal of this IP/ mass spectrometry interaction study was to investigate if Rev7 exerts its diverse cellular functions by mediating different protein-protein interactions. In particular, I investigated if Rev7 interacts with varied interaction partners in response to different

environmental conditions, i.e. in cells that are G2/M arrested or in cells that have been subject to DNA damaging conditions.

Interestingly, an analysis of all three mass spectrometry experiments revealed that Rev7 may indeed form distinct protein-protein interactions depending on a cell's environmental conditions. In particular, while a number of interacting proteins, such as ZNF828, were identified in all treatment conditions assayed in the mass spectrometry analysis, several proteins were only identified in the hRev7-LAP samples treated with the DNA-damaging agent MMC (mitomycin C). The putative Rev7 interactors identified in only in MMC-treated hRev7-LAP cells are: the chromatin-binding protein ZNF262, the single-stranded DNA binding protein RPA1, the AAA+ ATPase TRIP13, and the chromatin-binding, DNA damage repair protein p75 (Fig. 3). The identification of these proteins in the MMC-treated hRev7-LAP mass spectrometry data set is particularly intriguing for to date there are no published studies suggesting Rev7 interacts with any of these protein partners. Consequently, their identification in this hRev7 IP/mass spectrometry study indicates that they are novel Rev7 mediated protein-protein interactions. Additionally, their detection in only hRev7-LAP cells treated with MMC may suggest that their interactions with Rev7 are induced following DNA damage.

Considering that the novel Rev7 interactors detected in the MMC treated samples were only identified under this condition, I decided to investigate the literature to see if any of these proteins had any characterized functions relevant to DNA damage response. This literature search revealed that all of the proteins in question had functions linked to DDR. Out of this set of proteins, RPA1, TRIP13, and p75 all have well characterized DNA damage repair roles. In particular, RPA1 functions as DDR protein by binding to and helping stabilize single stranded DNA intermediates that form following DNA damage, such as during DSB repair where RPA1

mutation/ loss is associated with defective DSB repair (Y. Wang et al., 2005). Additionally, TRIP13 and p75 also have roles in DDR that are linked to DSB repair.

IV. Validation of selected uncharacterized novel Rev7 protein-protein interactions

Having identified a number of uncharacterized and putative Rev7 protein interactors with cellular functions that may help better inform how Rev7 regulates a diverse set of cellular functions, I conducted co-immunoprecipitation experiments with a select set of these proteins to verify that they are indeed Rev7-mediated protein-protein interactions. Due to the roles they play in regulating Rev7-related functions, such as the cell cycle and/or DSB repair, the set of Rev7-mediated protein-protein interactions I sought to validate were Rev7's interactions with: POGZ, HP1-gamma, TRIP13, and p75.

I first sought to validate that I can detect Rev7-mediated interactions with the uncharacterized Rev7 protein interactors POGZ and HP1-gamma in G2/M arrested HeLa cells. This was important because to date the only reports of Rev7-mediated protein-protein interactions with POGZ and HP1-gamma, respectively, were detected in studies investigating Rev7-mediated protein-protein interactions in untreated cells. To do this work, I carried out co-immunoprecipitation experiments in which POGZ and HP1-gamma, respectively, were immunoprecipitated from HeLa cells that had been treated with nocodazole to induce a G2/M arrest. Western blots for POGZ or HP1-gamma immunopreciptated cell lysates were run and probed with a Rev7 specific antibody. These experiments validated that Rev7 interacts with POGZ and HP1-gamma, respectively, for when either protein is immunoprecipitated from G2/M arrested HeLa cells (Fig.4a,b) interactions with Rev7 are detected.

Having validated that Rev7 interacts with HP1-gamma and POGZ in G2/M arrested HeLa cells, I also conducted co-immunoprecipitation experiments to validate if Rev7 also interacts

with uncharacterized protein partners, such as the protein POGZ, in DNA damaged cells. This was crucial because there are no published studies investigating the impact that DNA damage induction may have on promoting Rev7-mediated interactions with POGZ or HP1-gamma protein. To do this, I carried out co-immunoprecipitation experiments where POGZ was immunoprecipitated from MMC-treated HeLa cells and then western blots for Rev7 immunopreciptated cell lysates were run and probed with GFP antibody targeting hRev7_LAP. These data validated that Rev7 interacts with uncharacterized protein interactors, like POGZ, in MMC-treated DNA damaged HeLa cells (data not shown), for these data reveal that when POGZ is immunoprecipitated in MMC-treated cells interactions with Rev7 are detected.

I also sought to confirm that Rev7 interacts with the novel protein Rev7 interactors detected in the MMC-treated samples. In particular, I conducted experiments to verify that I could validate Rev7 mediated protein-protein interactions with TRIP13 and p75, respectively. To do this I carried out co-immunoprecipitation experiments where Rev7 was immunoprecipitated from HeLa cells treated with MMC, which was used to induce DNA damage, and then western blots for Rev7 immunopreciptated cell lysates were run and probed with TRIP13 or p75 specific antibodies. These experiments validated that when Rev7 is immunoprecipitated from MMC treated DNA damaged HeLa cells (Fig.5) interactions with TRIP13 and p75 are indeed detected.

Intrigued by TRIP13's ability to regulate HORMA domain containing proteins by using its AAA+ ATPase activity to remodel their structure, I also sought evidence suggesting that TRIP13's interaction with Rev7 might play a role in remodeling Rev7's structure as well. To begin to investigate this question, I conducted co-immunoprecipitation experiments where Rev7 was immunoprecipitated from untreated HeLa cells and then western blots for Rev7 immunopreciptated cell lysates were run and probed with a TRIP13 specific antibody.

Intriguingly, these data revealed that when Rev7 is immunoprecipitated from untreated HeLa cells (Fig. S2) interactions with TRIP13 are detected. While TRIP13's interaction with Rev7 was not initially identified in the untreated sample from my hRev7-LAP IP/mass spectrometry studies, it is possible that the interaction that TRIP13 makes with Rev7 is present but not as abundant in the absence of DNA damage. It is possible that TRIP13's putative ability to structurally remodel Rev7's structure might normally occur in untreated cells, but is enriched in the presence of a cell stress like DNA damage.

Importantly, taken together these data confirm that TRIP13 and p75 are indeed novel Rev7 interactors and encouraged me to investigate the functional relevance of Rev7-mediated protein-protein interactions with TRIP13 and p75, respectively.

V. Investigating the functional relevance of Rev7 protein-protein interactions that Rev7 forms with TRIP13

To begin to investigate if there is any functional relevance between the interaction between Rev7 and TRIP13, I first investigated whether TRIP13 is also able to modulate chemotherapeutic efficacy in drug-resistant cancer cells. I sought to look at TRIP13 in this context due to the crucial role Rev7 plays in regulating DDR mechanisms, such as TLS DNA damage tolerance and DSB repair. In particular, I tested, if like Rev7, that TRIP13 depletion results in cisplatin sensitization in the KP-drug resistant lung cells. To conduct these experiments, I used RNAi technology and designed short-hairpin RNAs (shRNA) targeting mouse TRIP13 (mTRIP13). After generating 5 sequences (shT13_1-5) that specifically target mTRIP13 (Fig.S4), I cloned these sequences into E2-Crimson labeled MLS vectors and transfected KP lungs cells with the resulting TRIP13 shRNA constructs. Following the transfections, I carried out flow-cytometry

analysis to sort for E2-Crimson positive KP cells, to ensure that I have a population of cells enriched for TRIP13 depletion. After sorting the KP cells for E2-crimson labeled TRIP13 shRNAs, I then used qPCR analysis to assess the impact that each TRIP13 shRNA construct has on TRIP13 depletion in KP cells. These mRNA transcript data reveal that the TRIP13 shRNA constructs with the best knockdown, shT13_3, reduces mTRIP13 transcript levels to ~30% in KP wild-type lung cells and ~10% in Rev7 knockout (KO) KP lung cells (Fig. 6a).

After identifying TRIP13 targeted shRNAs that efficiently deplete TRIP13 levels in wild-type and Rev7 KO KP lung cells, I then sought to analyze the impact that TRIP13 depletion has on cisplatin sensitivity in KPWT and REV7 KO KP cells, respectively. I investigated this question by using the Cell Titer-Glo assay to determine the cell viability of TRIP13 knockdown KPWT and REV7 KO KP cells following cisplatin treatment. These data reveal that TRIP13 depletion enhances cisplatin sensitivity in KPWT cells, which are intrinsically resistant to cisplatin (Fig. 6b). After establishing that TRIP13 depletion does indeed modulate cisplatin response in KPWT cells, I then sought to explore the impact that TRIP13 depletion has on cisplatin sensitivity in Rev7 KO KP cells. Interestingly, these cell viability experiments suggest that TRIP13 knockdown acts in an additive or synergistic manner with Rev7 KO and in turn drastically enhances cisplatin sensitivity in KP cells (Fig. 6c). These results are particularly interesting, for they suggest that simultaneously targeting Rev7 and TRIP13 may represent one approach to overcome cisplatin resistance and improve chemotherapeutic efficacy in drug-resistant lung cancer treatment.

VI. Investigating the functional relevance of Rev7 protein-protein interactions that Rev7 forms with P75

Additionally, I sought to investigate if there is any functional relevance to the interaction between Rev7 and p75. Similar to my TRIP13 cisplatin sensitivity work, I also investigated whether p75 depletion affects cisplatin sensitization in KP-drug resistant lung cancer cells. To conduct these experiments, I used RNAi technology and designed short-hairpin RNAs (shRNA) targeting mouse P75 (mp75). Upon generating 5 sequences (shp75_1-5) that specifically target mp75 (Fig. S5). I cloned these sequences into E2-Crimson labeled MLS vectors and transfected KP lungs cells with the resulting p75 shRNA constructs. Following the transfections, I carried out flow-cytometry analysis to sort for E2-Crimson positive KP cells, to ensure that I have a population of cells enriched for p75 depletion. After sorting the KP cells for E2-crimson labeled p75 shRNAs, I then used qPCR analysis to assess the impact that each p75 shRNA construct has on p75 depletion in KP cells. These mRNA transcript data reveal that the p75 shRNA constructs with the best knockdown, shp75 _3, reduces p75 transcript levels to ~40% in KP wild-type (WT) lung cells and ~10% in Rev7 knockout (KO) KP lung cells (Fig.7a).

Upon identifying p75-targeted shRNAs that efficiently deplete p75 levels in wild-type and Rev7-KO KP lung cells, I then analyzed the impact that p75 knockdown has on cisplatin sensitivity in KPWT and Rev7-KO KP cells by using the Cell Titer-Glo assay to determine the cell viability following cisplatin treatment. These data reveal that p75 depletion enhances cisplatin sensitivity in KPWT cells, which are intrinsically resistant to cisplatin (Fig.7b). After establishing that p75 depletion modulates cisplatin response in KPWT cells, I then explored the impact that p75 depletion has on cisplatin sensitivity in Rev7-KO KP cells. Intriguingly, these cell viability experiments suggest that p75 may have an epistatic relationship with Rev7 because Rev7KO KP cells in which p75 has been depleted have a similar sensitivity to cisplatin as Rev7KO KP cells alone (Fig.7c). These results are very interesting because they suggest that

Rev7 and p75 may act in a shared DDR pathway, which in turn could provide an explanation for why Rev7-p75 protein-protein interactions are detected specifically in MMC-treated DNA damaged mammalian cells.

Given that these cisplatin sensitivity studies in drug-resistant KP lung cancer cells suggest that Rev7 and p75 may have an epistatic relationship, I also explored whether an interaction between Rev7 and p75 can be detected in this lung cancer cell line. To begin to investigate this question, I conducted co-immunoprecipitation experiments where Rev7 was immunoprecipitated from MMC treated KPWT cells and then western blots for Rev7 immunopreciptated cell lysates were run and probed with a p75 specific antibody.

Notably, these experiments (Fig. 8) reveal that Rev7 interacts with p75 in DNA-damaged KPWT cells, thus further suggesting that Rev7 and p75 may have an epistatic relationship in drug-resistant lung cells and act in a common DDR pathway. Upon detecting that Rev7 and p75 interact in KPWT cells that are treated with agents that can induce DSBs, like MMC and cisplatin, I also sought to explore if other Rev7 interacts with any other proteins linked to DSB repair. In particular, due to the role that p75 plays in regulating DSB repair via its interaction with the DSB repair protein CtIP, I conducted preliminary experiments to explore if Rev7 also interacts with CtIP in KP cells. Rev7 was immunoprecipitated from MMC-treated KPWT and Rev7KO KP cells, respectively, and then western blots for Rev7 immunopreciptated cell lysates were run and probed with a CtIP specific antibody. Intriguingly, data from these experiments (Fig. 8) also suggest that Rev7 may interact with the DSB repair protein CtIP under DNA-damage conditions. Importantly, these data suggest that any potential protein-protein interactions that Rev7 makes with CtIP may provide one possible explanation for Rev7's ability to regulate DSB repair pathway choice and strongly supports further exploration of the functional

significance of Rev7's protein-protein interactions with p75 and CtIP.

VII. Probing the structural basis of Rev7-TRIP13 and Rev7-p75

After validating that Rev7 forms a novel interaction with TRIP13 in both undamaged and MMC damaged mammalian cells, I also explored whether I could gain insights into the structural basis of the REV7-TRIP13 protein-protein interactions. In particular, research elucidating how TRIP13 remodels and in turn regulates other HORMA domain containing proteins, such as the spindle activity checkpoint protein MAD2 and the meiotic protein HORMAD1, reveal that TRIP13 binds these HORMA domain proteins via its N-terminal domain (TRIP13-NTD), which is similar to how other related AAA+ remodelers, e.g. the protein AAA+ ATPase NSF, carry out their substrate recognition (Ye et al., 2015). In the case of TRIP13's interaction with MAD2, structural studies have revealed that TRIP13, via its NTD, can structurally remodel MAD2. These studies reveal that TRIP13 is able to do this by disrupting interactions that MAD2's N-terminus forms with its safety-belt region in its c-terminal domain (Ye et al., 2015). Subsequently, by disrupting this interaction, TRIP13 is able to remodel MAD2's structure by destabilizing MAD2's interactions with its protein-protein interactions (Ye et al., 2015). Considering the structural relevance of TRIP13-NTD and HORMA domain interactions, I first sought to prove the basis of the Rev7-TRIP13 protein-protein interactions by conducting structural studies using TRIP13-NTD.

To address this question, I worked with a structural collaborator, Alex Rizzo in the Korzhnev lab, at the University of Connecticut to conduct NMR experiments in which unlabeled hRev7, namely hRev7_ R124A/Rev3-Rev7 binding motif 2 (RBM2), was incubated with a ^{15}N-labeled

TRIP13-NTD (TRIP13 residues 1-106). The hRev7_ R124A/Rev3-RBM2 version of Rev7 was used in this initial study because wild-type Rev7 forms a homodimer, which would be too large to investigate via NMR. Interestingly, these NMR data do not provide evidence (Fig.9) that TRIP13-NTD and hRev7-R124A/Rev3-RBM2 interact. However, this does not rule out the possibility that the TRIP13-NTD is key for mediating interactions with TRIP13 and Rev7, for it is possible that the formation of other Rev7 protein complexes, such as the Rev7-homodimer, may also be required for any interactions that TRIP13 may form with Rev7 in cells. This said, in future Rev7-TRIP13 structural studies there would be much value in conducting additional experiments, like gel filtration studies, that would allow for the use of full length Rev7 and TRIP13.

VIII. Probing the structural basis of Rev7-p75 PPI

Prompted by the discovery that Rev7 forms a novel interaction with the DNA damage repair protein p75 and data from cisplatin sensitivity assays that suggest that Rev7 and p75 form an epistatic relationship, I also sought to explore if I could gain insights into the structural basis of the REV7-p75 protein-protein interactions. To investigate this question, I first used the literature to determine if there are key modes of TRIP13-based protein-protein interactions with other characterized TRIP13 protein-protein interactions. In particular, published structural studies on p75's mediated interactions reveal that p75 interacts with chromatin and chromatin interacting protein partners via a region in its N-terminal domain called a "PWWP" motif and interacts with multiple proteins partners, such as POGZ and MLL-menin fusion oncoprotein, via a region in its C-terminal domain called the integrase-binding motif (IBD) (Tesina et al., 2015).

Based on this structural data that reveals that p75 mediates varied protein interactions via its N-terminal (p75-NTD) PWWP motif and C-terminal (p75-CTD) IBD motif, I sought to

determine if Rev7's interactions with p75 are mediated by either p75 domain. To explore this question, I worked with my structural collaborator, Alex Rizzo in the Korzhnev lab, at the University of Connecticut to conduct NMR and gel filtration experiments. In particular, given the key role Rev7 plays in regulating the TLS DNA damage tolerance and DSB repair, we first sought to explore if Rev7's interaction with p75 is mediated via p75's chromatin binding "PWWP" motif in the N-terminal domain.

We first conducted NMR experiments in which unlabeled p75-NTD (p75 residues 1-93) was incubated with a ^{15}N-labeled hRev7-R124A/Rev3-RBM2 but the data we obtained (Fig. 10a) did not indicate an interaction of p75-NTD with hRev7. However, considering we did not use wild-type hRev7 in these NMR studies because it homodimerizes and as such is too large, it is possible that p75-NTD only interacts with Rev7 when it is a homodimer. Because of this consideration, we also conducted gel filtration experiments to assess if p75-NTD interacts with wild-type hRev7. In particular, we attempted to co-elute p75-NTD with wild type hRev7 to see if wild type monomeric hRev7 and/or homodimeric hRev7 is needed to mediate an interaction with p75-NTD. Data from these experiments (Fig10b) reveal that the proteins eluted in two separate peaks, therefore failing to provide evidence for binding with p75-NTD and wild type hRev7. However, it is possible that interactions that may exist between p75-NTD and Rev7 may be dependent on other interacting proteins, such as DNA damage repair proteins like CtIP. It is also possible that interactions between p75-NTD and Rev7, may be dependent on interactions that p75's PWWP motif, found in the p75-NTD, makes with DNA, since the interaction and the PWWP motif in p75 has been shown to have functional relevance for other p75 protein interactors (Tesina et al., 2015).

To further probe the structural basis of p75's interaction with Rev7 we also sought to

investigate if Rev7 interacts with p75's IBD motif, present in p75-CTD. We explored this particular interaction because many of the characterized interactions between p75 and p75 protein interactors occur in this domain. To begin to examine this question we first conducted NMR experiments in which unlabeled p75-CTD (p75 residues 343-424) was incubated with a ^{15}N-labeled hRev7-R124A/Rev3-RBM2. These data (Fig.10c) did not indicate an interaction between p75-CTD and hRev7-R124A/Rev3-RBM2. However, it is possible that any interactions that may exist between Rev7 and p75-CTD may be dependent on Rev7 homodimerization. Additionally, it is possible that interactions that p75-CTD may make with Rev7 may be dependent on interactions that p75-CTD forms with Rev7 and other shared Rev7 and p75 interacting proteins, such as POGZ (Bartholomeeusen et al., 2009; Tesina et al., 2015).

VIIII. Exploring the functional relevance of Rev7 in DSB repair in drug-resistant lung cancer cells

Due to the recent discovery that Rev7 also plays an important role regulating DSB repair pathway choice, it is particularly interesting that my cisplatin sensitivity experiments in KP cells suggest that Rev7 and the DSB repair protein p75 are epistatic to one another. Motivated by these findings, I sought to investigate if Rev7 may play a role in regulating DSB repair in drug-resistant lung cancer cells. This question was of particular interest in the context of drug-resistant lung cancer because my research has shown that Rev7 loss drastically enhances sensitivity to cisplatin in these cells and in turn it is possible that loss of Rev7's DSB repair regulatory functions may aid in sensitizing these intrinsically drug-resistant cells to cisplatin-induced DNA damage.

To begin to investigate this question, I conducted DSB repair activity experiments to investigate if Rev7 loss has an impact on DSB repair capacity in these cells using two different

assays, the CometChip assay and FM-HCR DNA damage reporter assay, respectively. To use the CometChip assay to probe if Rev7 may help regulate DSB repair activity in KP lung cancer cells, cells were treated with 100 GY of ionizing radiation (IR) to induce DSBs. Additionally, the CometChip assay was conducted under neutral (non-denaturing conditions), which permits detection of DSBs at the single cell level (Ge et al., 2014). Specifically, in this assay the presence of DSBs was assessed in both KPWT and Rev7KO KP cells at four different time points: untreated cells "-1 hours", time "0 hours" treatment with 100 GY IR, time "1 hour" post treatment with 100GY IR treatment, and time "4 hours" post treatment with 100 GY IR treatment. These data (Fig.11) reveal that Rev7 KO KP cells display markedly increased levels of DSB breaks, as measured by comet tail moment, when compared to KP WT cells. These results are intriguing for the increase in DSBs observed in Rev7 KO cells reveal that KP cells have inefficient DSB repair when Rev7 is deleted. Importantly, these data suggest that Rev7 loss may indeed play a role in regulating DSB repair in KP cells.

To further investigate how Rev7 may impact DSB repair in drug-resistant lung cells, I also used the FM-HCR assay to assess DSB repair capacity in KP cells. The FM-HCR DNA damage reporter assay is a fluorescence-based multiplex flow-cytometric host cell reactivation assay (FM-HCR) that measures the ability of mammalian cells to repair plasmid reporters, each bearing a different type of DNA damage, such as DSBs that are repaired by the HR pathway or DSBs that are repaired by the NHEJ pathway (Nagel et al., 2014). Thus, using the FM-HCR assay to assess DSB repair in these studies is particularly advantageous because it will allow me to distinguish if Rev7 loss impacts HR DSB repair or NHEJ DSB repair, respectively.

Notably, data from the FM-HCR experiments (Fig.12a,b) indicate that Rev7 loss significantly decreases HR DSB repair activity in KP cells, as compared to KPWT cells, and also

that Rev7 loss has little to no impact on NHEJ DSB repair activity, as compared to KPWT cells. These data are interesting because they differ from a few of the recently published studies assessing the role that Rev7 has on DSB repair capacity, which argue that Rev7 depletion results in a decrease in NHEJ DSB repair activity (Boersma et al., 2015; Leland et al., 2018; Xu et al., 2015). However, independent published work has shown that in HeLa cells Rev7 depletion leads to a decrease in HR DSB repair activity (Shilpy Sharma et al., 2012).

Encouragingly, I also conducted FM-HCR experiments in Rev7 deficient HeLa cells (Fig. S5), which also suggest that Rev7 depletion may decrease HR DSB repair activity. Additionally, unpublished DSB repair activity studies from the D'Andrea lab, conducted in Rev7KO U2OS osteosarcoma cells also suggest that Rev7 loss may result in a decrease in HR DSB repair. Importantly, my data in combination with published and unpublished studies investigating Rev7's impact on DSB repair strongly suggest that Rev7 plays dual roles regulating DSB Repair, for it appears that in certain contexts Rev7 may promote NHEJ and in other contexts Rev7 may promote HR. Furthermore, my Rev7 DSB repair findings indicate that there is much value in further dissecting the mechanisms behind Rev7's regulatory control of DSB repair because it may provide insights into what conditions enable Rev7 to promote NHEJ or HR DSB repair pathway choice.

Discussion

As the number of studies aimed at the functional and structural characterization of Rev7 grows, it is becoming increasingly evident that Rev7 is a multifunctional protein with regulatory roles beyond the TLS DNA damage tolerance pathway. This study has focused on employing immunoprecipitation and mass spectrometry analyses, using the LAP (Localization and Purification)-tagged system, to further elucidate Rev7's diverse cell regulatory roles. In this

study, to help further elucidate Rev7's diverse regulatory roles I conducted immunoprecipitation and mass spectrometry experiments under varied cellular conditions studies to explore the impact that these may have on the induction of different Rev7 mediated protein-protein interactions. I showed that by immunopurifying hRev7-LAP tagged complexes from asynchronous, G2/M arrested, and MMC-treated cells and conducting mass spectrometry analyses, I can use the LAP-tagged system to detect that Rev7 interacts with previously characterized partners such as transcription factor TFII-I. These analyses also revealed that in asynchronous, G2/M arrested, and MMC-treated cells Rev7 consistently interacts with several relatively uncharacterized protein partners: POGZ, ZNF828, and HP1-gamma.

Most notably, mass spectrometry analysis of MMC-treated cells revealed two novel Rev7 interactions partners: the AAA+ ATPase TRIP13 and the anti-apoptotic protein, DNA damage repair protein p75. The discovery of Rev7-mediated interactions with TRIP13 was of particular interest, for via TRIP13's AAA+ ATPase activity, TRIP13 has been shown to structurally remodel and regulate the activity other HORMA domain containing proteins (Ye et al., 2015), which may help explain how Rev7 is able to interact with different protein partners. Additionally, my discovery of Rev7s interaction with TRIP13 and p75 (Banerjee et al., 2014, Daugaard et al., 2012) is also of great interest because both TRIP13 and p75 have been shown to play important roles in regulating DSB repair.

Consequently, since both TRIP13 and p75 have characterized DDR regulatory functions that, if aberrant, can negatively impact chemotherapeutic efficacy in some cancer cells, I sought to explore if we could gain any functional insights into how TRIP13 or p75's activity may impact Rev7's modulation of cisplatin efficacy in drug-resistant cancer. In particular, these studies suggest that Rev7 may act additively or synergistically with TRIP13 in drug-resistant

cancers, for TRIP13 depletion in Rev7 KO KP cells enhances their sensitivity to cisplatin. Thus, my findings suggest that co-targeting Rev7 and TRIP13 function may provide a novel way to modulate chemotherapeutic efficacy in chemoresistant cancer cells. Interestingly, these cisplatin sensitivity studies also reveal that p75 co-depleted Rev7 KO cells are as sensitive to cisplatin as Rev7 KO cells, which suggest that Rev7 may interact epistatically with p75. These findings also give us new insights for they reveal that Rev7 may modulate chemotherapeutic efficacy in drug-resistant lung cells through the help of protein partners, like p75, via a shared DDR pathway.

Additionally, my discovery that Rev7 forms novel protein interactions and potentially acts in a shared DDR response pathway with DSB repair proteins like p75 prompted me to explore if Rev7 plays a role regulating DSB repair in drug-resistant lung cancers. These findings were intriguing, for they revealed that Rev7 loss in KP cells results in an increase in DSB, which suggests that Rev7 plays a role in promoting DSB repair in these cells. Additionally, these DSB repair activity functional studies are also impactful because they suggest that Rev7 loss results in a decrease in HR DSB repair activity in KP cells. This finding is intriguing for it expands the field's understanding of how Rev7 promotes DSB repair, which to date suggests that Rev7 inhibits 5' end resection and in turn promotes NHEJ DSB repair (Boersma et al., 2015; Leland et al., 2018; Tomida et al., 2018; Xu et al., 2015). My finding that Rev7 can also promote HR DSB repair highlights the fact that Rev7's role in DSB repair pathway choice is complex and warrants further elucidation. Importantly, from this work it is clear that a greater understanding of how Rev7 promotes its diverse regulatory roles will better enable researchers to determine under what contexts Rev7 may have functional relevance.

Furthermore, by both using immunoprecipation/mass spectromertry analyses to detect Rev7-mediated protein interactions and probing the functional relevance of these novel interactors in

non- TLS related Rev7 regulatory functions, my work suggests that one key way Rev7 is able to promote such diverse regulatory functions is through to its ability to form interactions with different protein partners. As our understanding of Rev7's biology increases, it becomes more apparent that Rev7, through still relatively uncharacterized mechanisms, plays a crucial role in regulating chemotherapeutic efficacy in a variety of tumors. This said, studies like this one aimed that are at better elucidating the impact that protein-protein interactions may have on regulating Rev7's multifunctional capabilities will help in the development of specific inhibitors that target critical Rev7 functions. This is particularly valuable in the context of cancer therapy because targeting particular Rev7-mediated protein interactions may aid in the development of personalized cancer therapy regimens that can help improve chemotherapeutic efficacy in cancer.

Methods:

Cell culture and chemicals:

HeLa cells and mouse $Kras^{G12D}$; $p53^{-/-}$ lung adenocarcinoma cells were cultured in standard DMEM/10% FBS media. Mitomycin C (used at 300nM) and Nocodazole (used at 100 ng/mL of culture medium for a duration of 12-18 hours to induce G2/M arrest) were purchased from Santa Cruz Biotechnology. Cisplatin was purchased from Calbiochem and used at the indicated concentrations (used at 10 μM).

Co-Immunoprecipitation (co-IP)

Antibodies were pre-cleaned before attaching to magnetic beads using the Pierce Antibody Clean-Up Kit (44600, Thermo Fisher Scientific). A total of 10μg of antibody were covalently attached to magnetic beads (88828, Pierce Direct Magnetic IP/Co-IP Kit, Thermo Fisher Scientific) and incubated with 1mg of protein for 2 hours at room temperature while rotating. Immunoprecipitation (IP) was performed according to manufacturer's directions (Pierce Direct Magnetic IP/Co-IP Kit, Thermo Fisher Scientific).

Western blotting

Cells were lysed with TRIS-SDS lysis buffer supplemented with 1X protease inhibitor solution (cOmplete EDTA-free, 11873580001, Roche). Protein concentration of cell lysates was determined by Pierce BCA protein assay (23225, Thermo Fisher Scientific). Total protein (50μg) was separated on 4-20% Mini-Protean-TGX gradient SDS-PAGE gels (BioRad) and then transferred to PVDF membranes (IPVH00010, EMD Millipore) for blotting.

Antibodies:

Rev7 was immunoprecipitated using anti-Mad2L2 antibody (ab180579, Abcam) and detected in western blots at 1:1000 dilution. TRIP13 was immunoprecipitated using anti-TRIP13 antibody (ab128153, Abcam) and detected in western blots at 1:1000 dilution. p75 was immunoprecipitated using LEDGF (C57G11, Cell Signaling Technologies) at 1:1000 dilution and detected in western blots at 1:1000 dilution. POGZ was immunoprecipitated using Anti-POGZ antibody (ab171934, Abcam) and detected in western blots at 1:1000 dilution. HP1γ was immunoprecipitated anti-HP1γ (Antibody #2619, Cell Signaling Technologies) and detected in western blots at 1:1000 dilution. CtIP was immunoprecipitated using anti-CtIP (CtIP Antibody, A300-488A, Bethyl) and detected in western blots at 1:2000 dilution.

shRNA design, cloning, and RT-qPCR validation

Short hairpin RNA (shRNA) constructs were designed and cloned as previously described (Dickins RA, et al). The vector used coexpressed E2Crimson under the control of the SV40 promotor and is identical to the published MSCV/LTRmiR30-SV40-GFP (LMS) vector. Retrovirally infected cells were then selected by fluorescence assisted cell sorting (FACS) for E2Crimson positive cells. RNA from 2 x 10^6 cells was prepared using RNeasy Mini Kit (Qiagen). RT-qPCR was performed using SYBR green on a BioRad thermal cycler. GAPDH, TRIP13, p75, and Rev7 primer sequences are available upon request.

***In vitro* viability assays and FACS:**

For short-term viability assays, cells were seeded in triplicate (8×10^3 per well) in 96-well plates and treated as indicated with 10 μM cisplatin. After 48 hours treatment, cell viability was measured using Cell- Titer-Glo (Promega) on an Applied Biosystems microplate luminometer.

CometChip assay

$Kras^{G12D}$; $p53^{-/-}$ lung adenocarcinoma cells were cultured in standard DMEM/10% FBS media seeded in 96-well plates. DSB repair activity was assessed by conducting the neutral CometChip assay as previously described (Ge et al., 2014).

FM-HCR assay

HeLa cells and $Kras^{G12D}$; $p53^{-/-}$ lung adenocarcinoma cells were cultured in standard DMEM/10% FBS media and seeded in 6 well plates. NHEJ DSB repair activity and HR DSB repair activity, respectively, was assessed using the FM-HCR assay as previously described (Nagel et al., 2014).

HeLa cell Localization and Affinity Purification (LAP) Tag and Mass Spectrometry analysis:

Human Rev7 (hREv7) was cloned into the pIC242 vector at its C and N termini, respectively, to generate hRev7-LAP constructs for use in immunoprecipitation and mass spectrometry studies. HeLa cells were lentivirally transfected with hRev7-LAP tag constructs and cells were then selected with blasticidin to generate HeLa cell lines stably expressing hRev7-LAP. hRev7-LAP constructs were immunoprecipitated from cells and mass spectrometry analyses were conducted as previously described (Cheeseman & Desai, 2005).

Protein expression, NMR and gel filtration analyses

Proteins/ plasmids

Rev7/Rev3-RBM2 (residues 1988-2014):coexpressed in pETDuet

Trip13 N-terminal domain (residues 1-106): pET28b+

p75 domain 1 (residues 1-93): pET28b+

p75 domain 2 (residues 346-424): pET28b+

Protein purification

All proteins were purified by the same general protocol. *E. coli* strain BL21(DE3) was transformed with a plasmid containing the gene of interest, grown to mid-log phase at 37 °C in either LB or M9 minimal media, and induced overnight at 20 °C with 1 mM final concentration of IPTG. Cells were harvested, lysed by sonication, centrifuged for 30 minutes at 18 000 rpm in an SS-34 rotor, and purified by affinity chromatography over Talon resin (Clontech). The proteins were then purified by gel filtration chromatography over a GE Superdex S75 column that was equilibrated with 20 mM HEPES, 100 mM NaCl, 10 mM DTT, pH = 7.4.

NMR spectroscopy

^{1}H-^{15}N HSQC spectra were collected at 25 °C on an 800 MHz Agilent spectrometer equipped with a 5 mm HCN salt tolerant inverse cryoprobe with z-axis gradients.

Trip13: ^{5}N-labeled Trip13 N-terminal domain starting at 500 μM was titrated with unlabeled Rev7-R124A/Rev3-RBM2 to 1:75 molar excess.

p75: ^{15}N-labeled Rev7-R124A/Rev3-RBM2 starting at 100 μM was titrated to a 2:1 molar excess with either p75 domain 1 (residues 1-93) or domain 2 (346-424).

Coelution of hRev7-WT/Rev3-RBM2 and p75 domain 1

Both proteins were mixed in a 1 mL sample loop at 1.5 mM final concentration and applied to a GE Superdex S75 gel filtration column.

Figures:

Fig.1: Table of hits identified in mass spectrometry data confirming Rev7 interacts with previously characterized Rev7 interactors, ZNF828 and TFII-I. Legend :"+" represents Rev7 protein interaction present in sample condition highlighted in column ; "-" represents Rev7 protein interaction not present in sample condition highlighted in column

Protein	Present in untreated sample	Present in nocodazole sample	Present in mitomycin C treated sample	Key functions
ZNF828	+	+	+	Chromosome alignment
TFII-I	+	+	+	Transcriptional regulation/ TLS

Fig.2a Table of hits identified in mass spectrometry data where several uncharacterized putative Rev7 interactors (MAD2, POGZ, HP1-Y and HP1-beta) were detected in sample conditions assayed. Legend : "+" represents Rev7 protein interaction present in sample condition highlighted in column ; "-" represents Rev7 protein interaction not present in sample condition highlighted in column

Protein	Present in untreated sample	Present in nocodazole sample	Present in mitomycin C treated sample	Key functions
MAD2	+	+	+	Spindle activity checkpoint regulator
HP1-beta	+	+	+	Promotes epigenetic repression
HP1-gamma	+	+	+	Promotes epigenetic repression
POGZ	+	+	+	Kinetochore regulator

Fig.2b: Table of hits identified in mass spectrometry data where several characterized and uncharacterized putative Rev7 interactors (ZNF828, TFII-I ,MAD2, POGZ, HP1-gamma and HP1-beta) were detected in sample conditions assayed. Legend :"+" represents Rev7 protein interaction present in sample condition highlighted in column ; "-" represents Rev7 protein interaction not present in sample condition highlighted in column

Protein	Present in untreated sample	Present in nocodazole sample	Present in mitomycin C treated sample	Key functions
ZNF828	+	+	+	Chromosome alignment
TFII-I	+	+	+	Transcriptional regulation/ TLS
MAD2	+	+	+	Spindle activity checkpoint regulator
HP1-beta	+	+	+	Promotes epigenetic repression
HP1-gamma	+	+	+	Promotes epigenetic repression
POGZ	+	+	+	Kinetochore regulator

Fig.3: Table of hits identified in mass spectrometry data where detecting several putative novel Rev7 interactors (p75,TRIP13, RPA1, ZNF262) were identified in mitomycin C DNA damaged cells. Legend :"+" represents Rev7 protein interaction present in sample condition highlighted in column ; "-" represents Rev7 protein interaction not present in sample condition highlighted in column

Protein	Present in untreated sample	Present in nocodazole sample	Present in mitomycin C treated sample	Key functions
p75	-	-	+	Anti-Apoptotic Protein
TRIP13	-	-	+	AAA+ ATPase that remodels HORMA proteins
RPA1	-	-	+	Binds single strand DNA/ DNA repair
ZNF262	-	-	+	Chromatin binding/ DNA repair

Fig.4a: Co-IP analysis probing Rev7-POGZ interaction in nocodazole treated HeLa cells

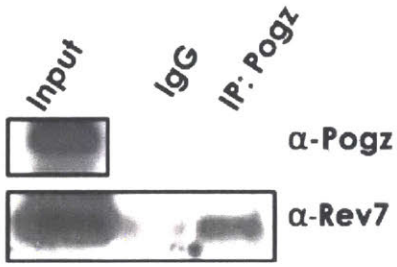

Fig.4b: Co-IP analysis probing Rev7-HP1-Y interaction in nocodazole treated HeLa cells

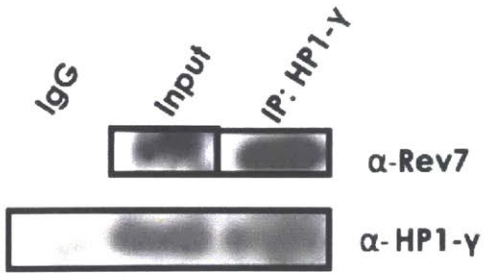

Fig.5: Co-IP analysis probing Rev7-TRIP13 and Rev7-p75 interaction in MMC treated HeLa cells

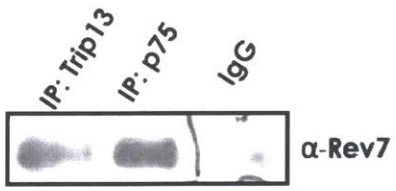

Fig.6a: Trip13 shRNA qPCR analysis

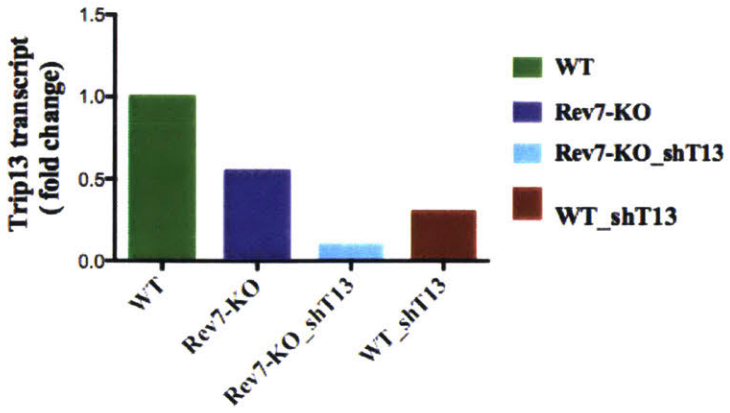

Fig.6b: Trip13 shRNA Cisplatin Sensitivity Assay

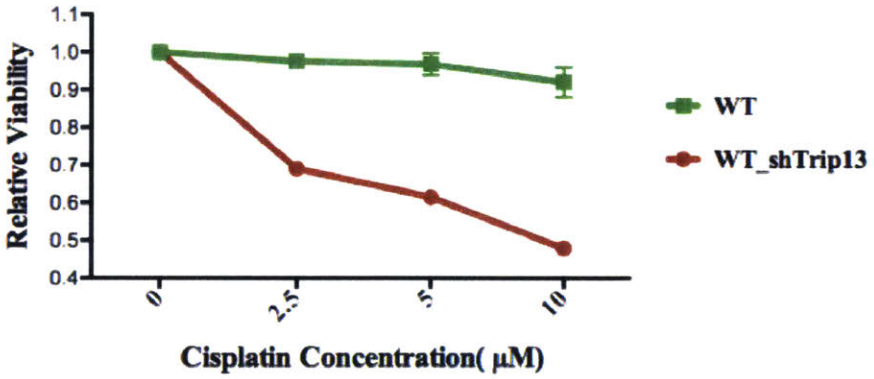

Fig.6c: Trip13 shRNA_Rev7KO cisplatin sensitivity assay

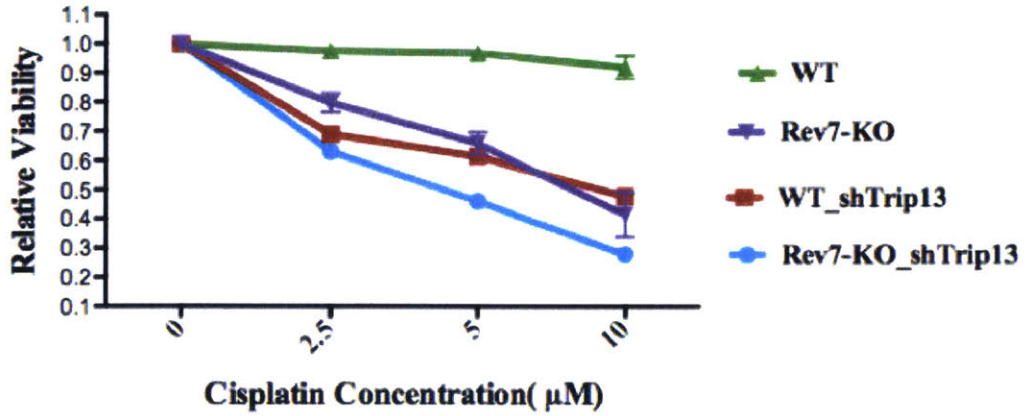

Fig.7a: p75 shRNA qPCR analysis

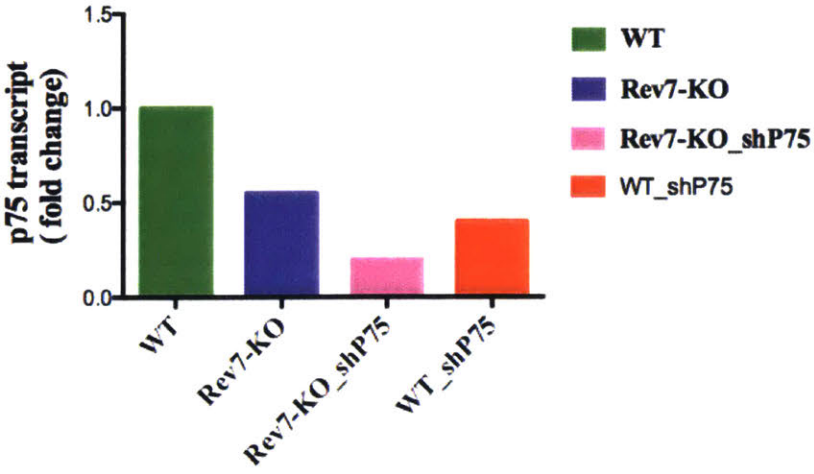

Fig.7b: Cell titer glo cisplatin sensitivity analysis of p75 knockdown KP cells

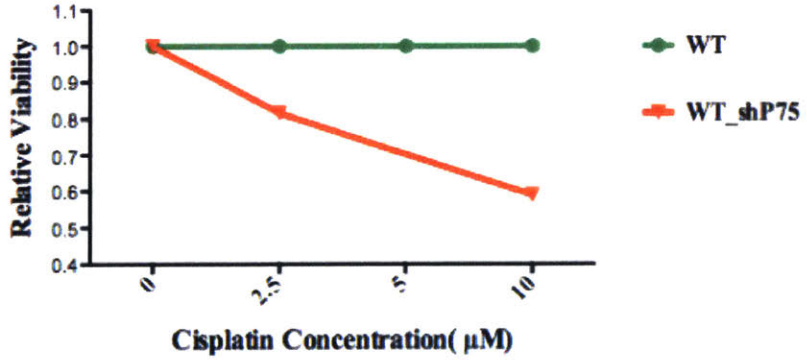

Fig.7c: Cell titer-glo cisplatin sensitivity analysis of p75 shRNA_Rev7KO cells

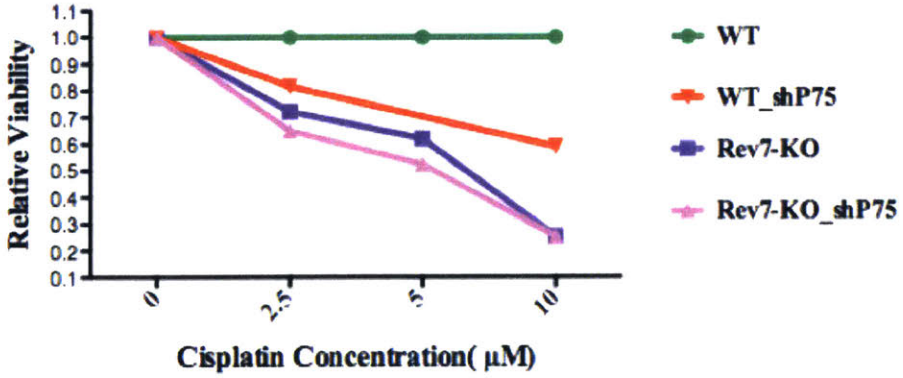

Fig.8: Co-IP analysis probing Rev7-p75 and Rev7-CtIP interaction in cisplatin treated KPWT cells

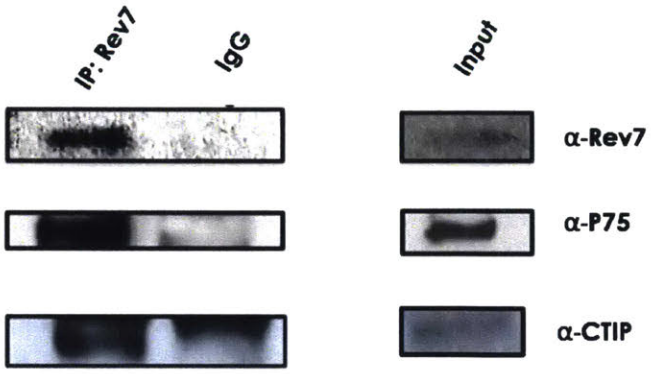

Fig.9: NMR analysis of Trip13-NTD and Rev7 interaction

NMR: mTRIP13 NTD; hRev7/Rev3RBM

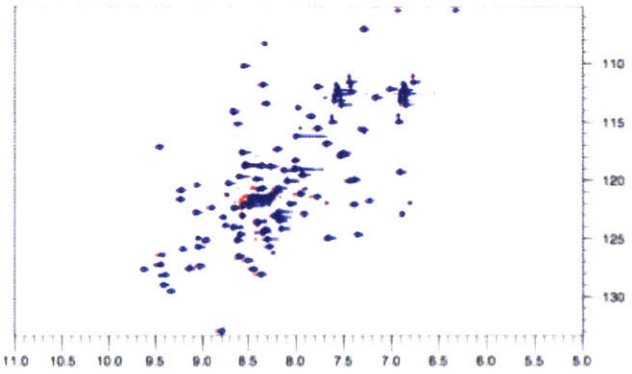

Red: only ^{15}N-labeled mTrip13 N-terminal domain (residues 1-106)

Blue: ^{15}N-labeled mTrip13 N-terminal domain (residues 1-106) plus hRev7-R124A/Rev3-RBM2

Fig.10a: NMR analysis of p75-NTD and Rev7 interaction

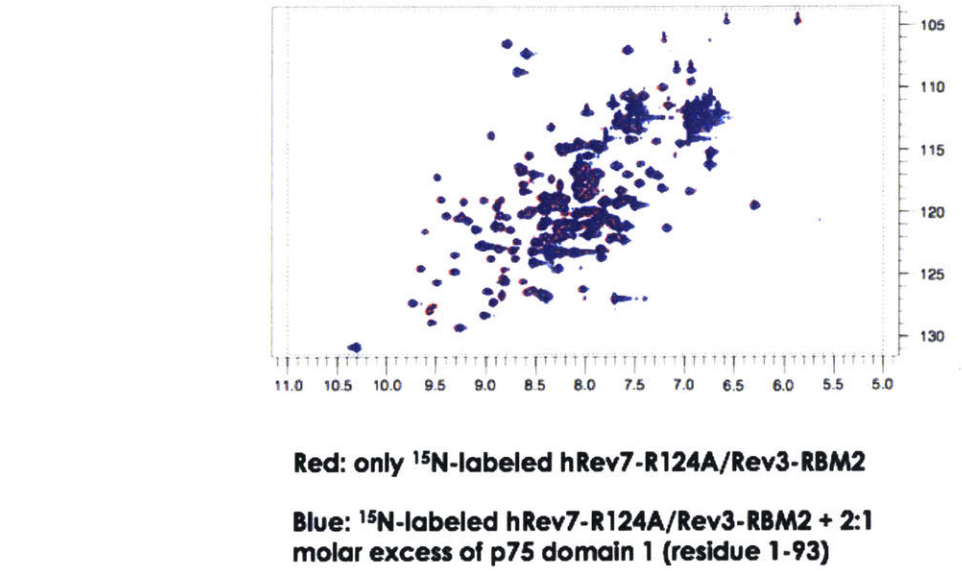

Fig.10b: Gel Filtration analysis of p75-NTD and Rev7 interaction

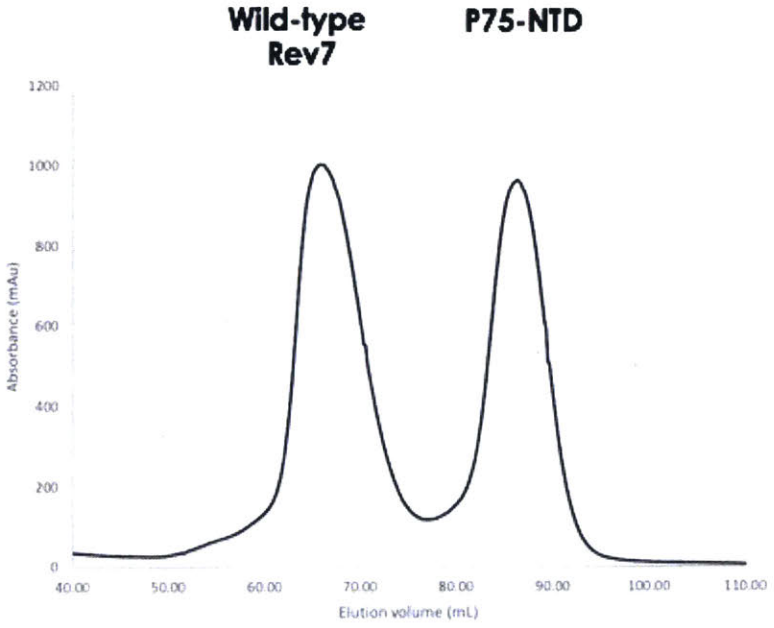

Fig.10c: NMR analysis of p75-CTD and Rev7 interaction

NMR: mP75 CTD; hRev7/Rev3RBM2

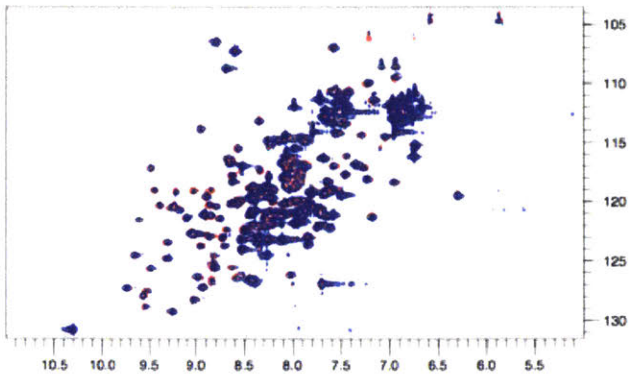

Red: only ^{15}N-labeled hRev7-R124A/Rev3-RBM2

Blue: ^{15}N-labeled hRev7-R124A/Rev3-RBM2 + 2:1 excess of p75 domain 2 (residue 346-424)

Fig.11: CometChip analysis of DSB repair, as seen in comet tail length, in Rev7KO treated with ionizing radiation vs KPWT treated with ionizing radiation cells, p-value <0.001

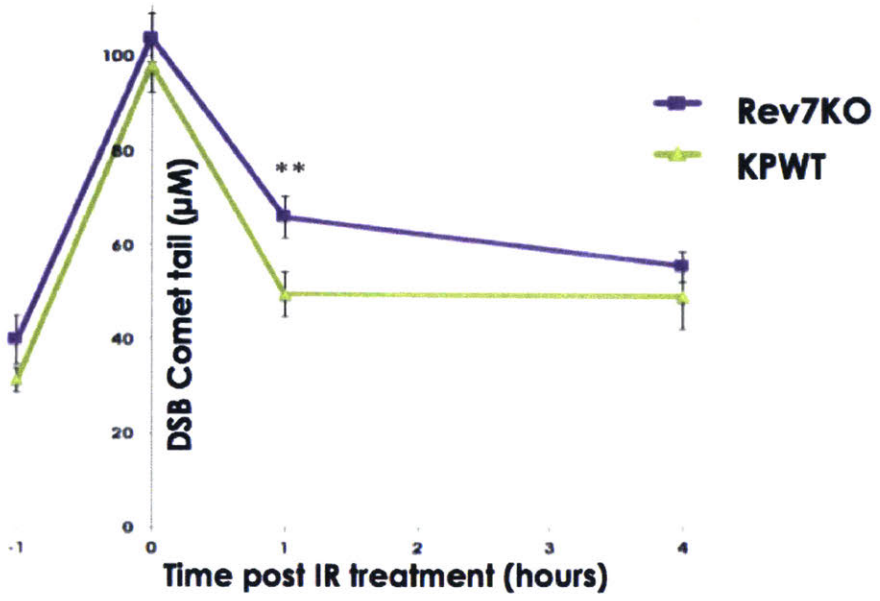

Fig.12a: FM-HCR assessing HR DSB repair activity in Rev7KO cells, p-value <0.001

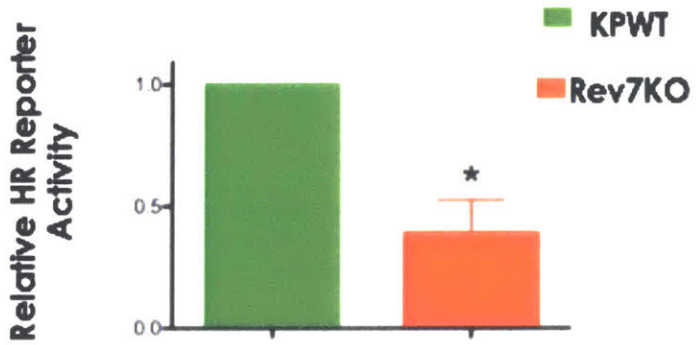

Fig.12b: FM-HCR assessing NHEJ DSB repair activity in Rev7KO cells, p-value <0.001

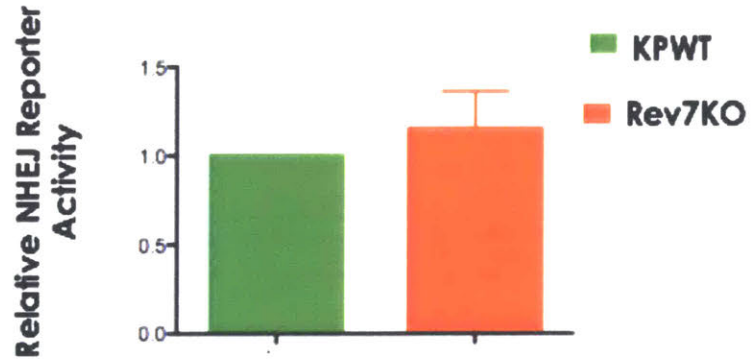

Supplemental Figures

Fig. S1: CoIP analysis of Rev7-TRIP13 interaction in untreated HeLa cells

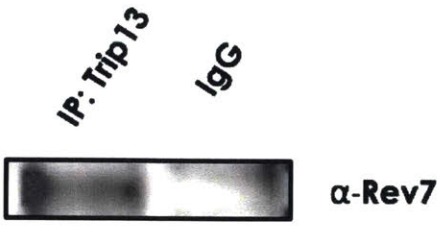

Fig. S2: Sequences for shRNAs targeting mouse TRIP13 (mTrip13)

Sequences for shRNAs targeting mouse TRIP13 (mTrip13)
mTrip13_shRNA1: **TGCTGTTGACAGTGAGCGCTAGAGCTGACATCAAGCAATATAGTGAAGCCACAGATGT** **ATATTGCTTGATGTCAGCTCTATTGCCTACTGCCTCGGA**
mTrip13_shRNA2: **TGCTGTTGACAGTGAGCGCCAGTGCATATCTAAAGGCAAATAGTGAAGCCACAGATGT** **ATTTGCCTTTAGATATGCACTGTTGCCTACTGCCTCGGA**
mTrip13_shRNA 3: **TGCTGTTGACAGTGAGCGCTGGGTGTACAATCTTTGTCAATAGTGAAGCCACAGATGT** **ATTGACAAAGATTGTACACCCATTGCCTACTGCCTCGGA**
mTrip13_shRNA 4:

TGCTGTTGACAGTGAGCGACACCGTACTCTTCTCAGACAATAGTGAAGCCACAGATGT ATTGTCTGAGAAGAGTACGGTGGTGCCTACTGCCTCGGA
mTrip13_shRNA5: TGCTGTTGACAGTGAGCGCTGGCCAGTTGATTGAAATAAATAGTGAAGCCACAGATGT ATTTATTTCAATCAACTGGCCATTGCCTACTGCCTCGGA

Fig. S3: Sequences for shRNAs targeting mouse p75 (mP75)

Sequences for shRNAs targeting mouse p75 (mP75)
mP75_shRNA1: TGCTGTTGACAGTGAGCGAACCAAAGGACATATTTCCTTATAGTGAAGCCACAGATGT ATAAGGAAATATGTCCTTTGGTCTGCCTACTGCCTCGGA
mP75_shRNA2: TGCTGTTGACAGTGAGCGCAGGATACATGCTGAAATTAAATAGTGAAGCCACAG ATGTATTTAATTTCAGCATGTATCCTTTGCCTACTGCCTCGGA
mP75_shRNA3: TGCTGTTGACAGTGAGCGCAGCCATAAGTGTCAATGTGTATAGTGAAGCCACAG

ATGTATACACATTGACACTTATGGCTTTGCCTACTGCCTCGGA
mP75_shRNA4: TGCTGTTGACAGTGAGCGCTAGAAGGTACAAATTTGTTTATAGTGAAGCCACAGATGT ATAAACAAATTTGTACCTTCTATTGCCTACTGCCTCGGA
mP75_shRNA5: TGCTGTTGACAGTGAGCGATCGGCAGACTTCAGATGTAAATAGTGAAGCCACAGATGT ATTTACATCTGAAGTCTGCCGACTGCCTACTGCCTCGGA

Fig. S4: FM-HCR assessing HR DSB repair activity in Rev7 deficient HeLa cells

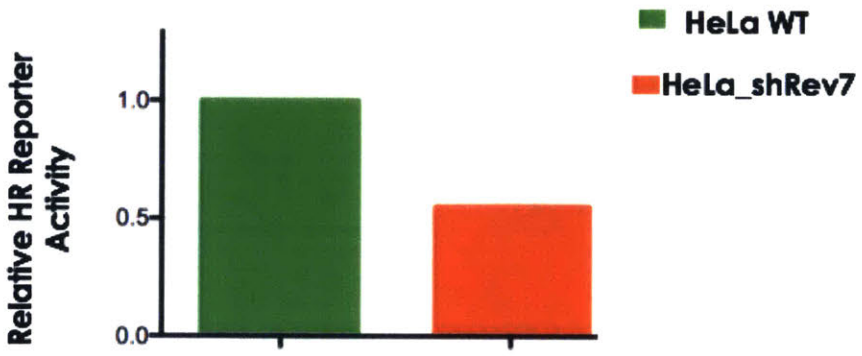

Chapter 4

Effect of Rev7 Dimerization on Structure and Function of the Rev1/Polz Translesion Synthesis Complex

Alessandro A. Rizzo[1], Faye-Marie Vassel[2], Nimrat Chatterjee[2], Sanjay D'Souza[2], Yunfeng Li[1], Bing Hao[1], Michael T. Hemann[2,3], Graham C. Walker[2] and Dmitry M. Korzhnev[1,*]

[1]Department of Molecular Biology and Biophysics, University of Connecticut Health Center, Farmington, CT 06030, USA

[2]Department of Biology, Massachusetts Institute of Technology, Cambridge, MA 02139, USA

[3]The David H. Koch Institute for Integrative Cancer Research, Massachusetts Institute of Technology, Cambridge, MA 02139, USA

Contributions: A.R., F.M.V., N.C. S.D., Y.L., B.H., G.C.W., M.T.H., and D.K conceived the idea for the research, designed experiments and interpreted data. A.R., G.C.W., and D.K. wrote the paper.

ABSTRACT

The translesion synthesis (TLS) polymerases Polz and Rev1 form a complex that enables replication of damaged DNA. The Rev7 subunit of Polz, which is a multifaceted HORMA protein with roles in TLS, DNA repair and cell cycle control, facilitates assembly of this complex by binding Rev1 and the catalytic subunit of Polz, Rev3. Rev7 interacts with Rev3 by a mechanism conserved among HORMA proteins, whereby an open-to-closed transition locks the ligand underneath the "safety belt" loop. Dimerization of HORMA proteins promotes binding and release of this ligand, as exemplified by the Rev7 homolog, Mad2. Here, we investigate the dimerization of Rev7 when bound to the two Rev7-binding motifs (RBMs) in Rev3 by combining *in vitro* analyses of Rev7 structure and interactions with a functional assay in a $Rev7^{-/-}$ cell line. We demonstrate that Rev7 uses the conventional HORMA dimerization interface to both form a homodimer when tethered by the two Rev7-binding motifs in Rev3, and to heterodimerize with other HORMA domains, Mad2 and $p31^{comet}$. Structurally, the Rev7 dimer can only bind one copy of Rev1, revealing an unexpected Rev1/Polz architecture. In cells, mutation of the Rev7 dimer interface increases sensitivity to DNA damage. These results provide new insights into the structure of the Rev1/Polz TLS assembly and highlight the function of Rev7 homo- and heterodimerization.

SIGNIFICANCE STATEMENT

We describe a novel class of protein-protein interactions mediated by the HORMA dimerization interface of the multitasking scaffolding protein Rev7 and unravel the significance of these interactions for the cellular response to DNA damage. Rev7 is an accessory subunit of the TLS DNA polymerase Polζ, which plays a central role in replication of damaged DNA.

Besides TLS, Rev7 has multiple functions in repair of double-strand breaks and cell cycle control. This study answers outstanding questions about the structure and function of the elusive Rev1/Polζ TLS complex and reveals the mechanism of Rev7 interactions with HORMA proteins from other pathways. These results contribute to the structural biology of DNA replication and to our understanding of the important class of HORMA proteins.

DNA damage creates replication blocks, leading to fork collapse, double-strand breaks and genomic rearrangements (1,2). To avert this scenario, specialized DNA polymerases (Y-family Rev1, Polh, Poli, Polk and B-family Polz) help human cells tolerate DNA damage by replicating opposite the lesions or filling single-stranded gaps left after replication in a process called translesion synthesis (TLS) (3-6). Rev1/Polz-dependent TLS occurs through a two-step mechanism in which one polymerase (typically Polh, Poli, Polk) inserts a nucleotide opposite the lesion, while another polymerase (typically Polz) extends the distorted primer terminus (7- 10). During this process, TLS DNA polymerases assemble into a multiprotein complex on the monoubiquitinated sliding clamp PCNA (11) with the aid of a scaffold protein, Rev1 (4,5).

Polz acts as the "extender" TLS DNA polymerase due to its proficiency in mismatched primer extension (7,8), although it can insert nucleotides across certain lesions (12,13). The catalytic subunit of Polz, Rev3, forms a complex with Rev7 (called Polz2), although Polz is now known to function as a four-subunit complex (called Polz4) composed of Rev3, Rev7, PolD2 and PolD3 (Fig. 1A) (14-18). PolD2 and PolD3 are subunits of the replicative DNA polymerase Polδ (19), but also enhance the efficiency of Polz4 relative to Polz2 (14-18). Polz4 is assembled by protein-protein interactions, including those between the Rev7-binding motifs (RBMs) of Rev3 and Rev7 (20-22), between the C-terminal domain of Rev3 and PolD2 (16), and between PolD2

and PolD3 (23). The activity of Polz4 is coordinated with other TLS polymerases through interactions of Rev7 and PolD3 with the Rev1 C-terminal (Rev1-CT) and polymerase-associated (Rev1-PAD) domains (Fig. 1A) (24-31).

Besides TLS, Polz participates in the repair of DNA interstrand crosslinks (ICLs) (32) and replication of "fragile-site" regions and non-B DNA structures (33,34), while the individual subunits also act in other pathways. Rev7 (*MAD2L2*) regulates the metaphase-to-anaphase transition by sequestering CDH1, thus preventing premature activation of the anaphase-promoting complex/cyclostome (APC/C) (35). In addition, Rev7's *in vitro* interactions with the spindle assembly checkpoint (SAC) protein Mad2 (36) and its interactions and colocalization with Ras-related nuclear (RAN) GTPase (37) are consistent with a role in regulation of the cell cycle. Rev7 also contributes to pathway choice for the repair of double-strand breaks (38,39).

Rev7 belongs to the HORMA (Hop1, Rev7, Mad2) domain family (21,40), whose members act as interaction modules in several cellular pathways (41). Structurally, HORMA domain proteins consist of a β-sheet flanked by three α-helices, and a "safety belt" region that can adopt two distinct conformations ("open" and "closed") (42-45). The interaction between Rev7 and the $Rev3^{1847\text{-}1898}$ peptide (below called Rev3-RBM1) (21) occurs by a mechanism conserved among HORMA domains, in which the "safety belt" loop closes around a partner protein (Fig. 1B). This mechanism is best characterized (46) for the interaction of a related HORMA protein, Mad2, with a peptide motif from the SAC proteins Mad1 or Cdc20 (42-44), whereby, upon binding, Mad2 converts from "open" to "closed" states (42-44). In the case of Mad2, this conformational change is induced by dimerization (46). Notably, although two copies of Mad2 are held in immediate proximity by Mad1, the Mad2 homodimer can only form between "open"

and "closed" monomers (47) or between the two "closed" apo-monomers (48), but not between two ligand-bound "closed" Mad2 even if tethered together (46-48). In turn, disassembly of the Mad2/Mad1 complex involves active opening of Mad2 by the AAA+ ATPase TRIP13 aided by Mad2 heterodimerization with another HORMA protein p31^{comet} (*MAD2L1BP*) (49-53). Taken together, these studies suggest that homo- and heterodimerization mediates formation and disassembly of HORMA domain complexes by the "safety belt" mechanism. Accordingly, Rev7 also forms a homodimer (20) as well as a heterodimer with Mad2 (36), although these structures are not available. Instead, most studies on Rev7 used a dimer-breaking mutation, R124A, to induce a monomeric state (20,21,27-29).

The role of Rev7 dimerization remained unexplored until its relevance was underscored by a study that identified a second Rev7-binding motif on Rev3 (within residues 1974-2025, referred to as RBM2), which is in proximity to Rev3-RBM1 (Rev3$^{1847-1898}$) (Fig. 1A,C) (22). This finding poses questions about the consequences of Rev7 dimerization for the assembly and function of the TLS machinery, given the role of Rev7 as an interaction module: (i) How many copies of Rev7 are present in human Polz? (ii) If both Rev3-RBMs can bind Rev7 simultaneously, can the two copies of Rev7 form a dimer within Polz (considering the two bound "closed" Mad2 do not form a dimer (46))? (iii) If the two Rev3-bound Rev7 can form a dimer, is it still competent to interact with known Rev7 partners, Rev1-CT and Rev1-PAD? (iv) If the Rev7 dimer can interact with these domains from Rev1, how many copies of Rev1 can bind Polz, considering Rev1 also functions as a scaffold? (v) And, finally, what is the role of Rev7 dimerization in the response to DNA damage?

To answer these questions, we have taken an *in vitro* biophysical and biochemical approach

combined with a functional assay in a Rev7$^{-/-}$ cell line. This study provides evidence that Rev7 can form a Rev3-tethered homodimer within Polz while retaining interaction with Rev1, as well as heterodimers with other HORMA domains through the conserved homodimerization interface. Our functional assay in a Rev7$^{-/-}$ cell line demonstrates that Rev7 homo- or heterodimerization is required for cell survival after treatment with the DNA crosslinking agent cisplatin. Overall, this work provides insights into the interactions that assemble the TLS machinery and highlights the role of Rev7 dimerization in mediating the response to DNA damage.

RESULTS Crystal structure of Rev7^{R124A}/Rev3-RBM2 confirms second Rev7 binding site on Rev3

Following previous reports identifying a second Rev7-binding motif in the Rev3 subunit of Polz (Fig. 1A,C) (22) and showing Rev7 and other HORMA domain proteins tend to form dimers (20,36,47-49,54), we set out to determine the consequences of Rev7 dimerization on the structure and function of the Rev1/Polz complex. First, given its significance for this study, we confirmed the second Rev7-binding motif in Rev3 (RBM2) (22) by solving a crystal structure of the Rev7^{R124A}/Rev3-RBM2 complex (Fig. 1B, green/orange; Table S1; PDB 6BD8). Similar to previous studies, we used the Rev7^{R124A} mutation that prevents homodimerization (20). Importantly, although a previous structure of Rev7^{R124A}/Rev3-RBM1 (PDB 3ABD (21)) was used for molecular replacement, Rev3-RBM1 was omitted. Still, the resulting map showed well-defined electron density corresponding to the Rev3-RBM2 peptide bound to Rev7.

Our structure shows Rev7^{R124A} in the "closed" conformation with Rev3-RBM2 bound by the "safety belt" of Rev7 (Fig. 1B, green/orange). It has 1.28 Å backbone RMSD against

$Rev7^{R124A}$/Rev3-RBM1 (3ABD (21) over residues 13-205; Fig. 1B, grey) but with one difference. In the safety belt region on Rev7 at residues 163-166, our structure shows a β-strand leading into a β-turn (Fig. 1B, green) whereas previous structures were either missing density (Fig. 1B, grey) (21) or modeled the density as an α-helix (28,29). With respect to Rev3, despite variation in sequence (Fig. 1C), Rev3-RBM1 and -RBM2 adopt nearly identical conformations when bound to Rev7 (Fig. 1D). Overall, our analysis verifies that Rev3-RBM2 (22) is a *bona fide* Rev7 interaction motif.

Rev7 uses conventional HORMA interface for homodimerization

Previously, Hara *et al.* showed that $Rev7^{WT}$ undergoes dimerization with a K_d of 13 μM (20). However, $Rev7^{WT}$/Rev3-RBM1 failed to crystallize, unlike $Rev7^{R124A}$/Rev3-RBM1 which harbors a dimer-breaking mutation (20). We attempted to determine the structure of the Rev7 dimer, but only obtained crystals of $Rev7^{WT}$/Rev3-RBM2 that diffracted to 2.80 Å under high-salt conditions where the protein crystallized as a monomer (Table S1; PDB 6BI7). This is not unexpected, considering the R124A mutation that abolishes electrostatic interactions of the arginine side-chain prevents formation of the dimer (20). Our structure of $Rev7^{WT}$/Rev3-RBM2 shows no substantial differences from structures of $Rev7^{R124A}$/Rev3-RBM1 (21) or $Rev7^{R124A}$/Rev3-RBM2 (Fig. S1).

To map the Rev7 dimerization interface, we introduced 32 single mutations to solvent- exposed residues and first determined the oligomeric state using gel filtration chromatography (Table S2). The Rev7/Rev3-RBM1 complexes were loaded on a gel filtration column so the concentration of eluted protein was about 0.3-0.4 mM. Under these conditions, $Rev7^{WT}$/Rev3- RBM1 and

Rev7^{R124A}/Rev3-RBM1 elute as distinct peaks corresponding to the monomer and the dimer (Fig. 2A) (20). Using this approach, we identified 8 mutations (in addition to R124A) that disrupt the Rev7 dimer, including E35A, V39R, K44A, L128A, K129A, V132A, D134A, and A135D. When mapped onto Rev7^{R124A}/Rev3-RBM2, these residues form a continuous surface centered on helix αC (Fig. 2B).

Next, we cross-validated the mutations with a yeast two-hybrid assay using fusions of Rev7 with the activation domain (AD) and DNA-binding domain (BD) of the *GAL4* transcription factor (55). As expected, transformation of yeast strain PJ69-4A with plasmids encoding AD- and BD-fused Rev7^{WT} resulted in growth on -AHLW plates (Fig. 2C, top; Fig. S2A), indicating this assay is sensitive to formation of the Rev7 dimer. In contrast, yeast did not grow on -AHLW plates when cells were transformed with AD-fused Rev7^{mutant} and BD-fused Rev7^{WT} despite the presence of viable transformants on –LW plates, suggesting that all mutations abolished Rev7 dimerization (Fig. 2C, top; Fig. S2A). In the reverse orientation (AD-fused Rev7^{WT}, BD-fused Rev7^{mutant}), the mutations K44A, R124A, K129A, D134A, and A135D abolished the interaction, while the mutations E35A, V39R, L128A, and V132A permitted growth on -AHLW plates (Fig. 2C, top). A possible explanation for this discrepancy is the difference in the number of mutations per Rev7 dimer. During the gel filtration analysis, both copies of Rev7 harbored a dimer- breaking mutation whereas during the yeast two-hybrid assay, only one protomer contained the mutation.

Overall, our analyses show that Rev7 homodimerization is mediated by the interface centered around helix αC. This is the canonical interface responsible for homo- and heterodimerization of other HORMA proteins (Fig. 2D) (47-49,54), providing us with confidence in the identification

of this region.

Rev7 interacts with Mad2 and p31^{comet} through the dimerization interface

Capitalizing on our analysis of Rev7 homodimerization, we used the yeast two-hybrid assay to probe heterodimerization of Rev7 with two other HORMA domains, Mad2 and p31^{comet}. Consistent with the previous report of a Rev7/Mad2 interaction (36), growth on -LW and -AHLW media plates was observed in both orientations when yeast strain PJ69-4A was transformed with Mad2 and Rev7^{WT} (Fig. 2C, center; Fig. S2B). We then tested our dimer-breaking mutations (Table S2) to determine whether the homodimerization interface in Rev7 mediates this interaction. In one orientation (AD-fused Rev7^{mutant}, BD-fused Mad2), all mutations broke the interaction. In the reverse orientation (AD-fused Mad2, BD-fused Rev7^{mutant}), K44A, R124A and A135D broke the interaction, while the remaining mutations still grew on -AHLW plates (Fig. 2C, center; Fig. S2B). The overlap in mutations that broke the Rev7 homodimer (Fig. 2C, top) and Rev7/Mad2 heterodimer (Fig. 2C, center) in this orientation is likely not a coincidence, but instead reports on the relative contributions of these residues to the binding energy.

To date, no interaction has been reported between p31^{comet} and Rev7, although a crystal structure of the p31^{comet}/Mad2 HORMA heterodimer is available (49). Considering the tendency of HORMA domain proteins for heterodimerization, we investigated whether Rev7 binds p31^{comet} and observed an interaction between AD-fused p31^{comet} and BD-fused Rev7^{WT} (Fig. 2C, bottom; Fig. S2C). The growth on -AHLW plates for Rev7^{WT}/p31^{comet}

transformants appears to be less robust than for Rev7^{WT}/Mad2 or Rev7^{WT} dimer, indicating a weaker interaction. We then tested the mutations to the Rev7 dimer interface (Table S2) and found that all mutations broke interaction between AD-fused p31^{comet} and BD-fused Rev7^{mutant} (Fig. 2C, bottom; Fig. S2C). Overall, our data corroborate the interaction between Rev7 and Mad2 (36), which we mapped to the Rev7 homodimerization interface. In addition, we identified an interaction between Rev7 and p31^{comet} through the same interface. These results demonstrate that Rev7 uses the dimerization interface for interaction with other HORMA domain proteins.

Two copies of Rev7 can bind adjacent sites on Rev3 and form a tethered dimer

Because Rev7 is an interaction module, the number of Rev7 in Polz and its oligomeric state will have implications for assembly of the TLS machinery. Therefore, we set out to determine if both Rev7-binding sites on Rev3 can be simultaneously occupied and, if so, test whether these tethered Rev7 form a dimer. Specifically, we used a fragment (Rev3-RBM12, residues 1871-2014) that includes both Rev7-binding motifs, which likely mimics the interaction with full-length Rev3 because both RBMs are located within a disordered region ~200 residues away from the nearest structured domain. Since RBM1 and RBM2 are separated by ~90 residues, one might assume there are no constraints preventing Rev3 from binding a Rev7 dimer. On the other hand, the Rev7 homolog Mad2 does not form a symmetric homodimer between two protomers that are similarly bound by two sites on Mad1 (46-48). Instead, Mad1- bound "closed" Mad2 interacts with an "open" apo-Mad2, promoting the "open" to "closed" transition and interaction with Mad1, followed by dissociation of the dimer (46). With this in mind, we investigated the stoichiometry of the Rev3/Rev7 interaction and asked whether Rev7 exhibits behavior similar to

Mad2.

Rev7^{WT}/Rev3-RBM12 elutes as a single peak from a gel filtration column at a volume consistent with a 2:1 stoichiometry (Fig. 3A, purple) and an SDS gel shows two proteins of the expected size in the peak fraction (Fig. 3A, inset). We then introduced a double mutation P1880A/P1885A to knock out Rev3-RBM1, which shifted the elution volume (Fig. 3A, orange) to nearly the volume of monomeric Rev7^{R124A}/Rev3-RBM2 (Fig. 3A, green) when loaded at low concentration to preclude intermolecular Rev7 dimerization (Fig. S3A). Still, an SDS gel of the mutant shows two bands corresponding to Rev7 and Rev3-RBM12$^{P1880A/P1885A}$ coeluting (not shown).

Furthermore, we collected SAXS measurements (Table S3, Fig. S3B) on Rev7^{WT}/Rev3-RBM12 and calculated a molecular weight consistent with a 2:1 stoichiometry (68.8±0.6 kDa *vs* theoretical 68.4 kDa) (Fig. S3C, left). We also collected SAXS measurements on Rev7^{R124A}/Rev3-RBM12, which is unable to form an intermolecular Rev7 dimer, resulting in a molecular weight of 72.5±4.2 kDa (Fig. S3C, right). This eliminates the possibility of a 2:2 complex held together by Rev7 dimerization. Taken together, the data indicate both Rev7 binding sites on Rev3 can be simultaneously occupied.

To address whether the two Rev7, tethered by Rev3, form a dimer, we collected SAXS measurements on Rev7^{WT}/Rev3-RBM12 and two complexes harboring one or three dimer-breaking mutations (Rev7^{R124A}/ or Rev7^{K44A,R124A,A135D}/Rev3-RBM12) (Fig. S3,4). Because SAXS can report on molecular shape, we reasoned that if Rev7 forms a tethered dimer, then mutating the dimer interface will alter the shape of the complex, and the inverse. Consistent

with a Rev7 dimer, the mutations altered the scattering intensity at low-q where the data is sensitive to larger scale structural perturbations (Fig. 3B). As expected, P(r) (pair-distance distribution functions) show the effect of the mutations was to expand the complex (Fig. 3C, Fig. S4B-D). Interestingly, the P(r) distributions point to a more extended conformation for $Rev7^{K44A,R124A,A135D}$ than for $Rev7^{R124A}$ when in complex with Rev3-RBM12 (Fig. 3C), suggesting $Rev7^{R124A}$ retains residual interaction when tethered.

To illustrate that neither the mutations themselves nor protomer-level conformational changes explain the mutation-induced variations in the SAXS data (Fig. 3B), we determined a crystal structure of $Rev7^{K44A,R124A,A135D}$/Rev3-RBM2 (Fig. S5A, Table S1; PDB 6BCD) and simulated SAXS data for this structure and the structures of $Rev7^{R124A}$/Rev3-RBM2 and $Rev7^{WT}$/Rev3-RBM2, which resulted in identical scattering intensity profiles at low-q (Fig. S5B,C *vs* Fig. 3B). Furthermore, we collected ^{1}H-^{15}N HSQC NMR spectra of $Rev7^{K44A,R124A,A135D}$/Rev3- RBM2 and $Rev7^{R124A}$/Rev3-RBM2, which confirmed the lack of mutation-induced conformational changes (Fig. S5D).

Finally, to cross-validate the formation of a tethered dimer, we collected ^{1}H-^{15}N HSQC spectra on $Rev7^{WT}$/ and $Rev7^{R124A}$/Rev3-RBM12 (MW 68 kDa) (Fig. S6). The $Rev7^{WT}$/Rev3- RBM12 spectrum displays little to no peak intensity for structured protein residues, consistent with slow tumbling of the Rev7 dimer that behaves as a single entity. When the R124A mutation is introduced to the dimer interface, which should loosen the tethered dimer, the spectrum improves, reflecting faster tumbling of independent Rev7 protomers connected by a flexible linker. Overall, the data indicate two copies of $Rev7^{WT}$ can bind Rev3, where they

form a tethered dimer.

Tethered Rev7 dimer retains interaction with Rev1-CT, but does not bind Rev1-PAD

After identifying the second Rev7 interaction motif on Rev3, Tomida *et al.* (22) proposed a model where Rev7 mediates a bivalent interaction with Rev1 by binding Rev1-CT (27-29) and Rev1-PAD (31). We tested this model and determined whether the tethered Rev7 dimer retains the ability to bind known Rev7 interaction partners. Because Rev7 interacts with Rev1-CT, which is known to also bind Polh, Poli, Polk and PolD3 through a second interface (25-30), the number of Rev1 attached to Polz through the Rev7/Rev1-CT interaction will have implications for assembly of the TLS machinery. With respect to Rev1-PAD, a previous report using a pull-down assay showed that yeast Rev7 can bind Rev1-PAD (31), although this has not been confirmed in higher eukaryotes.

First, we tested the interaction of human Rev1-PAD with Rev7^{R124A}/Rev3-RBM2 by NMR, which can detect weak binding. We collected ^{1}H-^{15}N HSQC spectra of ^{15}N-labeled monomeric Rev7^{R124A}/Rev3-RBM2 with unlabeled Rev1-PAD added to molar excess; however, chemical shift perturbations characteristic of binding were not observed (Fig. S7A). We next considered the possibility that Rev1-PAD can only interact with tethered dimeric Rev7 and tested the interaction of Rev1-PAD with Rev7^{WT}/Rev3-RBM12 using gel filtration chromatography; however, the proteins eluted as separate peaks despite concentrations of 750 mM and 150 mM in the elution fractions, respectively, again suggesting a lack of interaction (Fig. S7B). Overall, the data indicate human Rev1-PAD does not interact with Rev3-bound Rev7.

The interaction of human Rev1-CT with Rev7^{R124A}/Rev3-RBM1 has been shown by NMR

titrations and isothermal titration calorimetry (ITC) from our laboratory and subsequent crystal structures, which revealed a 1:1 stoichiometry for the Rev7^{R124A}/Rev1-CT complex (27-29). Here, we found Rev7^{WT}/Rev3-RBM12 still interacts with Rev1-CT, as the complex coelutes from a gel filtration column (Fig. S7C). We further validated this interaction by ITC (Fig. 4), which, surprisingly, indicates only one copy of Rev1-CT can bind Rev7^{WT}/Rev3-RBM12 despite the presence of two Rev7 (stoichiometry parameter n = 1.2). Notably, the dissociation constant (K_d) of 11.4 μM and association enthalpy (ΔH) of -42.9 kJ/mol for this complex are consistent with our previous ITC data for the interaction of Rev7^{R124A}/Rev3-RBM1 with Rev1-CT (K_d = 1.3 μM, ΔH = -39.2 kJ/mol) (27), reflecting the same heat is released when Rev1-CT binds to the Rev7^{R124A} monomer or the Rev7^{WT} dimer.

Model of the Rev7 dimer suggests 2:1 stoichiometry for Rev7:Rev1-CT interaction

To confirm and understand the 2:1 stoichiometry of the Rev7:Rev1 interaction when Rev7 is forming a tethered dimer in Polz, we modeled the structure of the Rev7^{WT}/Rev3-RBM2 dimer using HADDOCK (56) with the dimer-breaking mutations described above as input (Fig. 2B, Table S2). The resulting 200 models of the Rev7^{WT}/Rev3-RBM2 dimer were *all* grouped into a single cluster by HADDOCK and show the two Rev7 protomers in an antiparallel orientation with the C-terminus of helix αC forming the core of the interface (Fig. 5A, top). Encouragingly, the lowest-energy structure of the Rev7^{WT}/Rev3-RBM2 dimer exhibits remarkable similarity to the symmetric apo-Mad2 dimer (48) (Fig. 5A, bottom), providing us with confidence in our model.

To cross-validate our model, we collected SAXS/WAXS (small-angle / wide-angle X-ray

scattering) data on the dimeric Rev7^{WT}/Rev3-RBM2 construct and compared the experimental scattering with our model of the dimer (Fig. 5B; Fig. S8). Agreement was observed up to q = 0.16-0.18 Å^{-1}, suggesting our model captures the shape of the complex. To rationalize the discrepancy at higher q, we also collected SAXS/WAXS data on monomeric Rev7^{R124A}/Rev3-RBM2 and predicted data based on our crystal structure (Fig. 1B, green/orange), resulting in the same level of agreement up to q = 0.16-0.18 Å^{-1} (Fig. 5C). This discrepancy at high-q may be caused by dynamics of Rev7/Rev3 in solution, as a ^{1}H-^{15}N HSQC spectrum of Rev7^{R124A}/Rev3- RBM2 contains ~25% fewer peaks than expected presumably due to μs-ms exchange line- broadening (Fig. S5D).

With respect to the Rev7:Rev1 stoichiometry, superposition of the crystal structure of Rev7^{R124A}/Rev3-RBM1/Rev1-CT (29) onto our model of the Rev7 dimer reveals steric clash between the two Rev1-CT domains (Fig. 5D), providing an explanation for the 2:1 Rev7:Rev1 stoichiometry observed by ITC: once the first Rev1-CT domain binds the Rev7 dimer, binding of the second is occluded by the first. Furthermore, superposition of the Rev7^{R124A}/Rev3-RBM1/Rev1-CT structure (29) onto the dimer structures formed by other HORMA proteins, including the symmetric apo-Mad2 homodimer (48), p31^{comet}/Mad2 heterodimer (49), open/closed Mad2 dimer (47) and Atg13/Atg101 heterodimer (54) in *all* cases resulted in steric clash between the two Rev1-CT (Fig. S9).

Taken together, our ITC data for the Rev7^{WT}/Rev3-RBM12 - Rev1-CT interaction (Fig. 4) and a structural model for the Rev7^{WT}/Rev3-RBM2 dimer (Fig. 5) provide evidence that the Rev7 dimer can only bind one copy of Rev1-CT.

Rev7 dimerization mutant is unable to restore cisplatin resistance of Rev7$^{-/-}$ cells

Given the role of Rev7-mediated interactions in the assembly and function of Polz (7- 10), we were interested in whether Rev7 dimerization has a functional significance in DNA damage tolerance. To address this, we used a Rev7 knockout cell line developed by Vassel et al (to be published). This cell line was generated using CRISPR/Cas9 system in the *Kras*$^{G12D/+}$;Trp53$^{-/-}$ (KP) lung adenocarcinoma cell line background (57), which is a murine model for human non-small cell lung cancer that is intrinsically resistant to front-line chemotherapeutics like cisplatin (58). The resulting Rev7$^{-/-}$ cells were more sensitive to the DNA crosslinking agent cisplatin and showed reduced viability compared to the parental cell line (Fig. 6, grey *vs* black). To test whether the sensitivity to cisplatin is contingent upon Rev7 dimerization, the Rev7$^{-/-}$ cells were complemented with either Rev7^{WT} or the triple dimer interface mutant, Rev7^{K44A,R124A,A135D}. While complementation with Rev7^{WT} restored resistance to cisplatin, complementation with Rev7^{K44A,R124A,A135D} was unable to rescue the sensitized phenotype (Fig. 6A, purple *vs* brown) despite the appearance of stably-expressed protein by Western blot (Fig. 6B, brown). Overall, the data indicate that interactions mediated by the Rev7 HORMA dimerization interface are required for cell viability after treatment with cisplatin.

DISCUSSION

The TLS DNA polymerases Rev1, Polh, Poli, Polk and Polz are recruited to replication-blocking DNA lesions and assemble into a multiprotein complex that enables DNA synthesis (7-10). The B-family polymerase Polz participates in TLS by extending from the aberrant primer-template junction after another TLS polymerase has inserted a nucleotide opposite the lesion

(7,8,14). The subunit composition of Polz, which had been known as a complex of the catalytic Rev3 and accessory Rev7 subunits (12), was recently revised after several groups discovered that Polz contains two additional subunits, PolD2 and PolD3 (in humans) or Pol31 and Pol32 (in yeast) that are bound through interaction with the C-terminal domain of Rev3 (14-18). The latter two subunits are known subunits of the replicative DNA polymerase Polδ (19), suggesting Polz has an architecture typical for B-family polymerases. On the other hand, Rev7, which is a HORMA domain protein (21), is a unique component of Polz with no analogues in other DNA polymerases.

One function of Rev7 is to bridge Polz with other TLS polymerases through interaction with the scaffold protein Rev1 (4,5,25-30). With this in mind, a recent study from Tomida *et al.* (22) that revealed a second Rev7 interaction motif on human Rev3 (RBM2) in proximity to the previously described Rev3-RBM1 (20), raised several questions about the assembly and stoichiometry of the TLS machinery. The authors proposed a model where both Rev7 interaction sites can be simultaneously occupied by two copies of Rev7, whose function is to mediate a bivalent interaction with two binding modules on Rev1 (Rev1-PAD and Rev1-CT). Noting that, like other HORMA domain proteins (47-49,54), Rev7 is prone to dimerization (20), we tested this model and addressed whether Rev7 can bind the both sites on Rev3 and form a dimer in the context of Polz and whether the presence of two copies of Rev7 affects the interaction of Polz with Rev1.

We confirmed the second Rev7-binding motif on Rev3 and showed that both Rev3- RBMs can be occupied by two Rev7 at the same time, suggesting a 2:1 Rev7:Rev3 stoichiometry. Thus, human Polz includes two copies of Rev7, resulting in a five-subunit complex. When tethered together, these two Rev7 form a homodimer through the canonical HORMA interface (47-

49,54). However, we were unable to detect an interaction between human Rev7 and Rev1-PAD (that was shown in yeast by pull-down (31)). Instead, our binding studies and structural modeling revealed that the tethered Rev7 dimer is still able to interact with Rev1- CT, but with only a single copy. This suggests a 1:1 stoichiometry for assembly of the human Rev1:Polz complex. Beyond studying the role of Rev7 dimerization in Rev1/Polz-dependent TLS, we also established that Rev7 uses its dimerization interface for interaction with other HORMA domains, Mad2 and $p31^{comet}$. Importantly, we also demonstrated that the intact Rev7 dimerization interface is functionally significant *in vivo* as it required for cell viability after cisplatin treatment.

Our study raises questions about the mechanistic role of human Rev7 dimerization. One consequence of tethering two Rev7 by the high-affinity interaction sites on Rev3 is strengthening of the Rev7 dimer interaction relative to that of unbound Rev7. This will reduce the access of other Rev7 interaction partners that use the dimerization interface in a bimolecular interaction, such as other HORMA proteins, which often form heterodimers through the homodimerization interface (36,47-49,54). Given the multiple functions of Rev7 (14,35-39,41), the formation of a tight Rev3-tethered Rev7 dimer in the context of Polz may act as a mechanism to separate the functions of Rev7 by hiding the Rev7 dimerization interface from its interactors from other pathways. In line with this thinking, Rev7 is three orders of magnitude more abundant than Rev3 in human cells (293T) (22) and thus is mostly bound to other proteins. Here, we confirmed the interaction of Rev7 with Mad2 (36) and showed that it occurs through the canonical HORMA dimerization interface. Considering the role for Rev7 in the metaphase-to-anaphase transition (35) and the role of Mad2 as the spindle checkpoint (59), based on our model, a mitotically-relevant Rev7/Mad2 interaction would be disfavored through tethering of the two subunits when Rev7 is participating in TLS.

We have also demonstrated that Rev7 uses its dimerization interface to bind another HORMA protein, p31^{comet}, which plays a role in disassembly of the mitotic checkpoint complex by the AAA+ ATPase TRIP13. In this process, p31^{comet} recognizes a target HORMA protein (Mad2) and brings it in contact with TRIP13, which catalyzes the "closed" to "open" conversion (50-53). Considering the similarity between Mad2 and Rev7 (*MAD2L2*) (36) and the fact that both Mad2 and Rev7 interact with p31^{comet} through a conserved HORMA dimerization interface (49), one might hypothesize that p31^{comet} and TRIP13 also participate in active opening of Rev7 and its dissociation from Rev3. In this case, Rev3-mediated Rev7 dimerization would interfere with a Rev7/p31^{comet} interaction and thus prevent premature unloading of Rev7 and deactivation of Polz. In this regard, one should note that Rev7 and Mad2 exhibit differing behavior: the two Rev3-bound "closed" Rev7 interact to form a dimer, whereas Mad1-bound "closed" Mad2 interacts with ligand-free "open" Mad2 to facilitate ligand uptake accompanied by the conformational change and dissociation of the dimer (46-48).

Finally, this study demonstrates that the Rev7 dimerization interface is required for cell viability after treatment with cisplatin, although the mechanism is unresolved. Presumably, the loss of Rev7 dimerization affects Polz activity and sensitizes cells to cisplatin because Polz participates in TLS across cisplatin DNA adducts (18) and repair of cisplatin DNA interstrand crosslinks (32). However, the sensitization cannot be deductively attributed to a loss of Rev7 dimerization in Polz, as Rev7 contributes to pathway choice for the repair of double-strand breaks (38,39) and potentially functions in mitosis (35). A global loss of the Rev7 dimerization interface may also operate in other contexts including those with Mad2 or p31^{comet}. For example, one might envision a scenario where the dimerization-deficient Rev7 mutants cannot

be unloaded from their partner proteins by TRIP13 through interaction with $p31^{comet}$, resulting in a decrease in Rev7 available for interaction with Rev3.

In summary, this study yields insights into the role of Rev7 dimerization in mediating assembly of the TLS machinery and interactions of Rev7 with HORMA proteins from other cellular pathways. How and whether dimerization affects other functions of Rev7 in cell cycle control (35) or the repair of double-strand breaks (38,39), and any cross-talk between these functions and TLS remains to be determined.

METHODS

Subcloning and Mutagenesis

Subcloning and mutagenesis were carried out using standard molecular biology techniques. The pETDuet-1 (Novagen) based construct for co-expression of human $Rev7^{R124A}$ with Rev3-RBM1 fragment (the first Rev7-binding motif, $Rev3^{1847-1898}$) (20) was used as a template to design corresponding constructs for co-expression of $Rev7^{R124A}$ with other Rev3 fragments, including Rev3-RBM2 (the second Rev7-binding motif, $Rev3^{1988-2014}$) (22) and Rev3-RBM12 (a fragment containing two consecutive Rev7-binding motifs, $Rev3^{1871-2014}$). New fragments were introduced by PCR amplifying codon-optimized Rev3 from a custom-ordered gBlock Gene Fragment (Integrated DNA Technologies) using Q5 DNA polymerase (New England Biolabs), followed by ligating the digested product into the NdeI/XhoI restriction enzyme (ThermoFisher) sites of pETDuet-1 with T4 DNA ligase (New England Biolabs).

Mutations in the Rev7 and Rev3 genes were introduced using the modified inverse PCR procedure (60) without DPN1 digestion. After generating linear double-stranded DNA by amplification of the plasmid with Q5 DNA polymerase (New England Biolabs) using an extension time of 4 minutes, 2 μL of the PCR mixture was phosphorylated in a 25 μL reaction with T4 polynucleotide kinase (New England Biolabs) in T4 DNA ligase buffer. After heat inactivation, 3.5 μL of the phosphorylation mixture was ligated at room temperature for 30 minutes using T4 DNA ligase (New England Biolabs) in a 20 μL reaction and transformed into Top10 cells (ThermoFisher). The correct nucleotide sequence was confirmed in all cases by sequencing (Genewiz).

Protein Expression and Purification

All Rev7 complexes with Rev3-RBM fragments were expressed from pETDuet-1 (Novagen) constructs described above (20). Rev1 C-terminal (Rev1-CT) and Rev1 polymerase- associated (Rev1-PAD) domains were expressed from pET28b+ (Novagen) constructs described elsewhere (26). All proteins demonstrated excellent stability and were expressed and purified following a standard protocol. In brief, *Escherichia coli* BL21(DE3) cells were transformed with the plasmid encoding the protein(s) of interest, bacteria were grown to mid-log phase and then induced overnight with 1 mM IPTG at 20 °C. The following morning, cells were spun down in an F10S-6x500y rotor for 10 minutes at 6000 rpm. The cell pellet was resuspended in the Lysis Buffer consisting of 50 mM sodium phosphate, 300 mM NaCl, 10 mM imidazole, at pH 8 and lysed by sonication. The lysate was then centrifuged in an SS-34 rotor for 45 minutes at 18500 rpm and the supernatant was filtered through a 0.45 μM PVDF membrane directly into TALON cobalt resin that was equilibrated with Lysis Buffer for purification using the His_6 affinity tag. The column was run by gravity flow, washed extensively with Lysis Buffer and the protein was eluted using the Elution Buffer consisting of 50 mM sodium phosphate, 300 mM NaCl, 300 mM imidazole, at pH 8. The proteins were then purified by gel filtration chromatography on a HiLoad 16/600 Superdex75 pg column (GE Healthcare). During this step, the proteins were exchanged into their final buffers as noted. Proteins were concentrated using Amicon Ultra Centrifugal Filters (Millipore) when necessary.

The interaction of Rev7 with Rev3-RBM2 and Rev3-RBM12 was assessed by co- expressing the two proteins using pETDuet-1 and co-eluting the complex on a gel filtration column. After SDS gels of the peak fractions showed two proteins, corresponding to Rev7 and either Rev3-RBM2 or Rev3-RBM12, had eluted together, the identity of Rev3-RBM2 and Rev3- RBM12 was further

confirmed by in-gel trypsin digestion and LC-MS/MS.

Protein Crystallization, X-ray Data Collection and Structure Determination

$Rev7^{R124A}$/Rev3-RBM2, $Rev7^{K44A,R124A,A135D}$/Rev3-RBM2 and $Rev7^{WT}$/Rev3-RBM2 were exchanged into 5 mM HEPES, 100 mM NaCl, 10 mM DTT, at pH 7.4 (20) by gel filtration and concentrated to 45 mg/mL, 45 mg/mL and 60 mg/mL, respectively. In all cases, diffraction quality crystals were obtained by vapor diffusion in hanging drop format at 16 °C when protein solution was mixed at a 1:1 ratio with reservoir solution in 4 μL drops. For $Rev7^{R124A}$/Rev3-RBM2, the reservoir solution consisted of 100 mM sodium acetate, 200 mM NaCl, 1.4 M ammonium sulfate, at pH 5.0 and crystals were flash frozen in the reservoir solution containing 20% (v/v) PEG400. For $Rev7^{K44A,R124A,A135D}$/Rev3-RBM2, the reservoir solution contained 100 mM citrate, 1.6 M ammonium sulfate at pH 5.25 and crystals were frozen in the reservoir solution containing 20% (v/v) sucrose. For $Rev7^{WT}$/Rev3-RBM2, the reservoir solution contained 100 mM citrate, 1M LiCl, 7.5% (w/v) PEG6000 at pH 4.75 and crystals were frozen in the reservoir solution containing 20% (w/v) sucrose.

X-ray diffraction data were collected at the Cornell High Energy Synchrotron Source (CHESS) F1 beamline using a Pilatus 6M detector at a wavelength of 0.976 Å. For all structures, 360 frames were collected in 0.5° wedges with a collection time of 3-6 seconds per image over a total range of 180°. Data were processed using the HKL-2000 package(61). The structures were solved by molecular replacement using the previously reported structure of $Rev7^{R124A}$/Rev3-RBM1 (21) with the program Phaser (62) and refined by iterative cycles of model building and refinement with Coot and Refmac (as part of the CCP4i2 package) (63).

The details of data collection and structure refinement statistics are summarized in Table S1. Structures were deposited in the Protein Data Bank with accession IDs 6BC8, 6BCD and 6BI7.

Small-angle X-ray scattering

Small-angle X-ray scattering (SAXS) measurements were collected on $Rev7^{R124A}$/Rev3-RBM2, $Rev7^{WT}$/Rev3-RBM12, $Rev7^{R124A}$/Rev3-RBM12, and $Rev7^{K44A,R124A,A135D}$/Rev3-RBM12 complexes in buffer containing 50 mM Tris, 150 mM NaCl, 10 mM DTT, 1 mM EDTA, 5% glycerol, at pH 8.4. Measurements for $Rev7^{WT}$/Rev3-RBM2 were carried out in 20 mM HEPES, 10 mM DTT, 5% glycerol at pH 8.0. Buffers were matched by loading the proteins on a gel filtration column at a high enough concentration to ensure the peak fractions would be sufficient to take for measurement without concentrating. The concentration series for each construct is listed in Table S3. The matched buffer was taken from buffer that had passed through the column.

SAXS data collected for the above samples are summarized in Table S3. 10 x 1 s exposures were collected with the sample oscillating in the capillary flow-cell at the CHESS G1 station. The data were integrated, averaged, buffer subtracted and subjected to Guinier analysis to determine gyration radius R_g and forward scattering I(0) using the software RAW (64). To calculate the molecular weight of the complexes using the forward scattering, human PCNA (proliferating cell nuclear antigen) was used as a standard. For all samples, the R_g and molecular weight were consistent across concentrations, indicating concentration-dependent effects were not present (Table S3). The P(r) function (pair-distance distribution function) was calculated using the software GNOM as part of the ATSAS suite (65). Real-space values for R_g and I(0) derived

from the P(r) analysis are in agreement with the values derived from the Guinier analysis and also show no concentration dependence except in the case of Rev7^{WT}/Rev3- RBM2, as expected (Table S3).

To simulate SAXS curves from the Rev7/Rev3 coordinate files, the FoXS server was used with default parameters (66). Similar results were obtained with AXES (67). When simulating the SAXS data, residues at the N- and C-termini of Rev7 that were missing in the crystal structures were built in an extended conformation.

NMR Spectroscopy

^{1}H-^{15}N HSQC spectra of ^{15}N labeled Rev7^{WT}/Rev3-RBM12 and Rev7^{R124A}/Rev3-RBM12 were collected at 30 °C on an Agilent VNMRS 800 MHz (^{1}H) spectrometer equipped with a cold probe on protein samples dissolved in 20 mM Tris, 100 mM NaCl, 10 mM DTT, pH 8.4, at 240 μM Rev7 monomer concentration. Spectra of ^{15}N labeled Rev7^{R124A}/Rev3-RBM2 and Rev7^{K44A,R124A,A135D}/Rev3-RBM2 were collected at 30 °C in 20 mM HEPES, 100 mM NaCl, 10 mM DTT, pH 7.4. To probe Rev7/Rev1-PAD interaction, unlabeled Rev1-PAD was added to ^{15}N labeled Rev7^{R124A}/Rev3-RBM2 to molar excess (440 μM Rev1-PAD, 260 μM Rev7^{R124A}/Rev3- RBM2) in 20 mM HEPES, 100 mM NaCl, 10 mM DTT at pH 7.4, however, chemical shift perturbations indicating binding were not observed in the ^{1}H-^{15}N HSQC spectra. All spectra were processed with NMRPipe (68) and peak heights were determined using the software CCPNmr Analysis (69).

Mutational analysis of the Rev7 dimerization interface

A series of 32 site-directed mutations (Table S2) were introduced to solvent-exposed residues covering the entire surface of Rev7. Rev7^{WT}/Rev3-RBM2 or Rev7^{mutant}/Rev3-RBM2 was loaded onto a gel filtration column at ~1.5-1.7 mM, resulting in a peak concentration of ~300-400 μM (average of peak) after elution. At these concentrations, Rev7^{WT}/Rev3-RBM2 and the previously described dimer-breaking Rev7^{R124A}/Rev3-RBM2 mutant (20) elute as separate peaks at volumes corresponding to the dimer and the monomer. The oligomeric state of Rev7^{WT}/Rev3-RBM2 and Rev7^{R124A}/Rev3-RBM2 was cross-validated by SAXS measurements (Fig. S8) here and by analytical ultracentrifugation previously (20). All mutants identified in this study to break the Rev7 dimer (Fig. 2B) were also cross-validated with a yeast two-hybrid assay (Fig. 2C, Fig. S2A).

Yeast two-hybrid assay

Studies of Rev7 dimerization using the yeast two-hybrid assay were carried out in yeast strain PJ69-4A (55). DNA encoding for Rev7 (wild-type and/or mutants) was subcloned as fusions of the *GAL4* activation domain (AD) and *GAL4* DNA-binding domain (BD) in pGAD-C1 and pGBD-C1 plasmids marked with leucine and tryptophan, respectively. Yeast harboring the two plasmids, one encoding wild-type and another mutant Rev7, were grown at 30 °C for two days in a 3 mL culture lacking leucine and tryptophan and then spotted on –LW plates to confirm the presence of viable transformants and on –AHLW plates to score the interaction. This yeast two-hybrid protocol was also used to probe interactions between the wild-type or mutant Rev7 with the wild-type Mad2 and p31^{comet}.

Docking

Two PDB files of Rev7^{WT}/Rev3-RBM2 were used as input for the software HADDOCK (56) in combination with R124A and our 8 experimentally determined dimer-breaking mutations to guide the docking (Table S2). For all other parameters, the default setting was used. The structure used for docking was our 1.68 Å structure of Rev7^{R124A}/Rev3-RBM2 with the sequence mutated back to wild-type using PyMOL (70). This was done because our structure of Rev7^{WT}/Rev3-RMB2, while similar to that of the R124A mutant, is of lower quality, has residues missing and lacks side-chain density in loop regions (Fig. S1). *All* 200 lowest energy structures of the dimer calculated by HADDOCK were grouped into a single final cluster. To assess possible steric clash that may arise when Rev1-CT binds to the Rev7^{WT}/Rev3-RBM2 dimer, we used the "align" function in PyMOL (70) to superimpose two copies of Rev7^{R124A}/Rev3- RBM1/Rev1-CT (PDB: 3VU7 (29)) onto our structure of the Rev7^{WT}/Rev3-RBM2 dimer predicted by HADDOCK or other HORMA dimers as noted (Fig. 5D, Fig. S9).

Isothermal Titration Calorimetry

ITC measurement were collected on a TA instruments Nano ITC at the University of Connecticut Biophysics Core (Storrs, CT). 50 mL of 2 mM Rev1-CT was titrated in 2.5 mL aliquots into a solution of 250 mM Rev7 (125 mM Rev7^{WT}2/Rev3-RBM12) at 25 °C with 500 seconds of equilibration between each addition. The data were fit with the software NanoAnalyze using the independent and blank-constant models to extract the dissociation constant for the complex (K_d), association enthalpy (ΔH) and stoichiometry parameter (n).

DNA damage sensitivity assay in Rev7$^{-/-}$ cell line

The Rev7$^{-/-}$;*Kras*$^{G12D/+}$;Trp53$^{-/-}$ cells used in this study were generated by Vassel et al (to be published) using CRISPR/Cas9 system from the *Kras*$^{G12D/+}$;Trp53$^{-/-}$ murine lung adenocarcinoma cell line kindly provided Tyler Jack's lab at MIT (57). All cell lines were cultured in standard DMEM/10%FBS media.

To assess cell viability following cisplatin-induced DNA damage, cells were seeded in triplicate ($8x10^3$) in 96-well plates and treated as indicated with cisplatin. After 48h treatment, cell viability was assessed using Cell Titer-Glo (Promega) on an Applied Biosystems microplate luminometer.

DATA DEPOSITION

The crystal structures were deposited to the Protein Data Bank: Rev7^{R124A}/Rev3-RBM2: 6BC8; Rev7^{K44A,R124A,A135D}/Rev3-RBM2: 6BCD; Rev7^{WT}/Rev3-RBM2: 6BI7. The model of the (Rev7^{WT}/Rev3-RBM2)$_2$ dimer was deposited to PDB-dev with ID PDBDEV_00000009.

AUTHOR CONTRIBUTIONS

AAR conceived and performed the study advised by DMK. AAR and DMK wrote the manuscript. All authors contributed to the manuscript refinement. YL and BH contributed to the crystallography. F-MV, SD, NC, MTH and GCW performed the yeast-two hybrid assays, generated the Rev7$^{-/-}$ cell line and performed the cell-based DNA damage sensitivity assays.

CONFLICT OF INTEREST

The authors declare no conflict of interest.

ACKNOWLEDGMENTS

Research in the DMK laboratory is supported by NSF/MCB 1615866 and NIH/NIGMS R01-GM123239 grants. Work in the GCW laboratory is supported by NIH/NIEHS R01- ES015818 and R35-ES028303 grants and P30-ES002109 grant to the MIT Center of Environmental Health Sciences. GCW is an American Cancer Society Professor. BH is supported by NIH/NIGMS R01-GM099948 and Connecticut Regenerative Medicine Research Fund 15-RMA-UCHC-03 grants. The authors thank the faculty at CHESS, including Richard Gillilan and Jesse Hopkins (SAXS) and Irina Kriksunova and David Schuller (crystallography). CHESS is supported by the NSF and NIH/NIGMS via NSF award DMR-1332208, and the MacCHESS resource is supported by NIH/NIGMS award GM103485. The plasmid for human $Rev7^{R124A}$/Rev3-RBM1 in pETDuet-1 was provided by Dr. Hiroshi Hashimoto.

FIGURES

Fig. 1. Components of the Rev1/Polz4 complex: (**A**) the four subunits of TLS DNA polymerase Polz (top, in box) and the TLS DNA polymerase Rev1 (bottom). (**B**) Structure comparison of $Rev7^{R124A}$ complexes with the two Rev7-binding motifs of Rev3: Rev3-RBM1 (grey; PDB 3ABD (21)) and Rev3-RBM2 (green/orange, PDB 6BC8, this work). (**C**) Sequence alignment of the two Rev3-RBM motifs (20,22). (**D**) Close-up of the Rev3-RBM1 (grey) and Rev3-RBM2 (orange) interaction interfaces with $Rev7^{R124A}$ (green).

Fig. 2. Mutational mapping of the Rev7 homo- and heterodimerization interface. (**A**) An example of gel filtration profiles of the monomeric $Rev7^{R124A}$/Rev3-RBM1 (green) and dimeric $Rev7^{WT}$/Rev3-RBM1 (purple) complexes. (**B**) Yeast two-hybrid studies of Rev7 homo-dimerization (top) and its heterodimerization with Mad2 (center) or $p31^{comet}$ (bottom): growth on - LW and -AHLW plates of the PJ69-4A strain of yeast transformed with fusions to the *GAL4*-BD or *GAL4*-AD as indicated. (**C**) Rev7 residues whose mutation abolish dimerization (green) mapped on our structure of $Rev7^{R124A}$/Rev3-RBM2, outlining the Rev7 dimerization interface. Residues on helix aC are marked with "*". (**D**) Homo- and heterodimerization interface of other HORMA domains (47-49,54). All structures appear in the same orientation as in (C) and have residues on helix aC labeled.

Fig. 3. Two copies of Rev7 bind Rev3 and form a tethered dimer. (**A**) Gel filtration profiles of $Rev7^{WT}$/Rev3-RBM12 (purple), $Rev7^{WT}$/Rev3-$RBM12^{P1880A/P1885A}$ (orange) and $Rev7^{R124A}$/Rev3- RBM2 (green) suggesting a 2:1 stoichiometry for the Rev7:Rev3 interaction. Each curve was normalized to its maximum absorbance. Inset shows SDS gel of the $Rev7^{WT}$/Rev3-RBM12 peak fraction with the two bands corresponding to Rev7 (top) and Rev3-RBM12 (bottom). (**B**) SAXS scattering curves of $Rev7^{WT}$/Rev3-RBM12 (purple), $Rev7^{R124A}$/Rev3-RBM12 (green) and $Rev7^{K44A,R124A,A135D}$/Rev3-RBM12 (brown) at low-q. The first points from the scattering intensities were aligned to highlight the effect of the mutations on the shape of the curve. (**C**) P(r) distributions indicating the dimer-breaking mutations elongate the complex.

Fig. 4. ITC measurements suggest only one copy of Rev1-CT can bind the $Rev7^{WT}$ dimer when tethered by Rev3-RBM12. (**A**) Raw ITC data and (**B**) integrated heat changes obtained during titration of Rev1-CT into $Rev7^{WT}$/Rev3-RBM12. The best fit to the ITC data (solid line) results in dissociation constant (K_d) of 11.4±1.9 μM, association enthalpy (ΔH) of -42.9±1.4 kJ/mol and the stoichiometry parameter (n) of 1.24±0.02.

Fig. 5. Structural modeling of the Rev7 dimer and its complex with Rev1-CT. (**A**) Model of $Rev7^{WT}$/Rev3-RBM2 (purple) obtained using HADDOCK (56) based on mutational mapping of

the Rev7 dimerization interface and its comparison with the structure of the symmetric apo-Mad2 dimer (PDB: 3VFX, cyan) (48). "*" denotes the N-terminus of helix aC to demonstrate alignment. (**B**) Agreement between SAXS/WAXS scattering data (black dots) and scattering intensities calculated from the model of $Rev7^{WT}$/Rev3-RBM2 dimer in (A) using FoXS (66). (**C**) Comparison of experimental SAXS/WAXS data with scattering data predicted from our crystal structure of the $Rev7^{R124A}$/Rev3-RBM2 complex using FoXS (66). (**D**) Structure of $Rev7^{R124A}$/Rev3-RBM1/Rev1-CT (29) (Rev7 - purple; Rev3 - orange; Rev1-CT – yellow/red) superimposed on our model of the Rev7 dimer generated using HADDOCK (56) shown in (A). The Rev7 dimer is unable to bind a second Rev1-CT due to a steric clash.

Fig. 6. Interactions of the Rev7 dimer interface are required for resistance to cisplatin. **(A)** Relative viability of the parental *Kras*^{G12D};$p53^{-/-}$ cells (black), $Rev7^{-/-}$ cells (grey), and $Rev7^{-/-}$ cells complemented with $Rev7^{WT}$ (purple) and dimerization-deficient $Rev7^{K44A,R124A,A135D}$ (brown) after treatment with cisplatin for 48 hours. **(B)** Western blot showing knockout of Rev7 (grey) and expression of $Rev7^{WT}$ (purple) and $Rev7^{K44A,R124A,A135D}$ (brown) during complementation. In the lane marked "MW ladder", the black marker bands were traced by hand with marker.

Fig. 1.

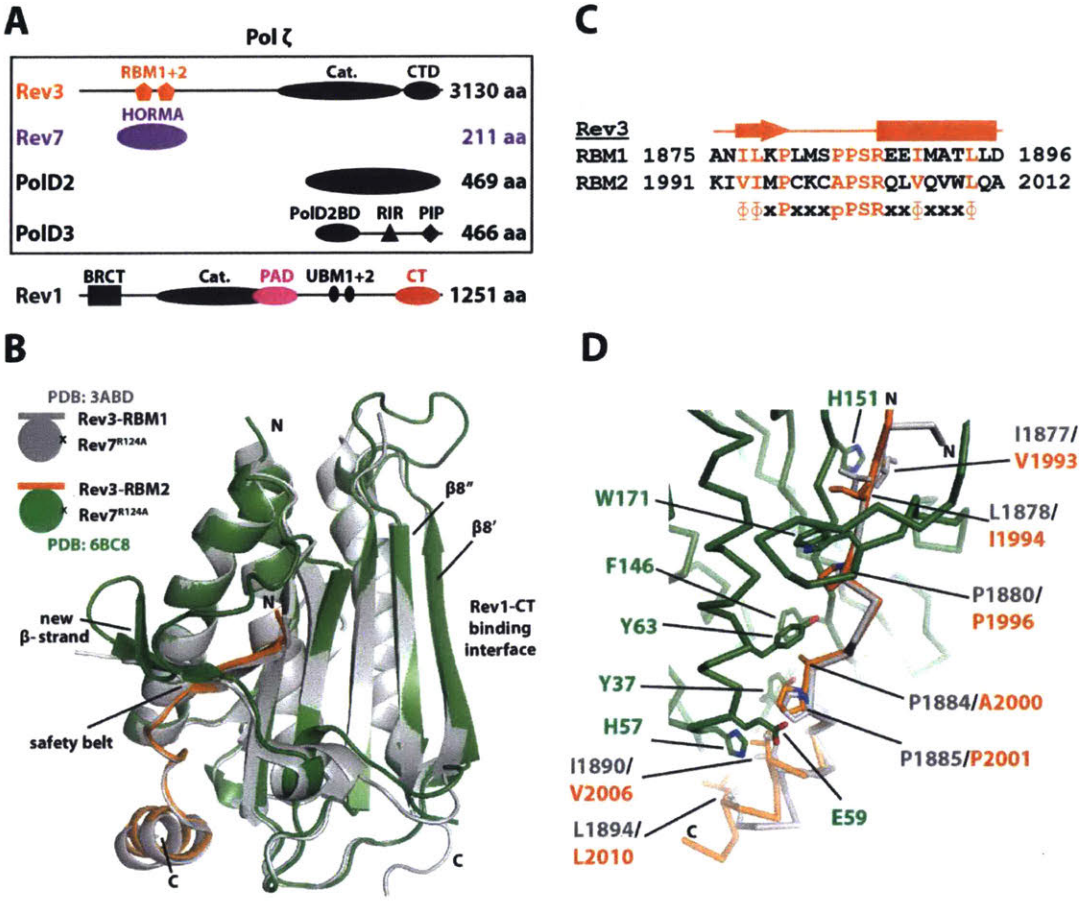
A
Pol ζ
Rev3
RBM1+2
Cat.
CTD
3130 aa
HORMA
Rev7
211 aa
PolD2
469 aa
PolD2BD
RIR
PIP
PolD3
466 aa
Rev1
BRCT
Cat.
PAD
UBM1+2
CT
1251 aa
B
PDB: 3ABD
Rev3-RBM1
Rev7R124A
Rev3-RBM2
Rev7R124A
PDB: 6BC8
N
β8″
β8′
Rev1-CT binding interface
new β-strand
safety belt
C
C
Rev3
RBM1 1875 ANILKPLMSPPSREEIMATLLD 1896
RBM2 1991 KIVIMPCKCAPSRQLVQVWLQA 2012
ΦΦxPxxxpPSRxxΦxxxΦ
D
H151
N
I1877/
V1993
W171
L1878/
I1994
F146
P1880/
P1996
Y63
Y37
P1884/A2000
H57
P1885/P2001
I1890/
V2006
E59
L1894/
L2010
C

Fig. 2.

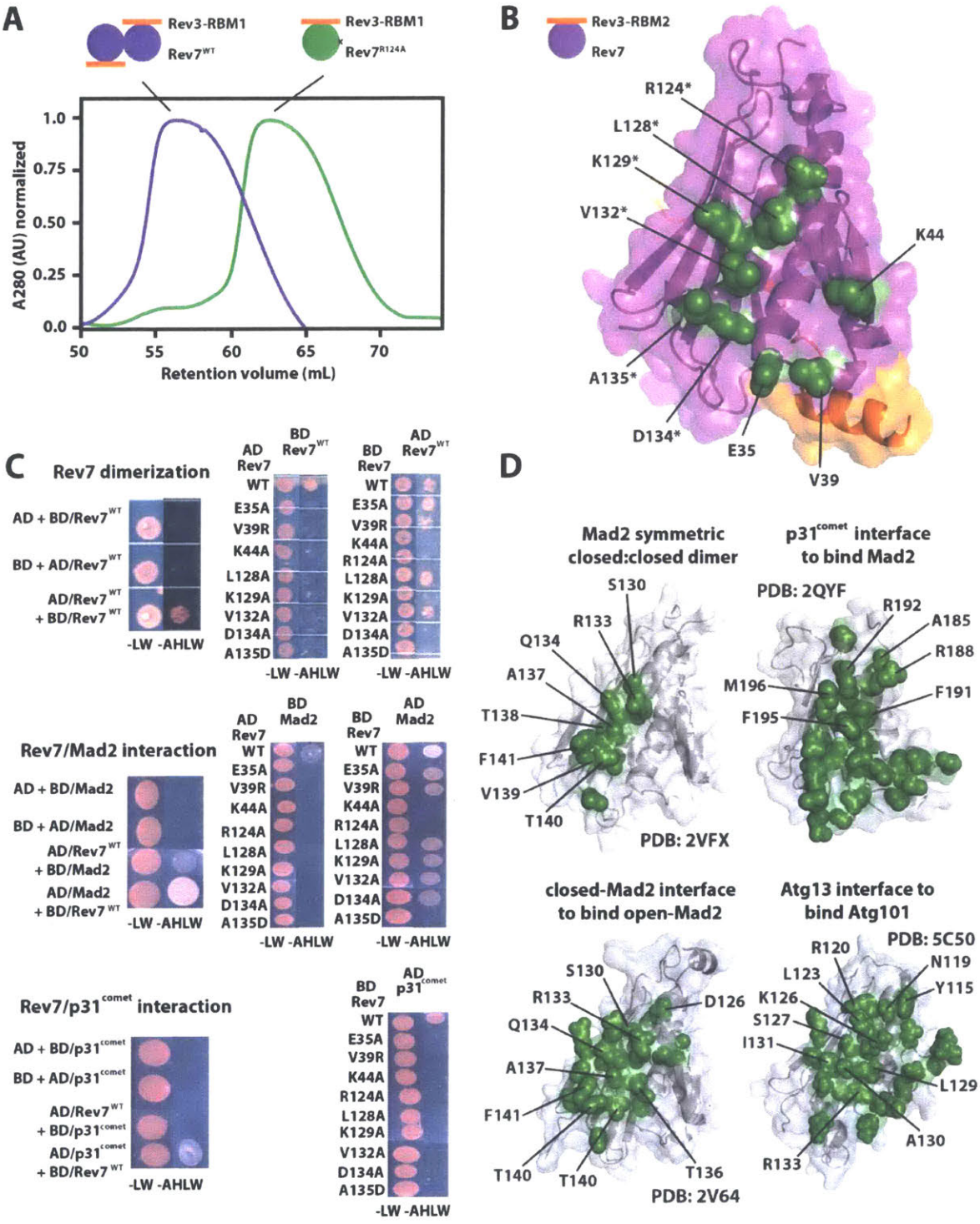
A
Rev3-RBM1
Rev7WT
Rev3-RBM1
Rev7R124A
A280 (AU) normalized
1.0
0.75
0.50
0.25
0.0
50
55
60
65
70
Retention volume (mL)
B
Rev3-RBM2
Rev7
R124*
L128*
K129*
V132*
K44
A135*
D134*
E35
V39
C
Rev7 dimerization
AD + BD/Rev7WT
BD + AD/Rev7WT
AD/Rev7WT + BD/Rev7WT
-LW -AHLW
AD Rev7
BD Rev7WT
BD Rev7
AD Rev7WT
WT
E35A
V39R
K44A
L128A
K129A
V132A
D134A
A135D
-LW -AHLW
Rev7/Mad2 interaction
AD + BD/Mad2
BD + AD/Mad2
AD/Rev7WT + BD/Mad2
AD/Mad2 + BD/Rev7WT
AD Rev7
BD Mad2
BD Rev7
AD Mad2
R124A
L128A
K129A
V132A
D134A
A135D
Rev7/p31comet interaction
AD + BD/p31comet
BD + AD/p31comet
AD/Rev7WT + BD/p31comet
AD/p31comet + BD/Rev7WT
BD Rev7
AD p31comet
D
Mad2 symmetric closed:closed dimer
p31comet interface to bind Mad2
PDB: 2QYF
S130
R133
Q134
A137
T138
F141
V139
T140
PDB: 2VFX
R192
A185
R188
M196
F191
F195
closed-Mad2 interface to bind open-Mad2
Atg13 interface to bind Atg101
PDB: 5C50
S130
R133
D126
Q134
A137
F141
T140
T140
T136
PDB: 2V64
R120
N119
L123
Y115
K126
S127
I131
L129
A130
R133

Fig. 3.

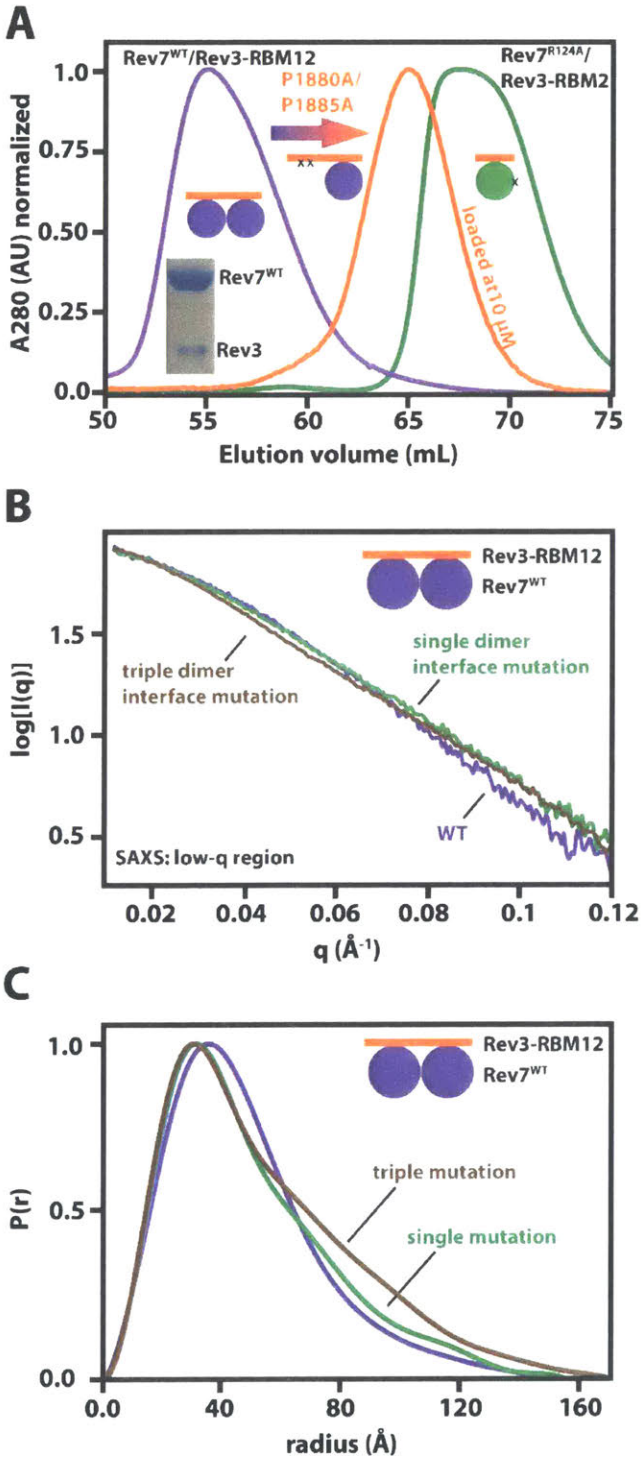
A
Rev7WT/Rev3-RBM12
P1880A/
P1885A
Rev7R124A/
Rev3-RBM2
loaded at 10 μM
Rev7WT
Rev3
A280 (AU) normalized
1.0
0.75
0.50
0.25
0.0
50
55
60
65
70
75
Elution volume (mL)
B
Rev3-RBM12
Rev7WT
single dimer
interface mutation
triple dimer
interface mutation
WT
SAXS: low-q region
log[I(q)]
1.5
1.0
0.5
0.02
0.04
0.06
0.08
0.1
0.12
q (Å-1)
C
Rev3-RBM12
Rev7WT
triple mutation
single mutation
P(r)
1.0
0.5
0.0
0.0
40
80
120
160
radius (Å)

Fig. 4.

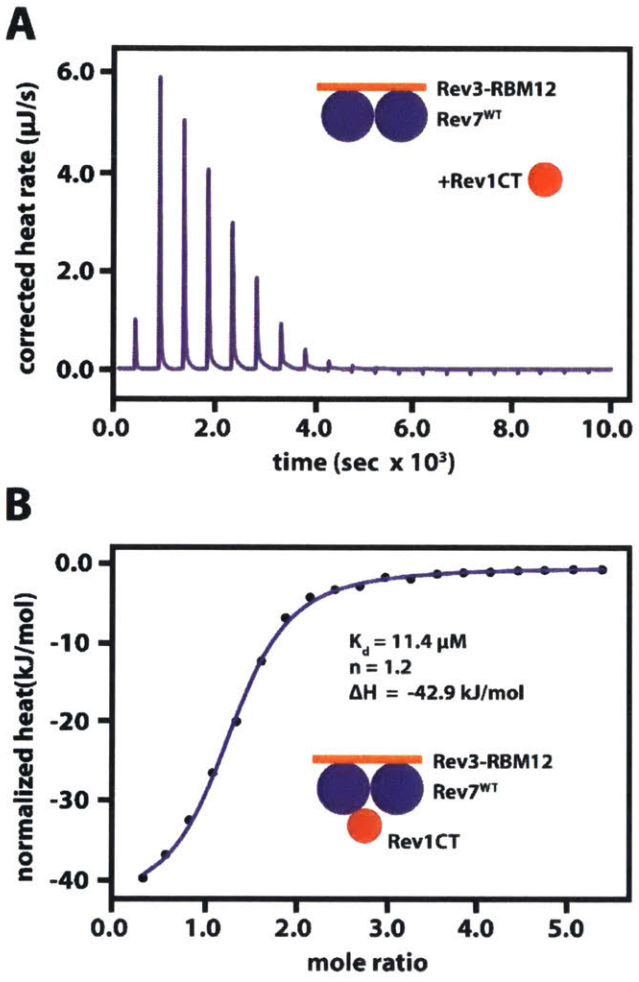
A
corrected heat rate (µJ/s)
6.0
4.0
2.0
0.0
Rev3-RBM12
Rev7WT
+Rev1CT
0.0
2.0
4.0
6.0
8.0
10.0
time (sec x 10³)
B
normalized heat(kJ/mol)
0.0
-10
-20
-30
-40
Kd = 11.4 µM
n = 1.2
ΔH = -42.9 kJ/mol
Rev3-RBM12
Rev7WT
Rev1CT
0.0
1.0
2.0
3.0
4.0
5.0
mole ratio

Fig. 5.

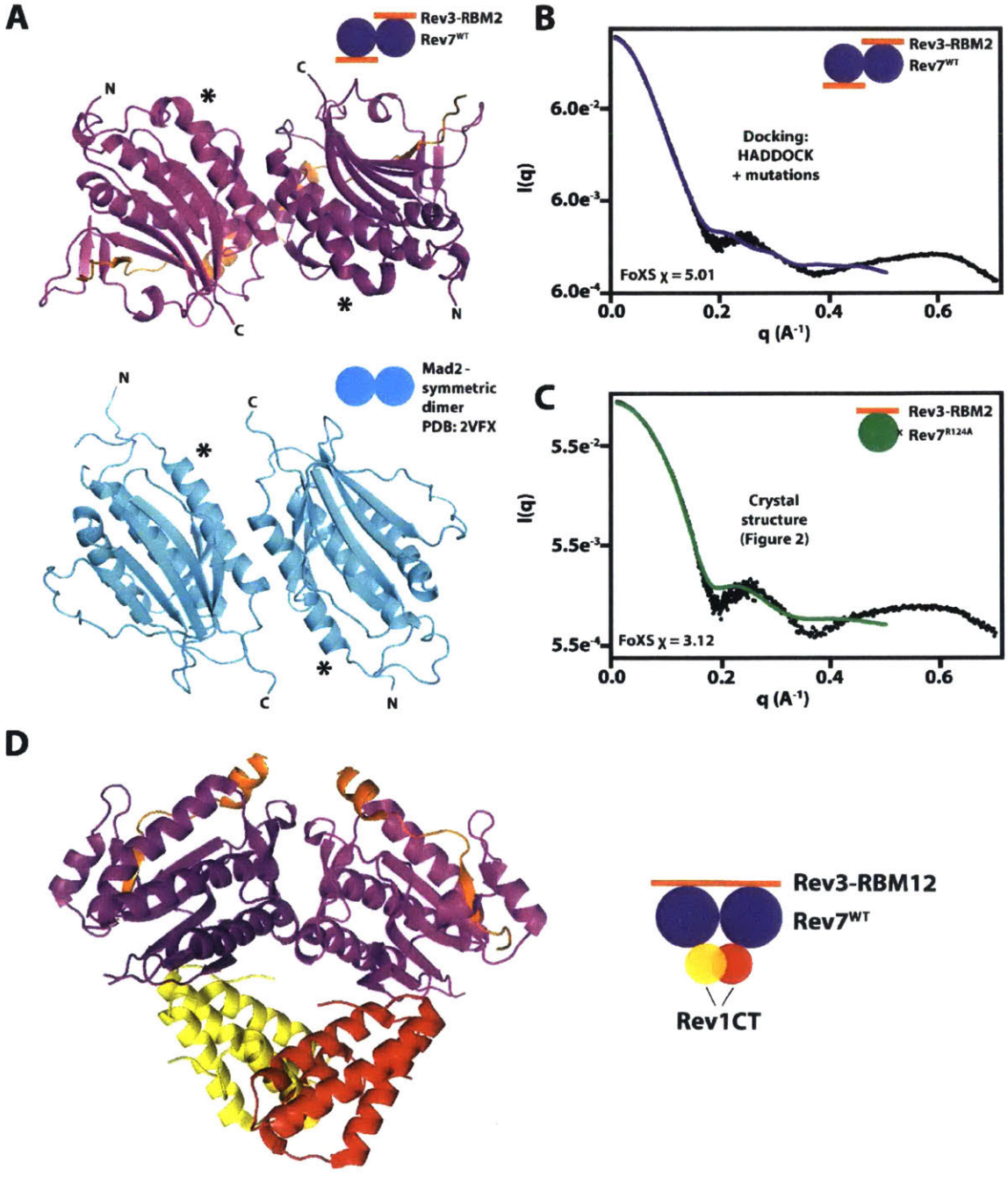
A
Rev3-RBM2
Rev7WT
N
C
C
N
Mad2 -
symmetric
dimer
PDB: 2VFX
N
C
C
N
B
Rev3-RBM2
Rev7WT
Docking:
HADDOCK
+ mutations
FoXS χ = 5.01
I(q)
6.0e-2
6.0e-3
6.0e-4
0.0
0.2
0.4
0.6
q (A-1)
C
Rev3-RBM2
Rev7R124A
Crystal
structure
(Figure 2)
FoXS χ = 3.12
I(q)
5.5e-2
5.5e-3
5.5e-4
0.0
0.2
0.4
0.6
q (A-1)
D
Rev3-RBM12
Rev7WT
Rev1CT

Fig. 6.

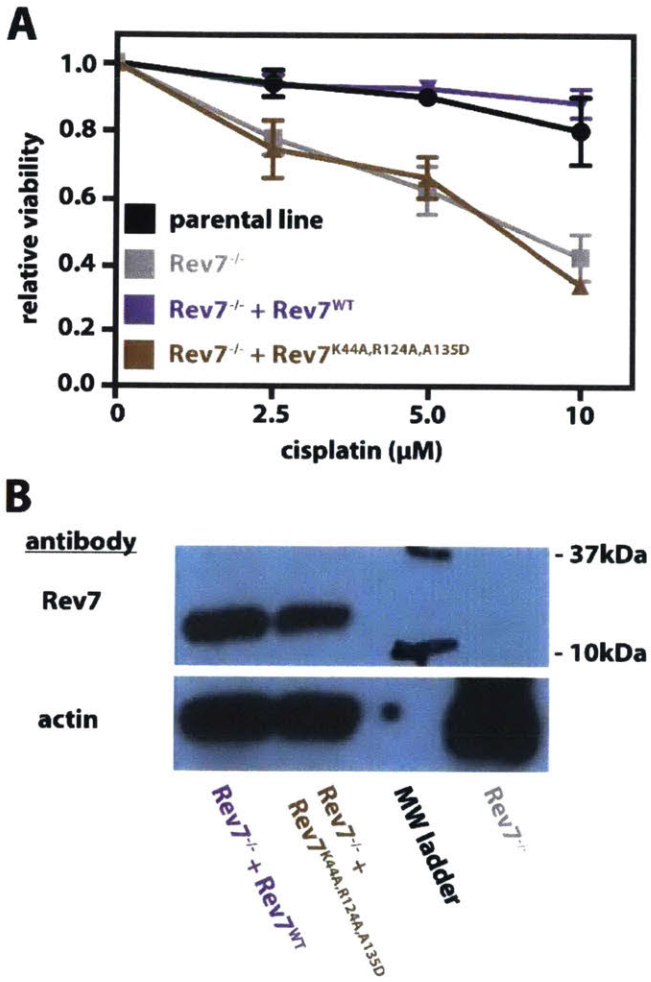
A
1.0
0.8
0.6
0.4
0.2
0.0
relative viability
parental line
Rev7-/-
Rev7-/- + Rev7WT
Rev7-/- + Rev7K44A,R124A,A135D
0
2.5
5.0
10
cisplatin (μM)
B
antibody
Rev7
actin
- 37kDa
- 10kDa
Rev7-/- + Rev7WT
Rev7-/- + Rev7K44A,R124A,A135D
MW ladder
Rev7-/-

SI FIGURES

Fig. S1: Superposition of crystal structures for Rev7^{R124A}/Rev3-RBM2 (green/orange, PDB: 6BC8) and Rev7^{WT}/Rev3-RBM2 (purple/orange, PDB: 6BI7) showing that the R124A mutation does not induce conformational changes to Rev7. See Table S1 for details of X-ray data collection and structure refinement statistics.

Fig. S2. Mutational mapping of the Rev7 homo- and heterodimerization interface by yeast two-hybrid assay (see Fig. 2C), including control plates. Growth on plates lacking leucine and tryptophan (-LW) and plates lacking adenine, histidine, leucine and tryptophan (-AHLW) of yeast strain PJ69-4A transformed with (i) an empty *GAL4*-BD vector, or plasmids encoding (**A**) Rev7^{WT}, (**B**) Mad2 or (**C**) p31^{comet} fused to *GAL4*-BD and (ii) an empty *GAL4*-AD vector, or Rev7^{WT} or Rev7^{mutant} fused to *GAL4*-AD, or the PJ69-4A strain of yeast transformed with the two plasmids in the opposite orientation.

Fig. S3. The stoichiometry of the Rev7:Rev3 interaction in human Polz is 2:1. (**A**) Gel filtration profiles (left) of a dilution series of Rev7^{WT}/Rev3-RBM12 (solid purple line) and Rev7^{WT}/Rev3- RBM2 (dashed purple line) with a schematic explaining the elution behavior (right). This panel shows that Rev7 elutes later as a monomer when not tethered and when loaded at 10 mM and also rules out formation of a 2:2 Rev7:Rev3-RBM12 complex through intermolecular Rev7 dimerization. (**B**) Guinier plots of SAXS measurements for Rev7^{WT}/Rev3-RBM12 (left), Rev7^{R124A}/Rev3-RBM2 (middle) and Rev7^{R124A}/Rev3-RBM12 (right). (**C**) Molecular weights of Rev7^{WT}/Rev3-RBM12, Rev7^{R124A}/Rev3-RBM12 and Rev7^{R124A}/Rev3-RBM2 complexes determined by SAXS. Note that the "1:1" marker represents the molecular weight of a complex that includes Rev3-RBM12 whereas the complex from which the green line derives includes RBM2 only. Inset shows 2:2 stoichiometry for Rev7/Rev3-RBM12 complex resulting from intermolecular Rev7 dimerization that data here and in (A) rule out.

Fig. S4. Rev7 forms a tethered dimer when bound to Rev3. (**A**) Guinier plot of SAXS measurements for Rev7^{K44A,R124A,A135D}/Rev3-RBM12. (**B**), (**C**), (**D**) The agreement between the P(r) models (lines) generated using GNOM in the ATSAS suite (1-3) and the experimental scattering intensities (colored symbols) for (**B**) Rev7^{WT}/Rev3-RBM12, (**C**) Rev7^{R124A}/Rev3- RBM12 and (**D**) Rev7^{K44A,R124A,A135D}/Rev3-RBM12. In all cases, the P(r) models agree with the raw scattering intensities and capture the experimentally observed differences at low-q.

5

Fig. S5: Changes in molecular shape of the tethered Rev7 dimer observed by SAXS (Fig. 3B, 3C) cannot be explained by the mutations themselves or conformational changes to a Rev7 protomer. (**A**) Superposition of Rev7^{R124A}/Rev3-RBM2 (green/orange; PDB 6BC8) and Rev7^{K44A,R124A,A135D}/Rev3-RBM2 (brown/orange; PDB 6BCD) crystal structures. (**B**) Simulated SAXS scattering intensities generated by FoXS (4,5) using the coordinate files for Rev7^{WT}/Rev3-RBM2 and Rev7^{R124A}/Rev3-RBM2. Only a single curve is visible because the two profiles are nearly identical. When simulating the SAXS data to compare the solution behavior of Rev7^{WT}/Rev3-RBM2 and Rev7^{R124A}/Rev3-RBM2, residues that were missing from loops of the lower quality Rev7^{WT}/Rev3-RBM2 structure were removed from the Rev7^{R124A}/Rev3-RBM2 coordinate file. (**C**) Same as (B) for the complexes of Rev7^{R124A}/Rev3-RBM2 and Rev7^{K44A,R124A,A135D}/Rev3-RBM2. In this case, the coordinate files were unaltered because both contained the same number of residues. (**D**) ^{1}H-^{15}N HSQC spectra of ^{15}N-labeled protonated Rev7^{WT}/Rev3-RBM2 (green) and Rev7^{K44A,R124A,A135D}/Rev3-RBM2 (brown). The two spectra are superimposable and illustrate that introduction of the two mutations in addition to R124A does not cause conformational changes to the Rev7 protomer.

Fig. S6: NMR spectra of Rev7^{WT}/Rev3-RBM12 and Rev7^{R124A}/Rev3-RBM12 support the tethered Rev7 dimer. (**A**) ^{1}H-^{15}N HSQC spectra of ^{15}N-labeled protonated Rev7^{WT}/Rev3-RBM12 (purple) and Rev7^{R124A}/Rev3-RBM12 (green) illustrating that Rev7^{WT} forms a tethered dimer that tumbles as a single 68 kDa entity. Addition of the R124A mutation to tethered complex improves the quality of the spectrum and shows the behavior expected for two independent 28 kDa protomers connected by a flexible linker. These spectra allow qualitative analysis of the solution behavior of the two constructs. However, expression levels for these constructs were too low to justify preparing a ^{2}H-labeled sample for quantification of the overall rotational correlation time (τ_c). (**B**) Quantification of peak intensities from the spectra in (A) for eight peaks corresponding to residues from dynamic regions of the proteins (left) and eight peaks corresponding to residues from structured parts of Rev7 (at >8.5 ppm, right). (**D**) Ratio of peak intensities in the Rev7^{WT} and Rev7^{R124A} spectra for the residues in (C). The increase in τ_c for the tethered Rev7^{WT} dimer results in a decrease in peak intensities for residues in structured protein regions, but has little effect on peaks from flexible regions undergoing rapid local motions. Note that the two spectra in (A) were collected with identical sample conditions (temperature, salt, pH, protein concentration) and processed with identical parameters. Therefore, the matching peak heights for dynamic residues in the two spectra indicate all

variables other than the mutation have been controlled.

6

Fig. S7: Interactions of the tethered Rev7 dimer. (**A**) NMR titration of ^{15}N labeled Rev7^{R124A}/Rev3-RBM2 with unlabeled Rev1-PAD added to molar excess does not show binding-induced chemical shift changes in ^{1}H-^{15}N HSQC spectra. (**B**) Rev1-PAD and Rev7^{WT}/Rev3-RBM12 elute as separate peaks from a gel filtration column, even when loaded at 3.7 and 0.75 mM, which results in elution at ~750 mM and 150 mM, respectively. (**C**) Rev1-CT and Rev7^{WT}/Rev3-RBM12 coelute from a gel filtration column, indicating the tethered Rev7 dimer remains competent to bind Rev1-CT.

Fig. S8: SAXS-derived molecular weight for the dimeric Rev7^{WT}/Rev3-RBM2 as a function of protein concentration. The molecular weight of Rev7^{WT}/Rev3-RBM2 (purple) and Rev7^{R124A}/Rev3-RBM2 (green) were determined using the Guinier analysis. Rev7^{WT}/Rev3-RBM2 reaches saturation between 6.1-10.6 mg/mL. Data at 12.1 mg/mL show interparticle repulsion and were not used in the analyses.

Fig. S9: Structures of Rev7^{R124A}/Rev3-RBM1/Rev1-CT (6) overlaid onto four other HORMA homo- and heterodimers (7-10) (only Rev7/Rev3-RBM1/Rev1-CT complexes are visible) showing steric clash of Rev1-CT would exist in a tethered Rev7 dimer as long as the Rev7 dimer structure lies within the variability of known HORMA homo- and heterodimerization structures.

Fig. S1

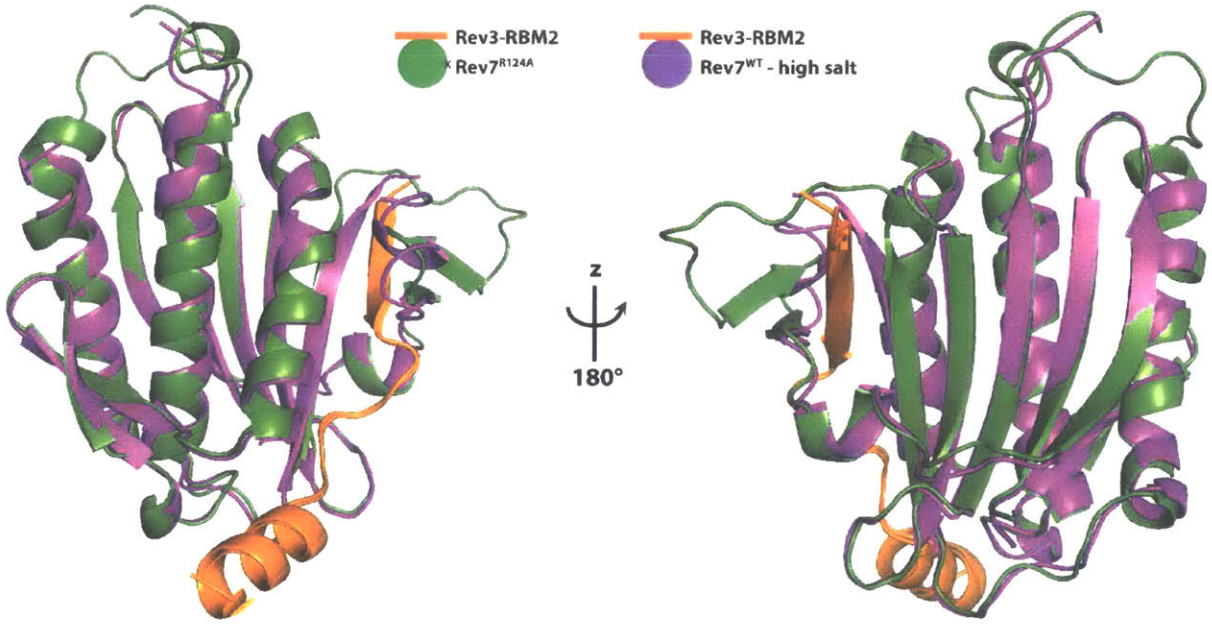

Fig. S2

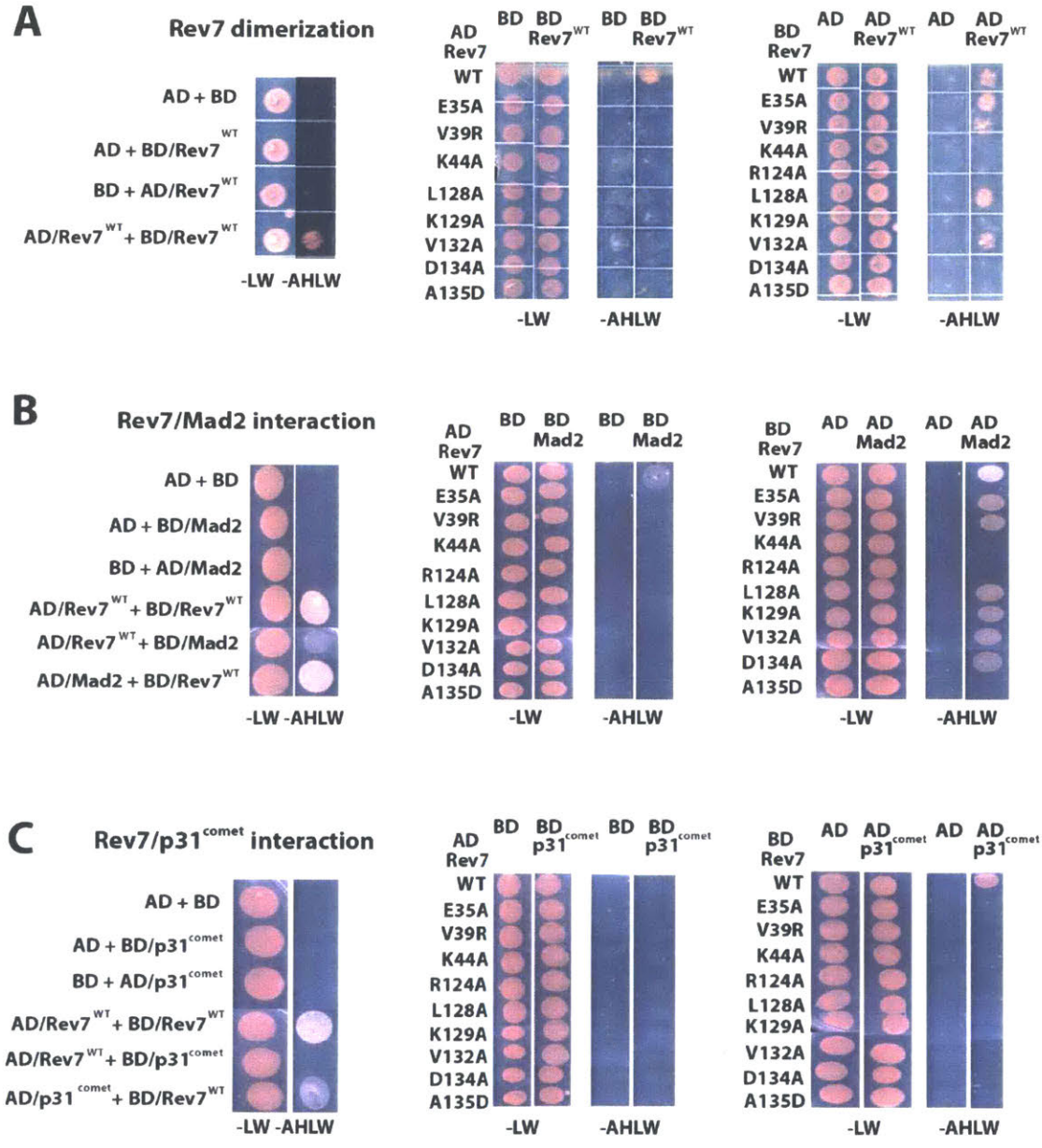
A
Rev7 dimerization
AD + BD
AD + BD/Rev7WT
BD + AD/Rev7WT
AD/Rev7WT + BD/Rev7WT
-LW -AHLW
AD Rev7
BD
BD Rev7WT
WT
E35A
V39R
K44A
L128A
K129A
V132A
D134A
A135D
-LW
-AHLW
BD Rev7
AD
AD Rev7WT
R124A
B
Rev7/Mad2 interaction
AD + BD/Mad2
BD + AD/Mad2
AD/Rev7WT + BD/Mad2
AD/Mad2 + BD/Rev7WT
Mad2
C
Rev7/p31comet interaction
AD + BD/p31comet
BD + AD/p31comet
AD/Rev7WT + BD/p31comet
AD/p31comet + BD/Rev7WT
p31comet

Fig. S3

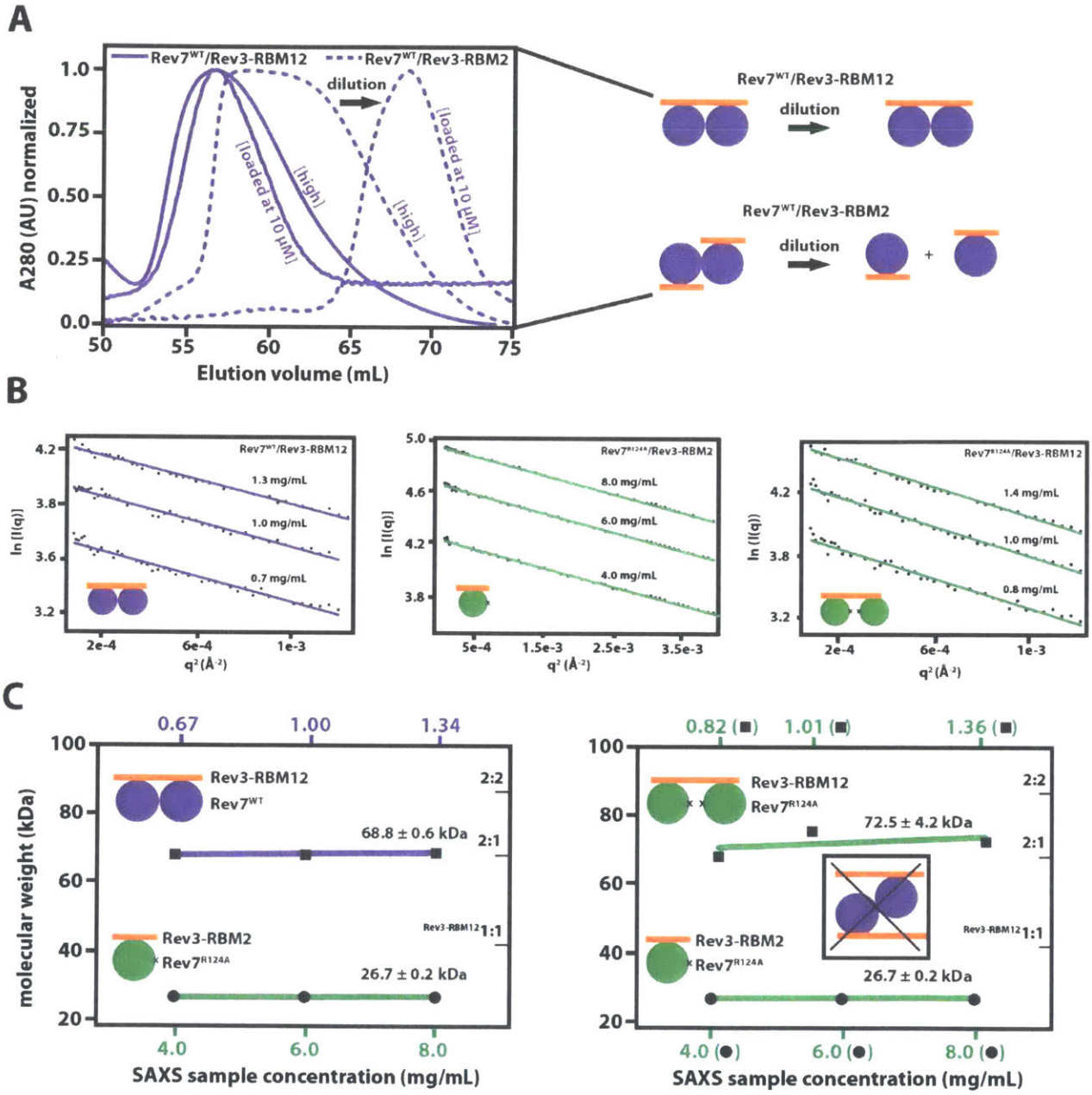
A
Rev7WT/Rev3-RBM12
Rev7WT/Rev3-RBM2
dilution
[loaded at 10 μM]
[high]
A280 (AU) normalized
Elution volume (mL)
B
Rev7WT/Rev3-RBM12
1.3 mg/mL
1.0 mg/mL
0.7 mg/mL
Rev7R124A/Rev3-RBM2
8.0 mg/mL
6.0 mg/mL
4.0 mg/mL
Rev7R124A/Rev3-RBM12
1.4 mg/mL
1.0 mg/mL
0.8 mg/mL
ln (I(q))
q² (Å⁻²)
C
molecular weight (kDa)
Rev3-RBM12
Rev7WT
68.8 ± 0.6 kDa
Rev3-RBM2
Rev7R124A
26.7 ± 0.2 kDa
72.5 ± 4.2 kDa
SAXS sample concentration (mg/mL)

Fig. S4

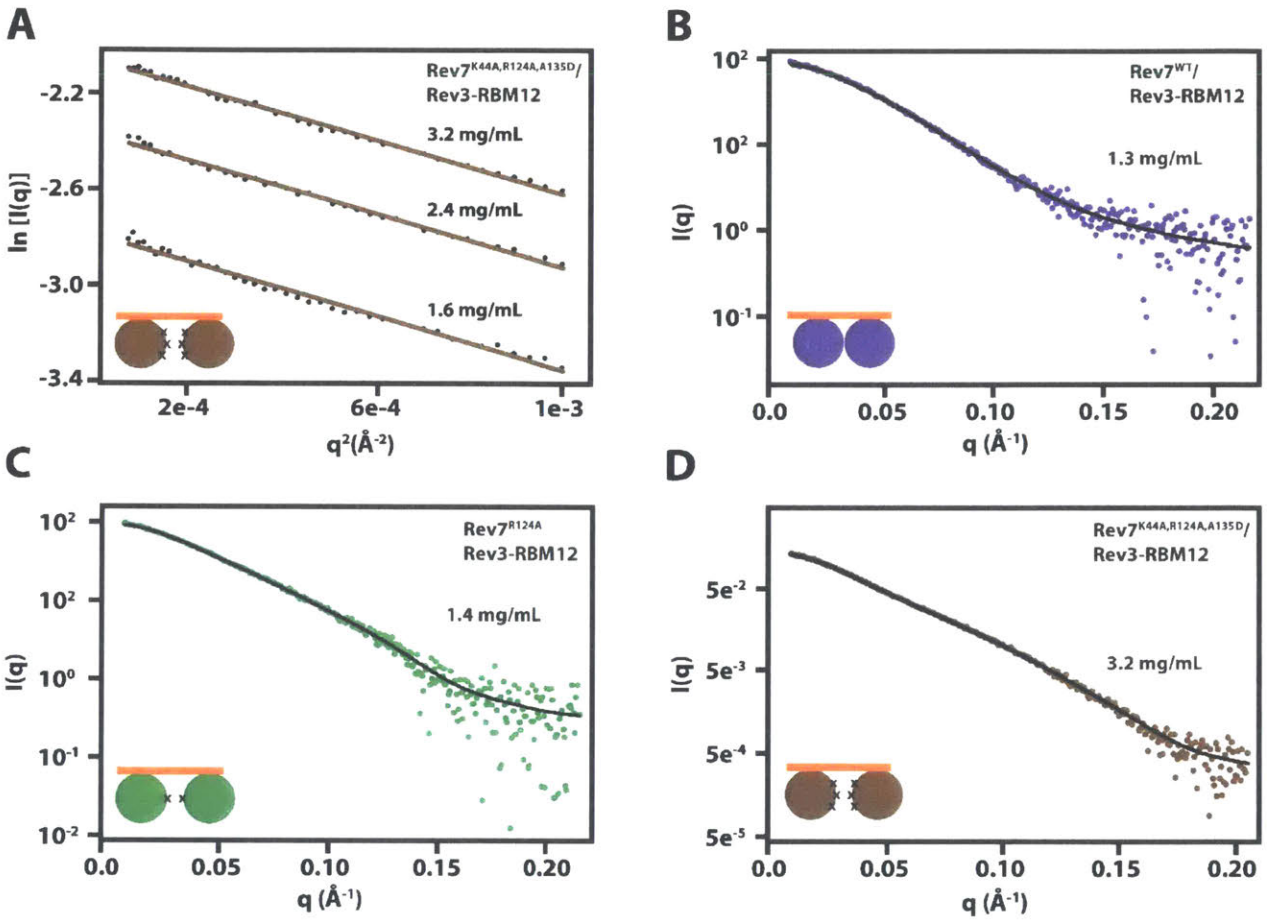
A
Rev7K44A,R124A,A135D/
Rev3-RBM12
3.2 mg/mL
2.4 mg/mL
1.6 mg/mL
ln [I(q)]
q²(Å⁻²)
B
Rev7WT/
Rev3-RBM12
1.3 mg/mL
I(q)
q (Å⁻¹)
C
Rev7R124A
Rev3-RBM12
1.4 mg/mL
I(q)
q (Å⁻¹)
D
Rev7K44A,R124A,A135D/
Rev3-RBM12
3.2 mg/mL
I(q)
q (Å⁻¹)

Fig. S5

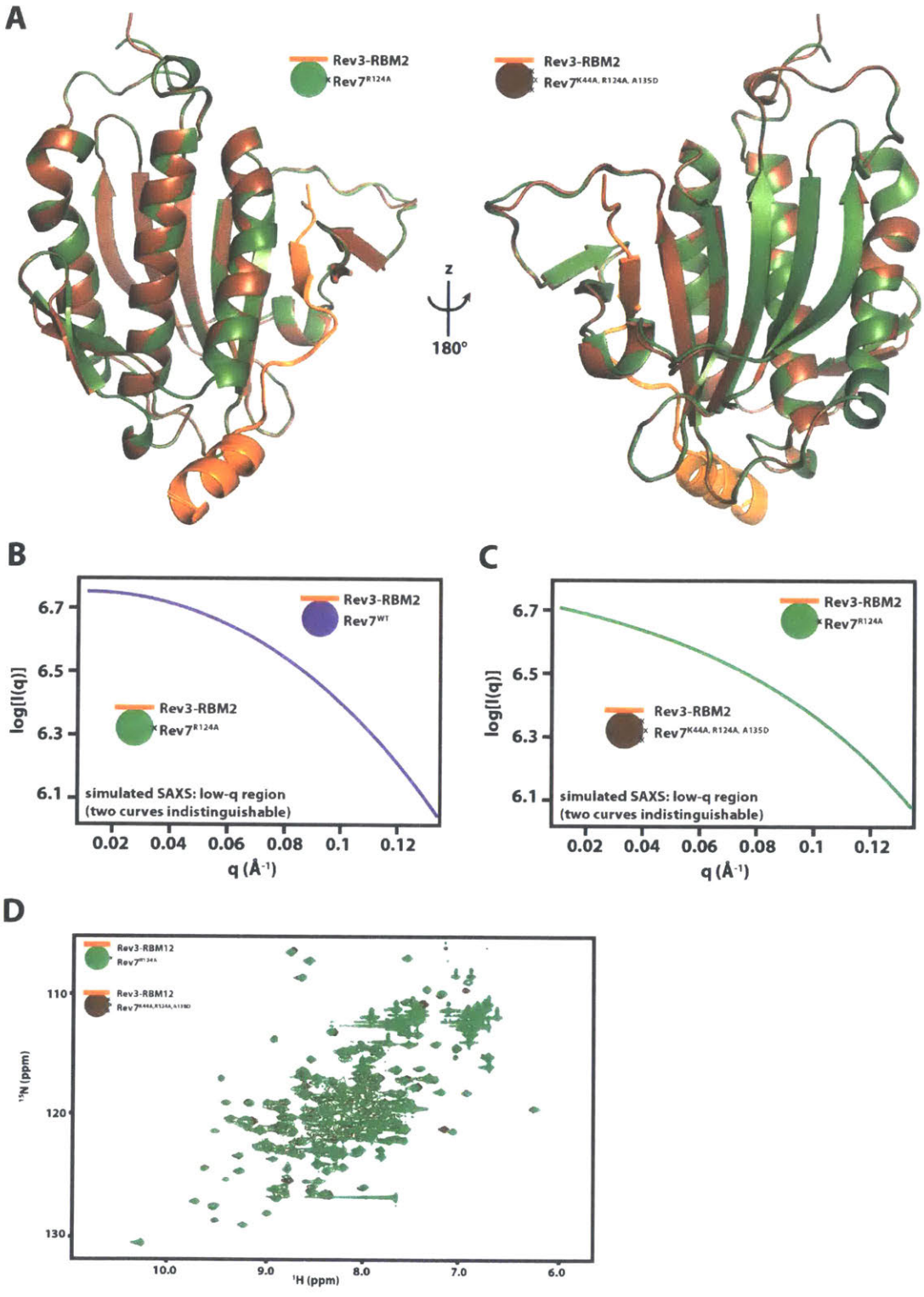
A
Rev3-RBM2
Rev7R124A
Rev3-RBM2
Rev7K44A, R124A, A135D
z
180°
B
Rev3-RBM2
Rev7WT
Rev3-RBM2
Rev7R124A
log[I(q)]
6.7
6.5
6.3
6.1
simulated SAXS: low-q region
(two curves indistinguishable)
0.02 0.04 0.06 0.08 0.1 0.12
q (Å-1)
C
Rev3-RBM2
Rev7R124A
Rev3-RBM2
Rev7K44A, R124A, A135D
log[I(q)]
6.7
6.5
6.3
6.1
simulated SAXS: low-q region
(two curves indistinguishable)
0.02 0.04 0.06 0.08 0.1 0.12
q (Å-1)
D
Rev3-RBM12
Rev7WT
Rev3-RBM12
Rev7K44A,R124A,A135D
110
120
130
15N (ppm)
10.0 9.0 8.0 7.0 6.0
1H (ppm)

Fig. S6

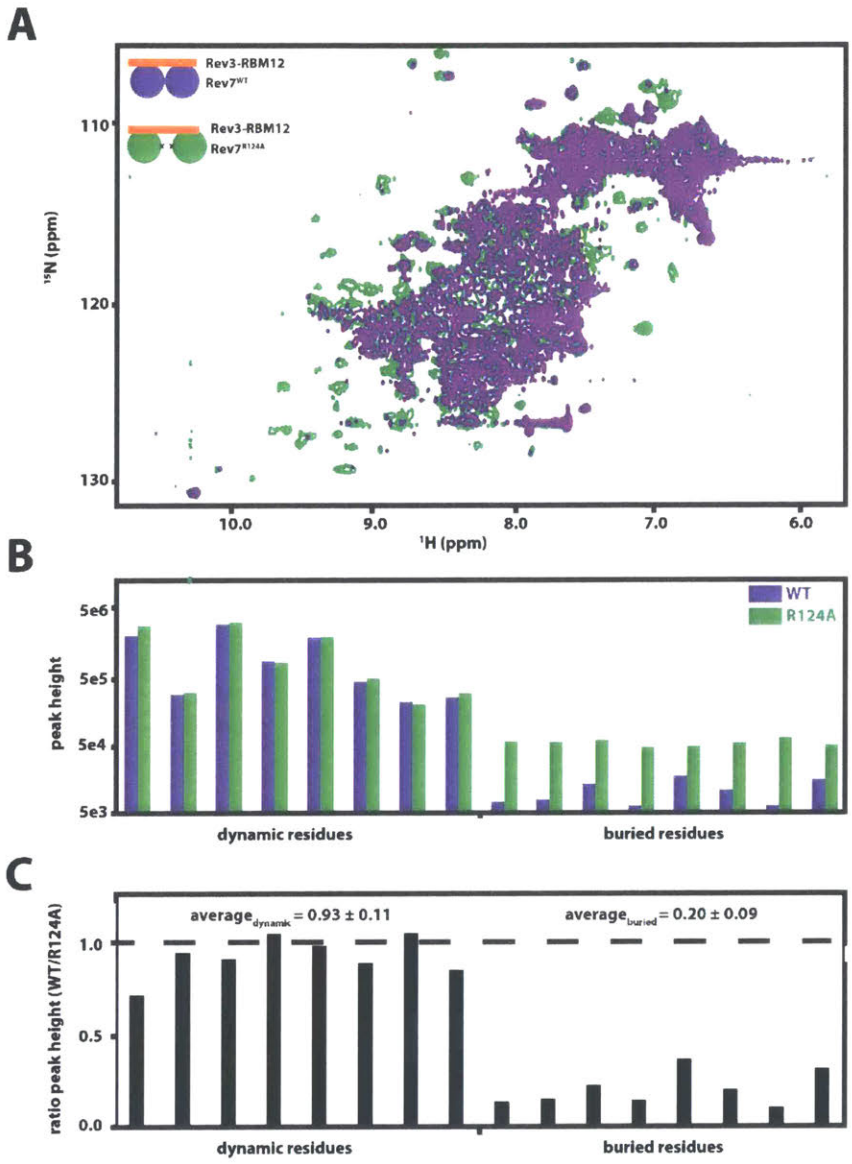
A
Rev3-RBM12
Rev7WT
Rev3-RBM12
Rev7R124A
110
120
130
15N (ppm)
10.0
9.0
8.0
7.0
6.0
1H (ppm)
B
WT
R124A
5e6
5e5
5e4
5e3
peak height
dynamic residues
buried residues
C
averagedynamic = 0.93 ± 0.11
averageburied = 0.20 ± 0.09
1.0
0.5
0.0
ratio peak height (WT/R124A)
dynamic residues
buried residues

Fig. S7

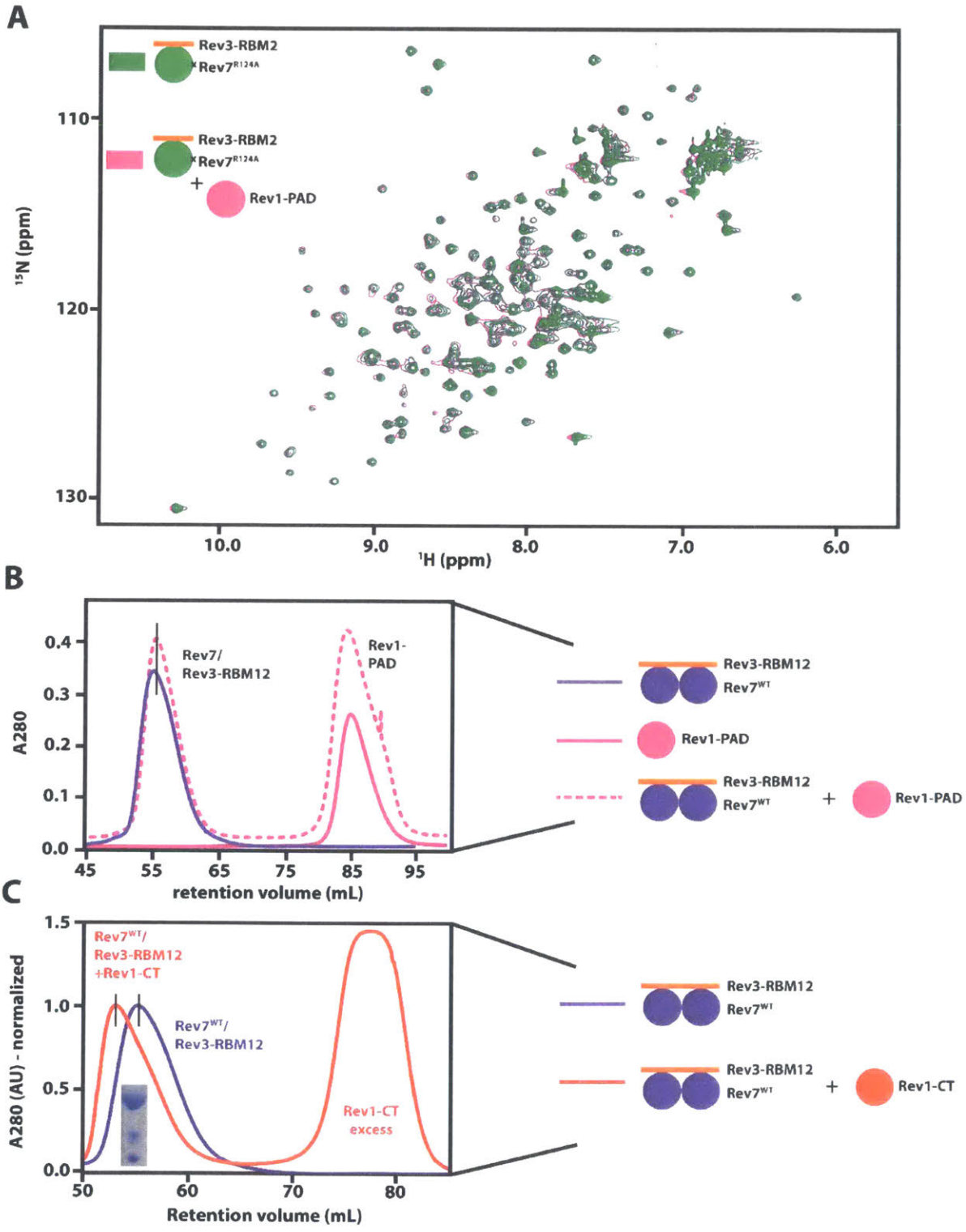
A
Rev3-RBM2
Rev7R124A
Rev3-RBM2
Rev7R124A
+
Rev1-PAD
15N (ppm)
1H (ppm)
B
Rev7/
Rev3-RBM12
Rev1-
PAD
A280
retention volume (mL)
Rev3-RBM12
Rev7WT
Rev1-PAD
Rev3-RBM12
Rev7WT
+
Rev1-PAD
C
Rev7WT/
Rev3-RBM12
+Rev1-CT
Rev7WT/
Rev3-RBM12
Rev1-CT
excess
A280 (AU) - normalized
Retention volume (mL)
Rev3-RBM12
Rev7WT
Rev3-RBM12
Rev7WT
+
Rev1-CT

Fig. S8

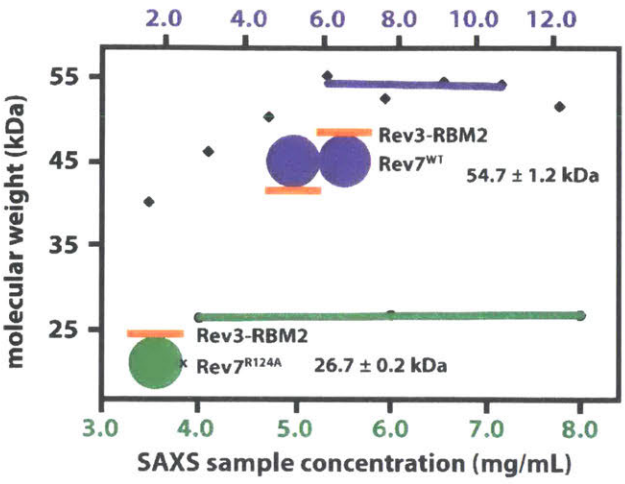
2.0
4.0
6.0
8.0
10.0
12.0
55
45
35
25
molecular weight (kDa)
Rev3-RBM2
Rev7WT
54.7 ± 1.2 kDa
Rev3-RBM2
Rev7R124A
26.7 ± 0.2 kDa
3.0
4.0
5.0
6.0
7.0
8.0
SAXS sample concentration (mg/mL)

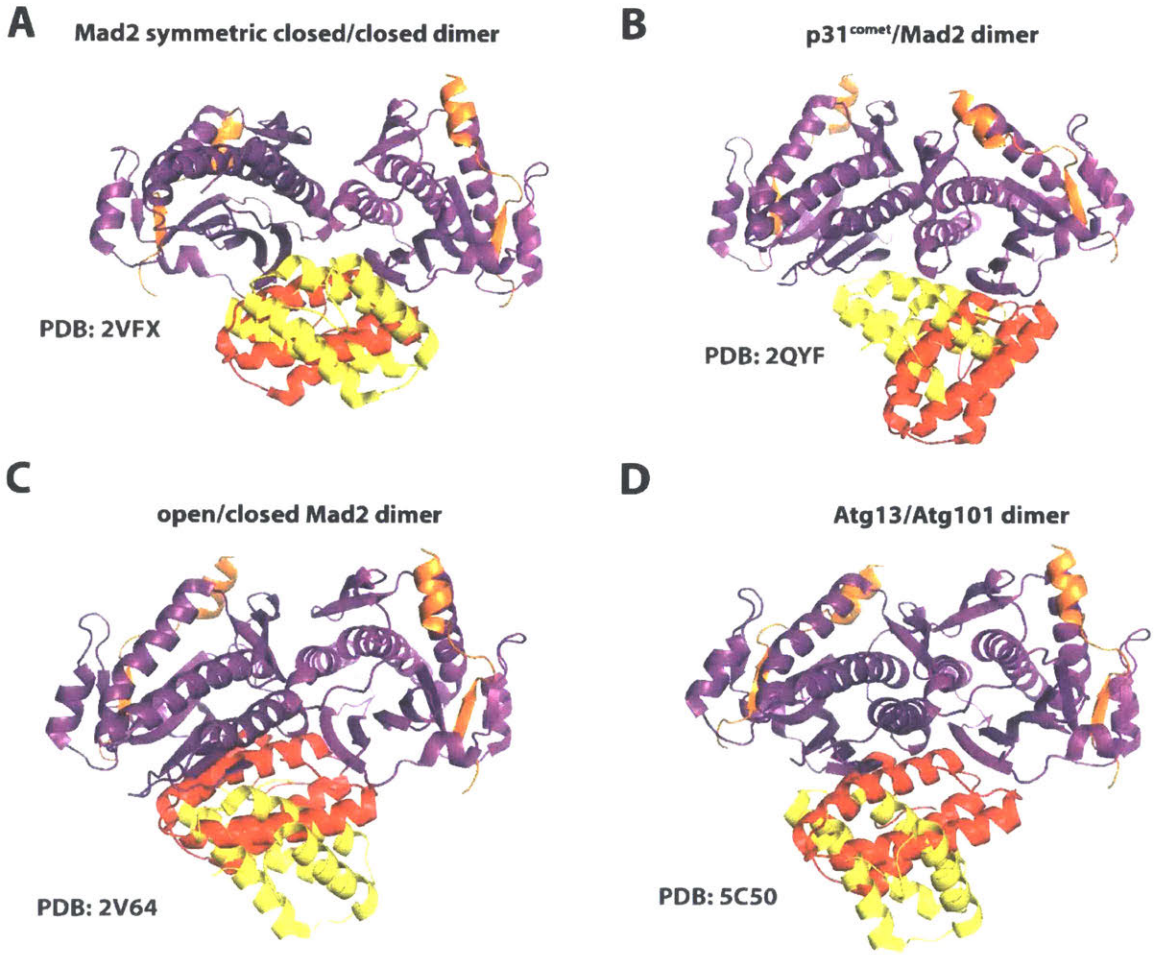
A
Mad2 symmetric closed/closed dimer
PDB: 2VFX
B
p31comet/Mad2 dimer
PDB: 2QYF
C
open/closed Mad2 dimer
PDB: 2V64
D
Atg13/Atg101 dimer
PDB: 5C50

Chapter 5

Discussion

In this thesis, CRISPR-Cas9 gene editing technologies, cell biology, and biochemical assays were employed to elucidate the functional relevance of the multifunctional protein Rev7 in drug-resistant cancer. The development of Rev7 knockout (Rev7KO) lung adenocarcinoma cells was key to the discoveries made in this thesis, for they were used to explore the role that Rev7 may play in mediating chemoresistance in drug-resistant lung cancer. In this work I discovered that Rev7 loss strikingly enhances cisplatin efficacy in drug-resistant "KP" lung cancer cells *in vitro*. Importantly, I also discovered that Rev7 loss enhances cisplatin efficacy in treating KP tumors *in vivo* and drastically increases overall survival of mice transplanted with KP tumors.

I also sought to gain new insights into the functional relevance of Rev7 by conducting analyses aimed at better elucidating Rev7 mediated protein-protein interactions (PPI). This approach was important, because historically studies examining Rev7's biological relevance have largely been focused on the role it plays as a structural subunit in the TLS DNA damage tolerance pathway. However, in the last decade it has become increasingly apparent that Rev7 plays important roles in regulating multiple cellular processes beyond the TLS pathway, such as DSB repair pathway choice, and may do so in part by interactions it forms with diverse protein partners.

To better understand the biological relevance of Rev7's diverse cell regulatory functions I employed immunoprecipitation and mass spectrometry studies that would allow me to detect Rev7-interacting proteins. In these studies I was able to demonstrate that under varied cellular

conditions, such as in G2/M arrested cells or mitomycin C (MMC) DNA damaged cells, Rev7 consistently interacts with several relatively uncharacterized protein interactors of interest. In these analyses I also discovered that Rev7 interacts with several novel protein interactors only in MMC DNA damaged cells. This discovery was particularly intriguing, for these findings reveal that Rev7 may form different protein-protein interactions depending on the cellular conditions. Additionally, this work led to the discovery that Rev7 forms novel interactions with proteins that have been shown to structurally remodel HORMA domain proteins like Rev7 and play important roles regulating DNA damage response (DDR) mechanisms, such as DSB repair.

I was particularly intrigued by the data that revealed Rev7 forms novel interactions with DSB repair proteins, which stimulated me to investigate if Rev7 plays any role regulating DSB repair in drug-resistant lung cancer cells. When I conducted DSB repair studies in Rev7 knockout KP cells, I observed a an increase in DSBs, which consistent with Rev7 loss reducing DSB repair capacity in KP cells. Most interestingly, these data reveal that the loss in DSB repair in in Rev7 KO KP cells is due to a reduction in HR DSB repair activity. Importantly, these findings suggest that Rev7 may play an important role in regulating DSB repair in drug-resistant lung cancer cells.

Altogether, my thesis research has demonstrated that Rev7 has functional relevance in modulating chemotherapeutic response in drug-resistant lung cancer. Importantly, these studies have revealed that Rev7's ability to modulate chemotherapeutic response in drug-resistant tumors model may be due to both its TLS and non-TLS DNA damage response regulatory functions. Furthermore, the work in this thesis strongly suggests that the development of small molecule inhibitors targeting specific Rev7 mediated protein interactions may provide new avenues to enhance chemotherapeutic efficacy in the clinic.

Rev7 expression and potential insights gained about Rev7's functional relevance in different cancer cells

One open question highlighted by that the findings in this thesis is whether Rev7 modulates chemotherapeutic response in the same manner in different malignancies. That is to say, to date published studies examining Rev7's role in chemotherapeutic efficacy have uncovered that Rev7 depletion does not always sensitize tumors to cancer treatment. For example, findings in several recent studies reveal that Rev7 depletion in BRCA-deficient cancer cells results in a decrease in sensitivity to PARP inhibitors, thus suggesting that in these cancer cells wild-type Rev7 may inhibit resistance to cancer treatment (Gupta et al., 2018; Xu et al., 2015). In contrast, recent studies conducted in ovarian cancer cells and glioma cells reveal that Rev7 depletion significantly sensitizes ovarian cancer cells to cisplatin enhances ionizing radiation (IR) sensitivity in glioma cells (Zhao et al., 2011). Additionally, findings in this thesis reveal that Rev7 loss sensitives drug-resistant lung cancer cells to cisplatin, further suggesting that in some contexts wild-type Rev7 may also promote chemoresistance in cancer cells.

Taken together, these findings highlight that while there may be much promise in developing small molecule inhibitors that target Rev7 that can be used to enhance the efficacy of chemotherapeutic agents like cisplatin certain contexts, it is also possible that inhibiting Rev7 function may also prove detrimental because it may promote chemoresistance mechanisms in other cancer contexts. Subsequently, more detailed characterizations of Rev7's biological relevance in different cell and tumor types is necessary to better determine which contexts abrogating Rev7 function may be beneficial.

To this point, one avenue that may help better elucidate how Rev7 may modulates chemotherapeutic response may be found in analyses focused on better understanding Rev7

expression in specific cell/ cancer contexts. This would be of value because Rev7 expression data in several of the studies highlighted in this thesis suggest that Rev7's expression may vary in different cancer contexts. For example, studies investigating the role the Rev7 may play in glioma cells reveal that Rev7 is overexpressed in IR-resistant glioma cells (Zhao et al., 2011). In contrast, studies investigating the role that Rev7 plays in BRCA-deficient cancer cells, specifically in BRCA-deficient breast and prostate cancer cells, reveal that these tumors often do not express Rev7 due to loss of functions in PARP inhibitor resistant cancer cells

Potential insights gained about Rev7's biological relevance from shRev7 versus Rev7KO studies

Interestingly, work in this thesis also highlights that more detailed studies focused on Rev7's expression may be important in elucidating how Rev7 modulates chemotherapeutic efficacy. Namely, findings in this thesis suggest that to truly unmask Rev7's functional relevance Rev7 knockout might be crucial. Specifically, while the findings in this thesis reveal that Rev7KO drastically enhance cisplatin sensitivity in drug-resistant lung cancer cells, other studies conducted during my PhD (Appendix Fig. 1a-d) focused on investigating the role Rev7 may play in modulating chemotherapeutic response in the *Eμ-myc arf*$^{-/-}$ mouse model of Burkitt's lymphoma, reveal that Rev7 knockdown has little to no impact on enhancing chemotherapeutic efficacy in these tumor cells.

In particular, the Rev7 Burkitt's lymphoma studies revealed that when short-hairpin RNAs (shRNAs) are used to knockdown Rev7, with only ~10% Rev7 transcript remaining, Burkitt's lymphoma cells are only moderately sensitized to cisplatin *in vitro* and Rev7 shRNAs fail to sensitize Burkitt's lymphoma cells to cisplatin *in vivo* (Appendix Fig. 1a,b). Additionally, these

data reveal that when Burkitt's lymphoma cells are treated with mafosfamide, an *in vitro* analog of the clinically relevant Burkitt's lymphoma drug cyclophosphamide, Rev7 knockdown Burkitt's lymphoma cells display little to no sensitivity to mafosfamide (Appendix Fig. 1d).). These data were striking for they are in stark contrast to Rev3 studies that reveal that Rev3 knockdown in Burkitt' s lymphoma cells drastically enhances sensitivity to cisplatin and mafosfamide in these cells (Xie, Doles, Hemann, & Walker, 2010). Importantly, the Rev3 findings suggest that Rev7, like Rev3, may indeed play a role in modulating chemotherapeutic response in these Burkitt's lymphoma cells but the fact that Rev7 knockdown and not knocked out in these cells may be masking this chemosensitivity phenotype.

Furthermore, these findings are of particular interest because studies suggest that Rev7 expression more be extremely abundant in cells. For example, studies have shown that Rev7 expression is about 4000 times that of Rev3 expression in mouse embryonic fibroblasts (cite.) Rev7's abundant expression has been linked to Rev7's ability to regulate interact with many different protein partners. This observation may help explain the variation in chemotherapeutic response phenotypes observed in this thesis in Rev7KO vs Rev7-knockdown cancer cells. Based on this hypothesis it is also possible that the half-life for Rev7 protein turnover might high and as such changes in Rev7 transcript levels might not significantly alter the amount of Rev7 present levels. Importantly, given Rev7's diverse cellular functions and ability to interact with many different protein partners, if this is the case, it is possible that residual Rev7 protein expression might be sufficient to form protein complexes with some of its protein interactors.

Altogether, findings highlighted in this section underscore the need for future studies investigating how Rev7 modulates chemotherapeutic response in drug-resistant lung cancer, to assess Rev7 mRNA and protein levels in drug-resistant lung cancer cells. More importantly, the

a better understanding of Rev7's expression status may help better inform cancer treatment regimens in drug-resistant lung tumors and other relevant drug-resistant malignancies.

Structural regulation of HORMA domain protein MAD2 and potential insights gained for Rev7 function

Work in this thesis is of particular value for it is the first to reveal that Rev7's DNA damage response roles beyond the TLS DNA damage tolerance pathway, namely Rev7's regulation of DSB repair, may also contribute to its ability to modulate chemotherapeutic efficacy in drug-resistant lung cancer. One key question that remains unclear is how Rev7 is able to promote its multifunctional capabilities and how this in turn impacts its ability to mediate chemoresistance in cancer.

Notably, work explored in this thesis has highlighted the importance that Rev7's conformational structure likely plays in regulating Rev7's ability to regulate chemotherapeutic response. Specifically, in this thesis in collaboration with the Korzhnev lab we have obtained structural data showing that wild-type Rev7 forms a homodimer and we have discovered that when we mutate Rev7's ability to homodimerize, drug-resistant lung cancer cells are strikingly sensitized to cisplatin treatment. As such, much insight into how Rev7's diverse functions are regulated may be gained from studies characterizing how other HORMA domain proteins are structurally, and in turn functionally, regulated.

In recent years, there have been a number of studies that have revealed that the diverse cellular functions of many HORMA domain proteins are regulated by the structural remodeling carried out by TRIP13, a AAA+ ATPase (Ye et al., 2015). Due to its significant sequence and

structural homology to Rev7, information on how the HORMA domain protein MAD2 is structurally regulated in cells may provide insights into how Rev7 mediates its diverse cellular functions. For MAD2, which like Rev7 is found in cells as a dimer, to correctly carry out its spindle activity checkpoint (SAC) function, MAD2 must be structurally remodeled in a manner that allows MAD2's HORMA domain to go from a closed (C-MAD2) to an open (O-MAD2) conformation. Structural studies have revealed that TRIP13's AAA+ ATPase activity is crucial for this remodeling to occur (Ma & Poon, 2018). In particular, these studies have revealed that TRIP13's AAA+ ATPase activity replenishes the cells pool of O-MAD2, which is needed for SAC to occur in the presence of unattached kinetochores, and as such when cells are TRIP13 deficient, MAD2 is unable to successfully promote SAC activation (Ma & Poon, 2018).

Consequently, future work investigating the biological relevance of Rev7 will benefit from insights gained from studies that have characterized how MAD2's structural remodeling impacts its cellular function. Additionally, given that work in this thesis has revealed that wild-type Rev7 dimerizes using the same HORMA domain interface that MAD2 uses to dimerize and, similar to MAD2, Rev7 interacts with proteins like $p31^{comet}$, which is an adaptor protein that TRIP13 uses to recognize a target HORMA domain protein, is it likely that Rev7 is indeed structurally remodeled by TRIP13. Taken together with my discovery in this thesis that Rev7 interacts with TRIP13, it is clear that that more detailed structure-function characterizations of Rev7's interaction with TRIP13 may help better elucidate how Rev7 is able to use its diverse cellular functions to modulate chemotherapeutic response in tumors.

Conclusion:

Work in this thesis presents striking evidence revealing that the multifunctional protein Rev7 modulates chemotherapeutic efficacy in drug-resistant lung cancer. This is important for it is the first study to suggest that Rev7's cellular functions beyond the TLS DNA damage tolerance pathway may also contribute to Rev7's ability to regulate chemotherapeutic efficacy in drug-resistant tumors. As our understanding of the mechanisms that promote chemoresistance increases, it is clear that targeting proteins like Rev7, which has multiple DNA damage response (DDR) functions, is advantageous because inhibiting multi-functional DDR proteins may provide a new way to improve the efficacy of chemotherapy in a wide-range of chemoresistant malignancies.

Appendix

Investigating the impact that Rev7 plays in modulating chemotherapeutic efficacy in Eμ-myc arf$^{-/-}$ Burkitt's lymphoma cells

Contributions F.M.V., G.C.W., and M.T.H. conceived the idea for the research, designed experiments and interpreted data.

Fig1a: qPCR analysis of Rev7 shRNA depletion in Eμ-myc arf$^{-/}$ Burkitt's lymphoma cells, $p<0.001$

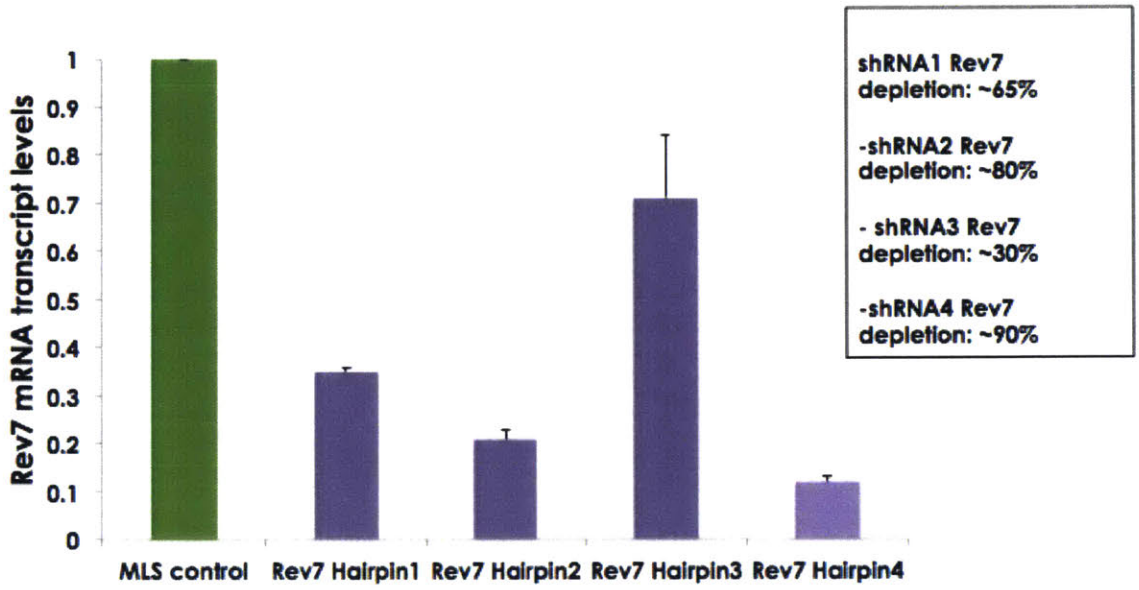

Fig1b: Schematic depicting *in vitro* GFP competition assay

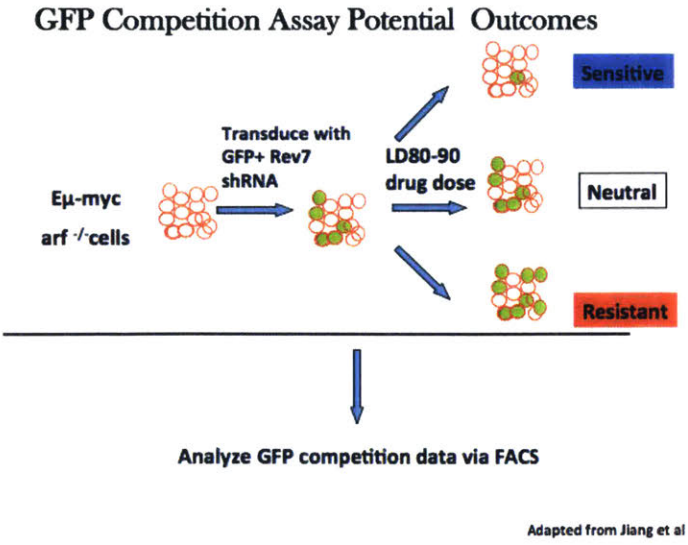

Fig1c: GFP competition assay assessing cisplatin sensitivity in Rev7 deficient (shRNA4) Eμ-myc arf$^{-/-}$ Burkitt's lymphoma cells, $p<0.001$

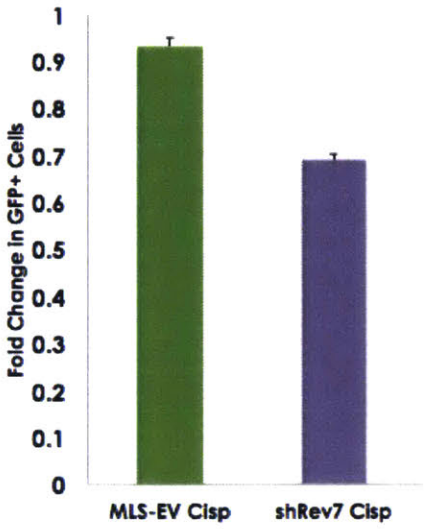

Fig1c: Kaplan-meier survival curve assessing overall survival following cisplatin treatment in mice transplanted with Rev7-deficient Eμ-myc arf$^{-/-}$ Burkitt's lymphoma tumors, $p<0.001$

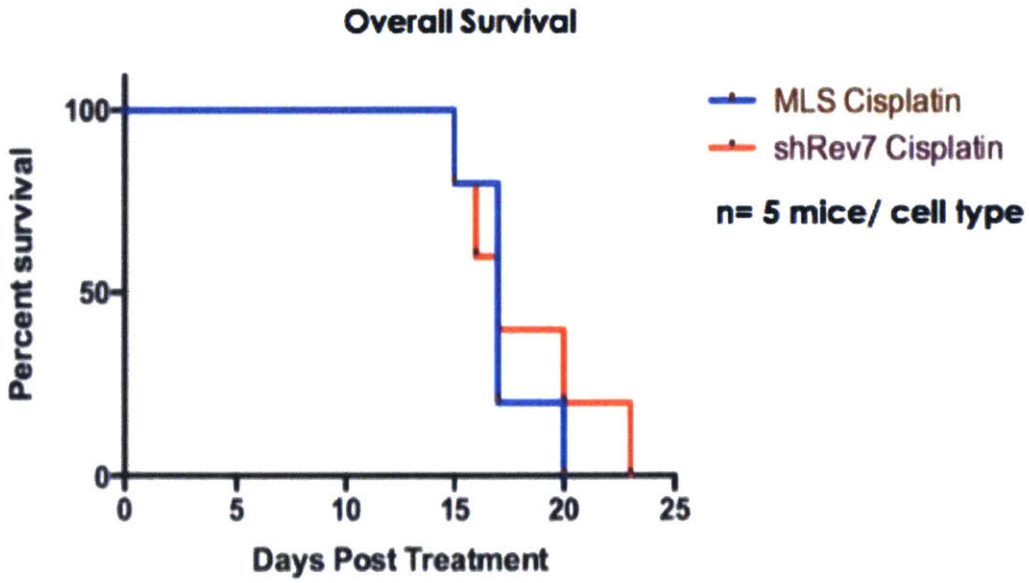

Fig.2: GFP competition assay assessing mafosfamide sensitivity in Rev7 deficient (shRNA4) Eμ-myc arf$^{-/-}$ Burkitt's lymphoma cells

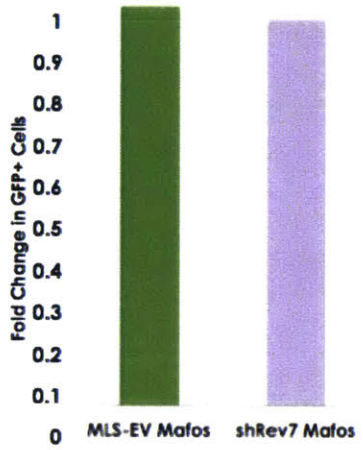

Methods

Cell Culture, Retroviral Vectors, and Chemicals

Eμ-myc Burkitt's lymphoma cells were cultured in B-cell medium (45% vol/vol DMEM/45% Iscove's Modified Dulbecco's Medium/10% FBS, supplemented with 2 mM L-glutamine and 5 μM β-mercaptoethanol). shRNA constructs were designed and cloned as previously described in this thesis. Cisplatin was purchased from Calbiochem and used at the indicated concentrations (used at 1 μM).

shRNA design, cloning, and RT-qPCR validation

Short hairpin RNA (shRNA) constructs were designed and cloned as previously described (Dickins RA, et al). The vector used coexpressed GFP under the control of the SV40 promotor and is identical to the published MSCV/LTRmiR30-SV40-GFP (LMS) vector. Retrovirally infected cells were then selected by fluorescence assisted cell sorting (FACS) for GFP positive cells. RNA from 2 x 10^6 cells was prepared using RNeasy Mini Kit (Qiagen). RT-qPCR was performed using SYBR green on a BioRad thermal cycler. GAPDH and Rev7 primer sequences are available upon request.

GFP Competition Assays

Eμ-Myc$^{p19arf-/-}$ lymphoma cells were infected with GFP-tagged shRNAs such that 15–25% of the population were GFP positive. An eighth of a million cells in 250μL B-cell media (BCM) were

then seeded into 24-well plates. For wells that would remain untreated as a control, only $1/16^{th}$ of a million cells were seeded. Next, 250μL of drug containing media was added to the cells. After 24 h, 300μL of cells from untreated wells are removed and replaced by 300μL fresh BCM. All wells then received 500μL BCM before being placed in the incubator for another 24 hours. At 48 h, cells transduced with the control vector, MLS, were checked for viability via flow cytometry on a BD FACScan using propidium iodide (PI) as a live/dead marker. Untreated wells then had 700μL of cells removed and replaced with 700μL fresh media followed by a further 1mL of fresh media. Wells for which drug had killed 80–90% of cells (LD80–90) were then diluted further by adding 1mL of BCM. Finally, at 72 h all wells for which an LD80–90 was achieved, as well as the untreated samples, were run via flow cytometry to determine GFP%.

***In vivo* transplantation:**

Eμ-Myc$^{p19arf-/-}$ lymphoma cells (~1×10^6) were intravenously injected into the tail vein of syngeneic C57BL6/Jx129-JAE female recipient mice. Upon tumor presentation, mice were administered with 10 mg/kg cisplatin. The Massachusetts Institute of Technology Committee on Animal Care reviewed and approved all mouse experiments described in this study.

Bibliography

Abbas, T., Keaton, M. A., & Dutta, A. (2013). Genomic Instability in Cancer. *Cold Spring Harb Perspect Biol*, *5*, 1–18. https://doi.org/10.1101/cshperspect.a012914

Abraham, R. T. (2001). cell cycle checkpoint signaling therough the ATM an ATR kinases.pdf. *Genes & Development*, *15*, 2177–2196. https://doi.org/10.1101/gad.914401.DNA

Acosta, J. C., & Gil, J. (2012). Senescence: A new weapon for cancer therapy. *Trends in Cell Biology*, *22*(4), 211–219. https://doi.org/10.1016/j.tcb.2011.11.006

Ahsan, A. (2016). *Lung Cancer and Personalized Medicine* (Vol. 893). https://doi.org/10.1007/978-3-319-24223-1

Albertella, M. R., Green, C. M., Lehmann, A. R., & O'Connor, M. J. (2005). A role for polymerase η in the cellular tolerance to cisplatin-induced damage. *Cancer Research*, *65*(21), 9799–9806. https://doi.org/10.1158/0008-5472.CAN-05-1095

Alcindor, T., & Beauger, N. (2011). Oxaliplatin: A review in the era of molecularly targeted therapy. *Current Oncology*, *18*(1), 18–25. https://doi.org/10.3747/co.v18i1.708

Aravind, L., & Koonin, E. V. (1998). The HORMA domain: a common structural denominator in mitotic checkpoints, chromosome synapsis and DNA repair. *Trends in Biochemical Sciences*, *23*(8), 284–286. https://doi.org/10.1016/S0968-0004(98)01257-2

Ashworth, A., & Lord, C. J. (2018). Synthetic lethal therapies for cancer : *Nature Reviews Clinical Oncology*. https://doi.org/10.1038/s41571-018-0055-6

Banerjee, R., Russo, N., Liu, M., Basrur, V., Bellile, E., Palanisamy, N., … D'Silva, N. J. (2014). TRIP13 promotes error-prone nonhomologous end joining and induces chemoresistance in head and neck cancer. *Nature Communications*, *5*. https://doi.org/10.1038/ncomms5527

Barazas, M., Annunziato, S., Pettitt, S. J., de Krijger, I., Ghezraoui, H., Roobol, S. J., … Rottenberg, S. (2018). The CST Complex Mediates End Protection at Double-Strand Breaks and Promotes PARP Inhibitor Sensitivity in BRCA1-Deficient Cells. *Cell Reports*, *23*(7), 2107–2118. https://doi.org/10.1016/j.celrep.2018.04.046

Bartholomeeusen, K., Christ, F., Hendrix, J., Rain, J. C., Emiliani, S., Benarous, R., … de Rijck, J. (2009). Lens epithelium-derived growth factor/p75 interacts with the transposase-derived

DDE domain of pogZ. *Journal of Biological Chemistry*, *284*(17), 11467–11477. https://doi.org/10.1074/jbc.M807781200

Bassett, E., King, N. M., Bryant, M. F., Hector, S., Pendyala, L., Chaney, S. G., & Cordeiro-Stone, M. (2004). The role of DNA polymerase eta in translesion synthesis past platinum-DNA adducts in human fibroblasts. *Cancer Research*, *64*(18), 6469–6475. https://doi.org/10.1158/0008-5472.CAN-04-1328

Basu, A., & Krishnamurthy, S. (2010). Cellular responses to cisplatin-induced DNA damage. *Journal of Nucleic Acids*, *2010*. https://doi.org/10.4061/2010/201367

Baude, A., Aaes, T. L., Zhai, B., Al-Nakouzi, N., Oo, H. Z., Daugaard, M., … Jäättelä, M. (2015). Hepatoma-derived growth factor-related protein 2 promotes DNA repair by homologous recombination. *Nucleic Acids Research*, *44*(5), 2214–2226. https://doi.org/10.1093/nar/gkv1526

Baudino, T. (2015). Targeted Cancer Therapy: The Next Generation of Cancer Treatment. *Current Drug Discovery Technologies*, *12*(1), 3–20. https://doi.org/10.2174/1570163812666150602144310

Bhat, A., Wu, Z., Maher, V. M., McCormick, J. J., & Xiao, W. (2015). Rev7/Mad2B plays a critical role in the assembly of a functional mitotic spindle. *Cell Cycle (Georgetown, Tex.)*, *14*(24), 3929–3938. https://doi.org/10.1080/15384101.2015.1120922

Blackford, A. N., & Jackson, S. P. (2017). ATM, ATR, and DNA-PK: The Trinity at the Heart of the DNA Damage Response. *Molecular Cell*, *66*(6), 801–817. https://doi.org/10.1016/j.molcel.2017.05.015

Boersma, V., Moatti, N., Segura-Bayona, S., Peuscher, M. H., Van Der Torre, J., Wevers, B. A., … Jacobs, J. J. L. (2015). MAD2L2 controls DNA repair at telomeres and DNA breaks by inhibiting 5′ end resection. *Nature*, *521*(7553), 537–540. https://doi.org/10.1038/nature14216

Cahill, D. P., Da Costa, L. T., Carson-Walter, E. B., Kinzler, K. W., Vogelstein, B., & Lengauer, C. (1999). Characterization of MAD2B and other mitotic spindle checkpoint genes. *Genomics*, *58*(2), 181–187. https://doi.org/10.1006/geno.1999.5831

Caiola, E., Salles, D., Frapolli, R., Lupi, M., Rotella, G., Ronchi, A., … Marabese, M. (2015). Base excision repair-mediated resistance to cisplatin in KRAS(G12C) mutant NSCLC cells. *Oncotarget*, *6*(30), 30072–30087. https://doi.org/10.18632/oncotarget.5019

Ceccaldi, R., Rondinelli, B., & D'Andrea, A. D. (2016). Repair Pathway Choices and Consequences at the Double-Strand Break. *Trends in Cell Biology*, *26*(1), 52–64. https://doi.org/10.1016/j.tcb.2015.07.009

Chabner, B. A., & Roberts, T. G. (2005). Timeline: Chemotherapy and the war on cancer. *Nature Reviews Cancer*, *5*(1), 65–72. https://doi.org/10.1038/nrc1529

Chang, A. (2011). Chemotherapy, chemoresistance and the changing treatment landscape for NSCLC. *Lung Cancer*, *71*(1), 3–10. https://doi.org/10.1016/j.lungcan.2010.08.022

Chapman, J. R., Taylor, M. R. G., & Boulton, S. J. (2012). Playing the End Game: DNA Double-Strand Break Repair Pathway Choice. *Molecular Cell*, *47*(4), 497–510. https://doi.org/10.1016/j.molcel.2012.07.029

Cheeseman, I. M., & Desai, A. (2005). P ROTOCOL A Combined Approach for the Localization and Tandem Affinity Purification of Protein Complexes from Metazoans RECIPES Coupling GFP Antibody to Protein A Beads Preparation of Tissue Culture Cells for Biochemistry. *Cancer*, 1–15. Retrieved from http://stke.sciencemag.org/content/sigtrans/2005/266/pl1.full.pdf

Chen, P., Li, J., Chen, Y. C., Qian, H., Chen, Y. J., Su, J. Y., … Lan, T. (2016). The functional status of DNA repair pathways determines the sensitization effect to cisplatin in non-small cell lung cancer cells. *Cellular Oncology*, *39*(6), 511–522. https://doi.org/10.1007/s13402-016-0291-7

Cheung-Ong, K., Giaever, G., & Nislow, C. (2013). DNA-damaging agents in cancer chemotherapy: Serendipity and chemical biology. *Chemistry and Biology*, *20*(5), 648–659. https://doi.org/10.1016/j.chembiol.2013.04.007

Cheung, H. W., Chun, A. C. S., Wang, Q., Deng, W., Hu, L., Guan, X. Y., … Wang, X. (2006). Inactivation of human MAD2b in nasopharyngeal carcinoma cells leads to chemosensitization to DNA-damaging agents. *Cancer Research*, *66*(8), 4357–4367. https://doi.org/10.1158/0008-5472.CAN-05-3602

Ciccia, A., & Elledge, S. J. (2010). The DNA Damage Response: Making It Safe to Play with Knives. *Molecular Cell*, *40*(2), 179–204. https://doi.org/10.1016/j.molcel.2010.09.019

Collado, M., Blasco, M. A., & Serrano, M. (2007). Cellular Senescence in Cancer and Aging. *Cell*, *130*(2), 223–233. https://doi.org/10.1016/j.cell.2007.07.003

Combs-cantrell, D. T., Cohen, M., Ed, D., Kalayjian, L. A., Kanner, A., Liporace, J. D., … Ph,

D. (2009). New England Journal. *Media*, *362*(1), 1597–1605. https://doi.org/10.1056/NEJMoa1215817

D'Adda Di Fagagna, F. (2008). Living on a break: Cellular senescence as a DNA-damage response. *Nature Reviews Cancer*, *8*(7), 512–522. https://doi.org/10.1038/nrc2440

d'Amato, T. A., Landreneau, R. J., Ricketts, W., Huang, W., Parker, R., Mechetner, E., … Luketich, J. D. (2007). Chemotherapy resistance and oncogene expression in non-small cell lung cancer. *Journal of Thoracic and Cardiovascular Surgery*, *133*(2), 352–363. https://doi.org/10.1016/j.jtcvs.2006.10.019

Daugaard, M., Baude, A., Fugger, K., Povlsen, L. K., Beck, H., Sørensen, C. S., … Jäättelä, M. (2012). LEDGF (p75) promotes DNA-end resection and homologous recombination. *Nature Structural and Molecular Biology*, *19*(8), 803–810. https://doi.org/10.1038/nsmb.2314

Deans, A. J., & West, S. C. (2011). DNA interstrand crosslink repair and cancer. *Nature Reviews Cancer*, *11*(7), 467–480. https://doi.org/10.1038/nrc3088

DeVita, V. T., & Chu, E. (2008). A history of cancer chemotherapy. *Cancer Research*, *68*(21), 8643–8653. https://doi.org/10.1158/0008-5472.CAN-07-6611

Dietlein, F., Thelen, L., & Reinhardt, H. C. (2014). Cancer-specific defects in DNA repair pathways as targets for personalized therapeutic approaches. *Trends in Genetics*, *30*(8), 326–339. https://doi.org/10.1016/j.tig.2014.06.003

Doles, J., Oliver, T. G., Cameron, E. R., Hsu, G., Jacks, T., Walker, G. C., & Hemann, M. T. (2010). Suppression of Rev3, the catalytic subunit of Pol , sensitizes drug-resistant lung tumors to chemotherapy. *Proceedings of the National Academy of Sciences*, *107*(48), 20786–20791. https://doi.org/10.1073/pnas.1011409107

Elmore, S. (2007). Apoptosis: A Review of Programmed Cell Death. *Toxicologic Pathology*, *35*(4), 495–516. https://doi.org/10.1080/01926230701320337

Fattah, F. J., Hara, K., Fattah, K. R., Yang, C., Wu, N., Warrington, R., … Yu, H. (2014). The Transcription Factor TFII-I Promotes DNA Translesion Synthesis and Genomic Stability. *PLoS Genetics*, *10*(6). https://doi.org/10.1371/journal.pgen.1004419

Fromme, J. C., & Verdine, G. L. (2004). Base Excision Repair. *Advances in Protein Chemistry*, *69*, 1–41. https://doi.org/10.1016/S0065-3233(04)69001-2

Fu, D., Calvo, J. A., & Samson, L. D. (2012). Balancing repair and tolerance of DNA damage

caused by alkylating agents. *Nature Reviews Cancer*, *12*(2), 104–120. https://doi.org/10.1038/nrc3185

Gan, G. N., Wittschieben, J. P., Wittschieben, B., & Wood, R. D. (2008). DNA polymerase zeta (pol) in higher eukaryotes. *Cell Research*, *18*(1), 174–183. https://doi.org/10.1038/cr.2007.117

Ge, J., Prasongtanakij, S., Wood, D. K., Weingeist, D. M., Fessler, J., Navasummrit, P., … Engelward, B. P. (2014). CometChip: A High-throughput 96-Well Platform for Measuring DNA Damage in Microarrayed Human Cells. *Journal of Visualized Experiments*, (92), 8–15. https://doi.org/10.3791/50607

Goodman, M. F., & Woodgate, R. (2013). Translesion DNA polymerases. *Cold Spring Harbor Perspectives in Biology*, *5*(10), 1–20. https://doi.org/10.1101/cshperspect.a010363

Gupta, R., Somyajit, K., Narita, T., Maskey, E., Stanlie, A., Kremer, M., … Choudhary, C. (2018). DNA Repair Network Analysis Reveals Shieldin as a Key Regulator of NHEJ and PARP Inhibitor Sensitivity. *Cell*, *173*(4), 972–988.e23. https://doi.org/10.1016/j.cell.2018.03.050

Hanahan, D., & Weinberg, R. A. (2011). Leading Edge Review Hallmarks of Cancer: The Next Generation. *Cell*, *144*, 646–674. https://doi.org/10.1016/j.cell.2011.02.013

Hara, K., Taharazako, S., Ikeda, M., Fujita, H., Mikami, Y., Kikuchi, S., … Hashimoto, H. (2017). Dynamic feature of mitotic arrest deficient 2–like protein 2 (MAD2L2) and structural basis for its interaction with chromosome Alignment–maintaining phosphoprotein (CAMP). *Journal of Biological Chemistry*, *292*(43), 17658–17667. https://doi.org/10.1074/jbc.M117.804237

Harper, J. W., & Elledge, S. J. (2007). The DNA Damage Response: Ten Years After. *Molecular Cell*, *28*(5), 739–745. https://doi.org/10.1016/j.molcel.2007.11.015

Helleday, T. (2010). Homologous recombination in cancer development, treatment and development of drug resistance. *Carcinogenesis*, *31*(6), 955–960. https://doi.org/10.1093/carcin/bgq064

Herbst, R. S., Morgensztern, D., & Boshoff, C. (2018). The biology and management of non-small cell lung cancer. *Nature*, *553*(7689), 446–454. https://doi.org/10.1038/nature25183

Hicks, J. K., Chute, C. L., Paulsen, M. T., Ragland, R. L., Howlett, N. G., Gueranger, Q., … Canman, C. E. (2010). Differential Roles for DNA Polymerases Eta, Zeta, and REV1 in

Lesion Bypass of Intrastrand versus Interstrand DNA Cross-Links. *Molecular and Cellular Biology*, *30*(5), 1217–1230. https://doi.org/10.1128/MCB.00993-09

Holohan, C., Van Schaeybroeck, S., Longley, D. B., & Johnston, P. G. (2013). Cancer drug resistance: An evolving paradigm. *Nature Reviews Cancer*, *13*(10), 714–726. https://doi.org/10.1038/nrc3599

Huang, Y., & Li, L. (2013). DNA crosslinking damage and cancer - a tale of friend and foe. *Translational Cancer Research*, *2*(3), 144–154. https://doi.org/10.3978/j.issn.2218-676X.2013.03.01

Jeggo, P. A., Pearl, L. H., & Carr, A. M. (2016). DNA repair, genome stability and cancer: A historical perspective. *Nature Reviews Cancer*, *16*(1), 35–42. https://doi.org/10.1038/nrc.2015.4

Jiang, H. G., Chen, P., Su, J. Y., Wu, M., Qian, H., Wang, Y., & Li, J. (2017). Knockdown of REV3 synergizes with ATR inhibition to promote apoptosis induced by cisplatin in lung cancer cells. *Journal of Cellular Physiology*, *232*(12), 3433–3443. https://doi.org/10.1002/jcp.25792

Jiricny, J. (2006). The multifaceted mismatch-repair system. *Nature Reviews Molecular Cell Biology*, *7*(5), 335–346. https://doi.org/10.1038/nrm1907

Kartal-Yandim, M., Adan-Gokbulut, A., & Baran, Y. (2016). Molecular mechanisms of drug resistance and its reversal in cancer. *Critical Reviews in Biotechnology*, *36*(4), 716–726. https://doi.org/10.3109/07388551.2015.1015957

Kelland, L. (2007). The resurgence of platinum-based cancer chemotherapy. *Nature Reviews Cancer*, *7*(8), 573–584. https://doi.org/10.1038/nrc2167

Kikuchi, S., Hara, K., Shimizu, T., Sato, M., & Hashimoto, H. (2012). Structural basis of recruitment of DNA polymerase ζ by interaction between REV1 and REV7 proteins. *Journal of Biological Chemistry*, *287*(40), 33847–33852. https://doi.org/10.1074/jbc.M112.396838

Kothandapani, A., Dangeti, V. S. M. N., Brown, A. R., Banze, L. A., Wang, X. H., Sobol, R. W., & Patrick, S. M. (2011). Novel role of base excision repair in mediating cisplatin cytotoxicity. *Journal of Biological Chemistry*, *286*(16), 14564–14574. https://doi.org/10.1074/jbc.M111.225375

Kurfurstova, D., Bartkova, J., Vrtel, R., Mickova, A., Burdova, A., Majera, D., … Bartek, J.

(2016). DNA damage signalling barrier, oxidative stress and treatment-relevant DNA repair factor alterations during progression of human prostate cancer. *Molecular Oncology*, *10*(6), 879–894. https://doi.org/10.1016/j.molonc.2016.02.005

Lange, S. S., Takata, K., & Wood, R. D. (2011). DNA polymerases and camcer. *Nature Reviews Cancer*, *11*(2), 96–110. https://doi.org/10.1038/nrc2998.DNA

Lawrence, C. W., Das, G., & Christensen, R. B. (1985). REV7, a new gene concerned with UV mutagenesis in yeast. *MGG Molecular & General Genetics*, *200*(1), 80–85. https://doi.org/10.1007/BF00383316

Lee, Y.-S., Gregory, M. T., & Yang, W. (2014). Human Pol purified with accessory subunits is active in translesion DNA synthesis and complements Pol in cisplatin bypass. *Proceedings of the National Academy of Sciences*, *111*(8), 2954–2959. https://doi.org/10.1073/pnas.1324001111

Lehmann, A. R., Niimi, A., Ogi, T., Brown, S., Sabbioneda, S., Wing, J. F., … Green, C. M. (2007). Translesion synthesis: Y-family polymerases and the polymerase switch. *DNA Repair*, *6*(7), 891–899. https://doi.org/10.1016/j.dnarep.2007.02.003

Leland, B. A., Chen, A. C., Zhao, A. Y., Wharton, R. C., & Megan, C. (2018). Rev7 and 53BP1 / Crb2 prevent RecQ helicase-dependent hyper- resection of DNA double-strand breaks, *1*, 1–14.

Lemontt, J. F., Waters, L. S., Minesinger, B. K., Wiltrout, M. E., D'Souza, S., Woodruff, R. V., & Walker, G. C. (1971). Mutants of yeast defective in mutation induced by ultraviolet light. *Genetics*, *68*(1), 21–33. https://doi.org/10.1128/MMBR.00034-08

Li, L., Zhu, T., Gao, Y.-F., Zheng, W., Wang, C.-J., Xiao, L., … Liu, Z.-Q. (2016). Targeting DNA Damage Response in the Radio(Chemo)therapy of Non-Small Cell Lung Cancer. *International Journal of Molecular Sciences*, *17*(6), 839. https://doi.org/10.3390/ijms17060839

Lin, X. (2006). Human REV1 Modulates the Cytotoxicity and Mutagenicity of Cisplatin in Human Ovarian Carcinoma Cells. *Molecular Pharmacology*, *69*(5), 1748–1754. https://doi.org/10.1124/mol.105.020446

Listovsky, T., & Sale, J. E. (2013). Sequestration of cdh1 by mad2l2 prevents premature apc/c activation prior to anaphase onset. *Journal of Cell Biology*, *203*(1), 87–100. https://doi.org/10.1083/jcb.201302060

Litchfield, K., Levy, M., Huddart, R. A., Shipley, J., & Turnbull, C. (2016). The genomic landscape of testicular germ cell tumours: From susceptibility to treatment. *Nature Reviews Urology*, *13*(7), 409–419. https://doi.org/10.1038/nrurol.2016.107

Longley, D. B., Harkin, D. P., & Johnston, P. G. (2003). 5-Fluorouracil: Mechanisms of action and clinical strategies. *Nature Reviews Cancer*, *3*(5), 330–338. https://doi.org/10.1038/nrc1074

Lopez-Martinez, D., Liang, C.-C., & Cohn, M. A. (2016). Cellular response to DNA interstrand crosslinks: the Fanconi anemia pathway. *Cellular and Molecular Life Sciences*, *73*(16), 3097–3114. https://doi.org/10.1007/s00018-016-2218-x

Luqmani, Y. A. (2008). Mechanisms of Drug Resistance in Cancer Chemotherapy. *Medical Principles and Practice*, *14*(1), 35–48. https://doi.org/10.1159/000086183

Ma, H. T., & Poon, R. Y. C. (2018). TRIP13 Functions in the Establishment of the Spindle Assembly Checkpoint by Replenishing O-MAD2. *Cell Reports*, *22*(6), 1439–1450. https://doi.org/10.1016/j.celrep.2018.01.027

Marteijn, J. A., Lans, H., Vermeulen, W., & Hoeijmakers, J. H. J. (2014). Understanding nucleotide excision repair and its roles in cancer and ageing. *Nature Reviews Molecular Cell Biology*, *15*(7), 465–481. https://doi.org/10.1038/nrm3822

Martin, L. P., Hamilton, T. C., & Schilder, R. J. (2008). Platinum resistance: The role of DNA repair pathways. *Clinical Cancer Research*, *14*(5), 1291–1295. https://doi.org/10.1158/1078-0432.CCR-07-2238

Matulonis, U. A., Sood, A. K., Fallowfield, L., Howitt, B. E., Sehouli, J., & Karlan, B. Y. (2016). Ovarian cancer. *Nature Reviews Disease Primers*, *2*, 1–22. https://doi.org/10.1038/nrdp.2016.61

Molina, J. R., Yang, P., Cassivi, S. D., Schild, S. E., & Adjei, A. A. (2008). Non-small cell lung cancer: epidemiology, risk factors, treatment, and survivorship. *Mayo Clinic Proceedings*, *83*(5), 584–594. https://doi.org/10.4065/83.5.584

Muniandy, P. A., Liu, J., Majumdar, A., Liu, S., & Seidman, M. M. (2010). DNA interstrand crosslink repair in mammalian cells: step by step. *Critical Reviews in Biochemistry and Molecular Biology*, *45*(1), 23–49. https://doi.org/10.3109/10409230903501819

Muniyappa, K., Kshirsagar, R., & Ghodke, I. (2014). The HORMA domain: An evolutionarily conserved domain discovered in chromatin-associated proteins, has unanticipated diverse

functions. *Gene*, *545*(2), 194–197. https://doi.org/10.1016/j.gene.2014.05.020

Murakumo, Y., Ogura, Y., Ishii, H., Numata, S. I., Ichihara, M., Croce, C. M., … Takahashi, M. (2001). Interactions in the Error-prone Postreplication Repair Proteins hREV1, hREV3, and hREV7. *Journal of Biological Chemistry*, *276*(38), 35644–35651. https://doi.org/10.1074/jbc.M102051200

Nagel, Z. D., Margulies, C. M., Chaim, I. A., McRee, S. K., Mazzucato, P., Ahmad, A., … Samson, L. D. (2014). Multiplexed DNA repair assays for multiple lesions and multiple doses via transcription inhibition and transcriptional mutagenesis. *Proceedings of the National Academy of Sciences*, *111*(18), E1823–E1832. https://doi.org/10.1073/pnas.1401182111

Negrini, S., Gorgoulis, V. G., & Halazonetis, T. D. (2010). Genomic instability an evolving hallmark of cancer. *Nature Reviews Molecular Cell Biology*, *11*(3), 220–228. https://doi.org/10.1038/nrm2858

Niimi, K., Murakumo, Y., Watanabe, N., Kato, T., Mii, S., Enomoto, A., … Takahashi, M. (2014). Suppression of REV7 enhances cisplatin sensitivity in ovarian clear cell carcinoma cells. *Cancer Science*, *105*(5), 545–552. https://doi.org/10.1111/cas.12390

O'Connor, M. J. (2015). Targeting the DNA Damage Response in Cancer. *Molecular Cell*, *60*(4), 547–560. https://doi.org/10.1016/j.molcel.2015.10.040

October, T. B. S., Zamble, D. B., & Lippard, S. J. (1995). Ci @ atin # NA repair in c cer ch othe py. *October*, *20*(Iv), 435–439. https://doi.org/10.1016/S0968-0004(00)89095-7

Ohashi, E., Murakumo, Y., Kanjo, N., Akagi, J. I., Masutani, C., Hanaoka, F., & Ohmori, H. (2004). Interaction of hREV1 with three human Y-family DNA polymerases. *Genes to Cells*, *9*(6), 523–531. https://doi.org/10.1111/j.1356-9597.2004.00747.x

Oliver, T. G., Mercer, K. L., Sayles, L. C., Burke, J. R., Mendus, D., Lovejoy, K. S., … Sweet-cordero, E. A. (2010). Chronic cisplatin treatment promotes enhanced damage repair and tumor progression in a mouse model of lung cancer, (Ii), 837–852. https://doi.org/10.1101/gad.1897010.with

Ouyang, L., Shi, Z., Zhao, S., Wang, F. T., Zhou, T. T., Liu, B., & Bao, J. K. (2012). Programmed cell death pathways in cancer: A review of apoptosis, autophagy and programmed necrosis. *Cell Proliferation*, *45*(6), 487–498. https://doi.org/10.1111/j.1365-2184.2012.00845.x

Pani, E., Stojic, L., El-Shemerly, M., Jiricny, J., & Ferrari, S. (2007). Mismatch repair status and the response of human cells to cisplatin. *Cell Cycle*, *6*(14), 1796–1802. https://doi.org/10.4161/cc.6.14.4472

Pirouz, M., Pilarski, S., & Kessel, M. (2013). A Critical Function of Mad2l2 in Primordial Germ Cell Development of Mice. *PLoS Genetics*, *9*(8). https://doi.org/10.1371/journal.pgen.1003712

Pommier, Y. (2013). Drugging topoisomerases: Lessons and Challenges. *ACS Chemical Biology*, *8*(1), 82–95. https://doi.org/10.1021/cb300648v

Raguz, S., & Yagüe, E. (2008). Resistance to chemotherapy: New treatments and novel insights into an old problem. *British Journal of Cancer*, *99*(3), 387–391. https://doi.org/10.1038/sj.bjc.6604510

Rahjouei, A., Pirouz, M., Di Virgilio, M., Kamin, D., & Kessel, M. (2017). MAD2L2 Promotes Open Chromatin in Embryonic Stem Cells and Derepresses the Dppa3 Locus. *Stem Cell Reports*, *8*(4), 813–821. https://doi.org/10.1016/j.stemcr.2017.02.011

Ran, F. A., Hsu, P. D., Wright, J., Agarwala, V., Scott, D. A., & Zhang, F. (2013). Genome engineering using the CRISPR-Cas9 system. *Nature Protocols*, *8*(11), 2281–2308. https://doi.org/10.1038/nprot.2013.143

Rosell, R., Taron, M., Barnadas, A., Scagliotti, G., Sarries, C., & Roig, B. (2003). Nucleotide excision repair pathways involved in Cisplatin resistance in non-small-cell lung cancer. *Cancer Control : Journal of the Moffitt Cancer Center*, *10*, 297–305. Retrieved from http://www.ncbi.nlm.nih.gov/pubmed/12915808

Rosenberg, B., Van Camp, L., Grimley, E. B., & Thompson, A. J. (1967). The Inhibition of Growth or Cell Division in Escherichia by Different Ionic Species of Platinum (IV) Complexes. *The Journal of Biological Chemistry*, *242*(6), 1347–1352.

Ross, A. L., Simpson, L. J., & Sale, J. E. (2005). Vertebrate DNA damage tolerance requires the C-terminus but not BRCT or transferase domains of REV1. *Nucleic Acids Research*, *33*(4), 1280–1289. https://doi.org/10.1093/nar/gki279

Sail, V., Rizzo, A. A., Chatterjee, N., Dash, R. C., Ozen, Z., Walker, G. C., … Hadden, M. K. (2017). Identification of Small Molecule Translesion Synthesis Inhibitors That Target the Rev1-CT/RIR Protein–Protein Interaction. *ACS Chemical Biology*, *12*(7), 1903–1912. https://doi.org/10.1021/acschembio.6b01144

Sale, J. E. (2015). REV7/MAD2L2: the multitasking maestro emerges as a barrier to recombination. *The EMBO Journal*, *34*(12), 1609–1611. https://doi.org/10.15252/embj.201591697

Sears, C. R., & Turchi, J. J. (2012). Complex cisplatin-double strand break (DSB) lesions directly impair cellular non-homologous end-joining (NHEJ) independent of downstream damage response (DDR) pathways. *Journal of Biological Chemistry*, *287*(29), 24263–24272. https://doi.org/10.1074/jbc.M112.344911

Shaloam Dasari and Paul Bernard Tchounwou. (2015). Cisplatin in cancer therapy : molecular mechanisms of action. *Eur J Pharmacol*, *5*(0), 364–378. https://doi.org/10.1016/j.ejphar.2014.07.025.Cisplatin

Sharma, S., Canman, C. E., & Arbor, A. (2017). repair, *53*(9), 725–740. https://doi.org/10.1002/em.21736.REV1

Sharma, S., Hicks, J. K., Chute, C. L., Brennan, J. R., Ahn, J. Y., Glover, T. W., & Canman, C. E. (2012). REV1 and polymerase ζ facilitate homologous recombination repair. *Nucleic Acids Research*, *40*(2), 682–691. https://doi.org/10.1093/nar/gkr769

Sharma, S., Shah, N. A., Joiner, A. M., Roberts, K. H., & Canman, C. E. (2012). DNA Polymerase Is a Major Determinant of Resistance to Platinum-Based Chemotherapeutic Agents. *Molecular Pharmacology*, *81*(6), 778–787. https://doi.org/10.1124/mol.111.076828

Shcherbakova, P. V., I. J. F. (2006). Translesion synthesis DNA polymerases. *Biochemistry*, (1), 2496–2517.

Siddik, Z. H. (2003). Cisplatin: Mode of cytotoxic action and molecular basis of resistance. *Oncogene*, *22*(47 REV. ISS. 6), 7265–7279. https://doi.org/10.1038/sj.onc.1206933

Soria, G., & Almouzni, G. (2013). Differential contribution of HP1 proteins to DNA end resection and homology-directed repair. *Cell Cycle*, *12*(3), 422–429. https://doi.org/10.4161/cc.23215

Taggart, D. J., Fredrickson, S. W., Gadkari, V. V., & Suo, Z. (2014). Mutagenic potential of 8-oxo-7,8-dihydro-2′-deoxyguanosine bypass catalyzed by human Y-family DNA polymerases. *Chemical Research in Toxicology*, *27*(5), 931–940. https://doi.org/10.1021/tx500088e

Tesina, P., Cermáková, K., Horejší, M., Procházková, K., Fábry, M., Sharma, S., … Rezácová, P. (2015). Multiple cellular proteins interact with LEDGF/p75 through a conserved

unstructured consensus motif. *Nature Communications*, *6*. https://doi.org/10.1038/ncomms8968

Tissier, a, McDonald, J. P., Frank, E. G., & Woodgate, R. (2000). poliota, a remarkably error-prone human DNA polymerase. *Genes & Development*, *14*(13), 1642–1650. https://doi.org/10.1101/gad.14.13.1642

Tomida, J., Takata, K.-I., Bhetawal, S., Person, M. D., Chao, H.-P., Tang, D. G., & Wood, R. D. (2018). FAM35A associates with REV7 and modulates DNA damage responses of normal and BRCA1-defective cells. *The EMBO Journal*, e99543. https://doi.org/10.15252/embj.201899543

Tomida, J., Takata, K. I., Lange, S. S., Schibler, A. C., Yousefzadeh, M. J., Bhetawal, S., … Wood, R. D. (2015). REV7 is essential for DNA damage tolerance via two REV3L binding sites in mammalian DNA polymerase ζ. *Nucleic Acids Research*, *43*(2), 1000–1011. https://doi.org/10.1093/nar/gku1385

Topping, R. P., Wilkinson, J. C., & Scarpinato, K. D. (2009). Mismatch repair protein deficiency compromises cisplatin-induced apoptotic signaling. *J Biol Chem*, *284*(21), 14029–14039. https://doi.org/10.1074/jbc.M809303200

Torpey, L. E., Gibbs, P. E., Nelson, J., & Lawrence, C. W. (1994). Cloning and sequence of REV7, a gene whose function is required for DNA damage-induced mutagenesis in Saccharomyces cerevisiae. *Yeast (Chichester, England)*, *10*(11), 1503–1509. https://doi.org/10.1002/yea.320101115

Tubbs, A., & Nussenzweig, A. (2017). Endogenous DNA Damage as a Source of Genomic Instability in Cancer. *Cell*, *168*(4), 644–656. https://doi.org/10.1016/j.cell.2017.01.002

Vermeulen, M., Eberl, H. C., Matarese, F., Marks, H., Denissov, S., Butter, F., … Mann, M. (2010). Quantitative Interaction Proteomics and Genome-wide Profiling of Epigenetic Histone Marks and Their Readers. *Cell*, *142*(6), 967–980. https://doi.org/10.1016/j.cell.2010.08.020

Wang, D., & Lippard, S. J. (2005). Cellular processing of platinum anticancer drugs. *Nature Reviews Drug Discovery*, *4*(4), 307–320. https://doi.org/10.1038/nrd1691

Wang, L., & Gautier, J. (2011). The Fanconi anemia and ICL repair: implications for cancer therapy. *Critical Reviews in Biochemistry and Molecular Biology*, *45*(5), 424–439. https://doi.org/10.3109/10409238.2010.502166.The

Wang, Y., Putnam, C. D., Kane, M. F., Zhang, W., Edelmann, L., Russell, R., … Edelmann, W. (2005). Mutation in Rpa1 results in defective DNA double-strand break repair, chromosomal instability and cancer in mice. *Nature Genetics*, *37*(7), 750–755. https://doi.org/10.1038/ng1587

Watanabe, N., Mii, S., Asai, N., Asai, M., Niimi, K., Ushida, K., … Murakumo, Y. (2013). The REV7 subunit of DNA polymerase ζ is essential for primordial germ cell maintenance in the mouse. *Journal of Biological Chemistry*, *288*(15), 10459–10471. https://doi.org/10.1074/jbc.M112.421966

Waters, L. S., Minesinger, B. K., Wiltrout, M. E., D'Souza, S., Woodruff, R. V., & Walker, G. C. (2009). Eukaryotic Translesion Polymerases and Their Roles and Regulation in DNA Damage Tolerance. *Microbiology and Molecular Biology Reviews*, *73*(1), 134–154. https://doi.org/10.1128/MMBR.00034-08

Wong, R. S. (2011). Apoptosis in cancer: from pathogenesis to treatment. *Journal of Experimental & Clinical Cancer Research*, *30*(1), 87. https://doi.org/10.1186/1756-9966-30-87

Xie, K., Doles, J., Hemann, M. T., & Walker, G. C. (2010). Error-prone translesion synthesis mediates acquired chemoresistance. *Proceedings of the National Academy of Sciences*, *107*(48), 20792–20797. https://doi.org/10.1073/pnas.1011412107

Xu, G., Ross Chapman, J., Brandsma, I., Yuan, J., Mistrik, M., Bouwman, P., … Rottenberg, S. (2015). REV7 counteracts DNA double-strand break resection and affects PARP inhibition. *Nature*, *521*(7553), 541–544. https://doi.org/10.1038/nature14328

Ye, Q., Rosenberg, S. C., Moeller, A., Speir, J. A., Su, T. Y., & Corbett, K. D. (2015). TRIP13 is a protein-remodeling AAA+ ATPase that catalyzes MAD2 conformation switching. *ELife*, *2015*(4), 1–44. https://doi.org/10.7554/eLife.07367

Yoon, J.-H., Prakash, L., & Prakash, S. (2009). Highly error-free role of DNA polymerase in the replicative bypass of UV-induced pyrimidine dimers in mouse and human cells. *Proceedings of the National Academy of Sciences*, *106*(43), 18219–18224. https://doi.org/10.1073/pnas.0910121106

Zafar, M. K., & Eoff, R. L. (2017). Translesion DNA Synthesis in Cancer: Molecular Mechanisms and Therapeutic Opportunities. *Chemical Research in Toxicology*, *30*(11), 1942–1955. https://doi.org/10.1021/acs.chemrestox.7b00157

Zafar, M. K., Maddukuri, L., Ketkar, A., Penthala, N. R., Reed, M. R., Eddy, S., … Eoff, R. L. (2018). A Small-Molecule Inhibitor of Human DNA Polymerase η Potentiates the Effects of Cisplatin in Tumor Cells. *Biochemistry*, *57*(7). https://doi.org/10.1021/acs.biochem.7b01176

Zheng, H.-C. (2017). The molecular mechanisms of chemoresistance in cancers. *Oncotarget*, *8*(35), 59950–59964. https://doi.org/10.18632/oncotarget.19048

Zhou, B. S., & Elledge, S. J. (2000). Checkpoints in perspective. *Nature*, *408*(November), 433–439. https://doi.org/10.1038/35044005

Zhu, F., & Zhang, M. (2003). DNA polymerase ζ: New insight into eukaryotic mutagenesis and mammalian embryonic development. *World Journal of Gastroenterology*, *9*(6), 1165–1169. https://doi.org/10.3748/wjg.v9.i6.1165